From Population to Protein: A Characterization of Inflammatory Breast Cancer via Epidemiology and Cell Biology

by

Hannah Grace Abraham

A dissertation submitted in partial fulfillment
of the requirements for the degree of
Doctor of Philosophy
(Cancer Biology)
in the University of Michigan
2021

Doctoral Committee:

Assistant Professor Corey W. Speers, Chair
Professor Howard C. Crawford
Professor Sofia D. Merajver
Associate Professor Ann L. Miller
Professor Max S. Wicha

Hannah G. Abraham

hcheriya@umich.edu

ORCID iD: 0000-0001-8871-3440

Dedication

"Not to us, O LORD, not to us

but to your name be the glory,

because of your love and faithfulness."

Psalm 115: 1

Acknowledgements

To Dr. Sofia Merajver, thank you from the bottom of my heart for your guidance and support over the past four years. I will always be grateful to have been given the opportunity to be a part of your lab and to be continually learning from the stellar team that you lead. You have taught me so many valuable lessons on conducting good science, caring well for patients, and life in general, which I will carry with me. Thank you for everything. Thank you also to my thesis committee members Corey Speers, Howard Crawford, Ann Miller, and Max Wicha for your encouragement and guidance throughout the progression of my dissertation.

To the past and current members of the Merajver lab, thank you for your generous mentorship. I could not have completed this work without the constructive feedback and technical advice and assistance you provided, and I have learned so much from you all. Thank you especially to Zhifen Wu and Li Wei Bao, whose expertise and dedication were invaluable to the success of this work. Thank you to Megan Altemus, Andrew Little, Laura Goo, Ryan Oliver, Trisha Westerhof, and Nathan Merrill for all the scientific discussions, life advice, and laughter we shared.

To the Cancer Biology Program faculty, staff, and students, thank you for welcoming me into the program and fostering a program ethos rich in scientific curiosity and the impulse to make the world better. I'm grateful to have had colleagues like you. Thank you especially to Dave Lombard and Dawn Storball for everything you do to support us students.

To the Medical Scientist Training Program faculty, staff, and students, I cannot thank you enough for the constant support, helpful advice, and inspiration you have given me all these

years. To Ron Koenig, thank you for believing in each of us and going above and beyond to support our growth as scientists and as people. Thank you Kathy Collins for building on that foundation to continue to improve the program. To Justine Hein and Ellen Elkin, thank you for everything you do and have done to help me and all the MSTP students when we most needed it.

To my parents, Jacob and Sheeba Cheriyan, and my sister Maria Cheriyan, words cannot express my gratitude for everything you have done for me. Thank you for your steadfast love and support and prayers. I am so grateful to have you, and could not have made it this far without you.

To my husband, Benjamin Abraham, thank you for taking this road with me. Your encouragement and love and prayers keep me afloat, and I am so blessed to have a partner like you.

Finally, to my Savior and Redeemer Jesus Christ, who has loved me despite everything—thank you, LORD, for your abundant grace and your mercies which are new every morning. Thank you that when I am weak, you are strong.

Financial Acknowledgements

I would like to acknowledge the many sources of funding that made this work possible. First, funds provided by the Medical Scientist Training Program, which supported my first year in the Cancer Biology Program. Also, the Sheth Research Fund, which supported my final year in the Cancer Biology Program. Additional funding for this work and the Merajver lab was provided by the Breast Cancer Research Foundation and the Rogel Cancer Center Core Grant (P30CA046592).

Table of Contents

List of Tables

List of Figures

Abstract

Inflammatory breast cancer (IBC) is a rare and extremely aggressive form of breast cancer, with high rates of metastasis at diagnosis and a relative 5-year survival rate of about 40%. There are currently no clinically validated molecular markers of IBC, leading both to difficulty in diagnosing IBC and to a lack of targeted therapies. Therefore, there is pressing need for a standard method of coding and recording IBC cases based on current knowledge of IBC in order to determine up-to-date prognoses for IBC survival. There is also need for a deeper understanding of molecular drivers of IBC's aggressively metastatic phenotype in order to develop treatments that could further improve survival outcomes. **In this work, we aim to 1) develop and utilize a clinically-relevant coding method to assess IBC incidence and survival in the US over four decades, and 2) determine the effects of candidate molecular markers RhoC, epithelial junction proteins, and type I interferons on IBC and other aggressive breast cancers' invasive potential.**

We find that using the clinical signs of edema, erythema, and "peau d'orange" to define IBC cases in the National Cancer Institute's Surveillance, Epidemiology and End Results (SEER) databases results in a cohort of patients with nearly identical survival curves compared to IBC cases defined by specifically stated pathologic or clinical diagnosis of IBC in the tumor registry record. We further report that the incidence of IBC has been largely stable over the past four decades, while IBC survival measured in mean survival months has significantly improved, doubling over the past three decades. However, we find significant racial disparities in the epidemiology of IBC; black patients have higher incidence, younger age at diagnosis, and worse

survival of IBC compared to white patients. Despite overall improved survival for all races, the differences in survival between black and white patients have persisted from the 1980s to the 2010s.

To explore potential molecular therapeutic targets that could be utilized to further improve survival outcomes for IBC patients, we move to assessing IBC from a cell biology perspective by using CRISPR-Cas9 knockout of RhoC, a small GTPase highly expressed in IBC and other aggressive breast cancers, to investigate the mechanism behind RhoC-driven metastasis. We determine that in these breast cancer cells, RhoC expression promotes cell invasion while decreasing the expression of cell-cell junction proteins and the functionality of epithelial junctions. RhoC expression also increases robust cellular Type I interferon signaling and response to interferon treatment, especially in triple-negative breast cancer cells. We further find that interferon treatment increases cell-cell adhesion and decreases cellular invasiveness, but these effects are dampened in RhoC knockout cells.

Overall, this thesis work contributes an updated picture of the state of IBC incidence and survival in the US, as well as a novel mechanistic linkage between RhoC, Type I interferon signaling, and epithelial junction proteins that could be useful in developing therapeutic interventions for metastatic IBC.

Chapter 1 : Introduction: Inflammatory Breast Cancer – Epidemiology and Molecular Underpinnings

Inflammatory Breast Cancer Clinical Features and Management

Among the different types of breast cancer, inflammatory breast cancers (IBCs) are notable for their aggressive progression. IBC is characterized pathologically by invasion of the dermal lymphatics by tumor emboli, which is thought to contribute to the classic clinical signs of edema, erythema, and "peau d'orange" (skin of an orange) skin changes that progress rapidly, within six months from onset of symptoms. As such, by definition IBC patients are classified to be at least Stage III at diagnosis; additionally, 20-30% of IBC patients present with distant metastases at diagnosis, while in non-inflammatory breast cancer (non-IBC) only 6-10% of patients present with distant metastases at diagnosis[1–3]. IBC is relatively rare, comprising about 2% of all breast cancer diagnoses in the US, though in Egypt and North Africa IBC comprises about 11% of all breast cancers[4,5].

Breast cancer overall is a heterogeneous disease, and IBC itself is equally heterogeneous. Breast cancers are commonly categorized by whether they express the estrogen receptor (ER), progesterone receptor (PR), or HER2. In terms of hormone receptor (HR) expression and HER2 status, on average about 44% of IBCs are HR+/HER2-, 14% are HR+/HER2+, 18% are HR-/HER2+, and 24% are HR-/HER2-, also known as triple-negative breast cancer (TNBC)[6–8]. These proportions contrast with the distribution of molecular subtypes in breast cancer overall, where 73% are HR+/HER2- and 12% are TNBC[9]. IBC is typically treated with anthracycline- and taxane-based neoadjuvant chemotherapy, followed by modified radical mastectomy and

locoregional radiation therapy; for HR+ and HER2+ patients, treatment includes adjuvant hormone therapy and trastuzumab before and after surgery, respectively[10]. This multimodality therapy was adopted for IBC treatment in the 1980s[11–13]; previously, IBC was treated with radiation and sometimes also mastectomy, but this approach resulted in dismal overall 5-year survival of 5.6% of patients and mean survival time of 22 months[14]. By the 2000s, trimodality therapy as well as the use of trastuzumab for HER2+ patients had increased IBC relative 5-year survival to 38.9%[15], with Stage III (no distant metastases at diagnosis) IBC overall 5-year survival increasing to 68%[16]. Despite the major improvements in IBC survival over the past several decades, the odds of survival are still much lower for IBC patients compared to Stage III non-IBC patients, who have a relative 5-year survival rate of 86%[9].

Challenges of IBC Diagnosis and Clinical Data Collection

Survival outcomes for IBC patients are also worsened by delays in determining an accurate diagnosis. Since IBC is rare, the clinical signs of erythema and edema of the breast can be ascribed to other etiologies, such as acute mastitis or cellulitis, although these typically present with fever and leukocytosis while IBC does not[17]. A patient given an initial diagnosis of infection would be treated with antibiotics; when their symptoms would not resolve after a week or two, IBC should be considered as a possible diagnosis and a biopsy performed without further delays. Due to the aggressive nature of IBC, even a few weeks' delay can significantly impact the spread of the cancer and thereby patient survival[18]. IBC is sometimes also misdiagnosed as non-inflammatory locally-advanced breast cancer (LABC)[19], which can mislead the patient and provider about the prognosis and in some cases change the treatment regimen offered to the patient—for instance, surgical resection has not been consistently demonstrated to provide

survival benefit for Stage IV non-IBC, while it does improve survival for Stage IV IBC patients if carried out after chemotherapy[20].

The difficulty of determining standard criteria to define and diagnose IBC has persisted since the earliest descriptions of IBC in scientific literature in 1816[21]. In 2006, Kim et al. reviewed the extant literature on cohort studies of IBC patients, and found that 52% of these studies did not report which clinical parameters they used to define IBC cases, while the studies that did define IBC cases used different clinical standards to do so[22]. The National Cancer Institute's Surveillance, Epidemiology and End Results (SEER) databases have also used differing codes to refer to IBC over the past four decades—the original SEER coding guidelines for IBC dictated that a case be defined as IBC, using the code 'ICD-O 8530', only if IBC or dermal lymphatic invasion were explicitly noted in the pathological report. By 1988 the American Joint Committee on Cancer (AJCC) clinical staging categories were also being used to code patients for SEER, and 'T4d' became the recommended coding for clinically presenting IBC, where T represents tumor size and T4d indicates that the tumor is diffuse, as quite frequently IBC does not present with a measurable mass. In the following decades the recommended coding for IBC has vacillated between emphasizing that clinical signs must be occurring in a majority of the breast to be IBC and not specifying a threshold amount of abnormal signs involving the breast skin[23,24].

To address these challenges and work towards standardized criteria for diagnosis and improved quality of data collection for IBC, a panel of international IBC experts was convened in 2008, and they put forth a consensus statement regarding diagnosis and clinical management of IBC. Thus the current consensus on minimum requirements for an IBC diagnosis is the presence of erythema, edema, and/or "peau d'orange" skin changes covering at least 1/3 of the

breast and having developed in less than six months, along with invasive carcinoma confirmed via biopsy[18]. For clinicians, it is also strongly recommended that if they suspect a diagnosis of IBC, detailed description of the patient's clinical signs and photographic evidence of the skin changes should be included in the medical record[16,19]. Notably, the presence of dermal lymphatic invasion on histologic analysis is not required for an IBC diagnosis. There is also no requirement for the presence of any specific molecular marker—for the simple reason that multiple studies have not found a robust IBC-specific genomic expression profile[25,26], nor yet identified and validated an IBC-specific molecular marker for clinical use[16].

Molecular Markers Characteristic to IBC: RhoC, E-cadherin, Interferon Response

Despite not yet being used in the clinic, differential expression of some candidate molecular markers has been observed in IBC compared to non-IBC. These include increased expression of RhoC, increased expression of E-cadherin, and increased expression of the interferon-α (IFN-α) signaling pathway in IBC.

RhoC, a member of the Rho GTPase family, is more highly expressed in IBC compared to non-IBC[27–29]. Furthermore, transfecting normal human mammary epithelial cells with RhoC led to the cells becoming more motile and invasive, and secreting levels of angiogenic factors similar to what IBC cells secrete[27,30]. Activation of RhoC by the kinase Akt1 phosphorylating serine 73 is also linked to increased IBC invasiveness[31,32]. Interestingly, the expression of RhoC is variable in the pathognomonic tumor emboli in the dermal lymphatics of IBC (**Figure 1.1A**), whereas RhoC expression was found to be consistently high in primary IBC tumors (**Figure 1.1B**)[28].

E-cadherin is a component of adherens junctions, helping epithelial cells adhere to one another. Regardless of molecular subtype, IBC has higher protein expression of E-cadherin than in non-IBC[29,33]; moreover, the expression of E-cadherin in IBC is visible within the tumor emboli invading the dermal lymphatics (**Figure 1.1C**)[34]. In one patient-derived xenograft IBC model, mRNA expression of E-cadherin was decreased compared to non-IBC, but nevertheless protein expression of E-cadherin was significantly elevated compared to non-IBC[35].

Interferons are cytokines originally discovered as important for immune anti-viral response but increasingly recognized as contributing to tumorigenesis and cancer progression. The type I interferon IFN-α specifically has been found to be more highly expressed in the cell lysates of IBC compared to non-IBC[36]. Several genes downstream of IFN-α are also more highly expressed in IBC[26].

Besides their association with IBC, these proteins have been more broadly studied in other cancers and in relation to each other.

RhoC and Other Rho GTPases in Cancer

Rho GTPases can be thought of as molecular switches, cycling between active GTP-bound states and inactive GDP-bound states, in order to regulate multiple signaling pathways in eukaryotic cells (**Figure 1.2A**). One of the most important parts of the cell that they are known to regulate is the actin cytoskeleton [37]. Rho GTPases are regulated by posttranslational modifications, one of which is the addition of a lipid group at the C-terminus, which occurs in all Rho GTPases except for RhoBTB1 and RhoBTB2. This lipid group can be a prenyl or a palmitoyl group, and the prenyl groups are further subdivided into 15-carbon farnesyl groups or 20-carbon geranylgeranyl groups. Such lipid modifications facilitate Rho GTPases' interaction

with phospholipid membranes, and bring them into closer proximity to activators like guanine nucleotide exchange factors, inactivators like GTPase-activating proteins, and downstream effectors which have Rho-binding domains [38]. The first Rho family genes were identified in 1985, and were found to be similar to Ras oncogenes in their molecular weight, their membrane-targeted C-terminal sequences, and internal structural homology [39]. These similarities inspired investigations into whether Rho GTPases, specifically the RhoA subclass of Rho GTPases (**Figure 1.2B**), were also involved in cancer biology.

RhoA, RhoB, and RhoC are Ras homologues, but do not have the oncogenic transforming capability of Ras. RhoA, RhoB and RhoC differ mostly in the 9-12 amino acids at their C-terminals, as well as in posttranslational modifications. RhoA and RhoC are geranylgeranylated, while RhoB is palmitoylated as well as geranylgeranylated or farnesylated[38]. Early work on the RhoA subclass was complicated by the difficulty of obtaining reagents specific for each member of the subclass, forcing researchers to develop creative methods of manipulating these proteins. For instance, Fritz et al. in 1999 assessed the amounts of RhoA, RhoB, and RhoC in different tumors by using the Clostridium botulinum exo-enzyme C3-mediated ^{32}P-ADP-ribosylation assay, which specifically detects RhoA subclass proteins. They found increased ^{32}P labeling in colon tumors compared to normal colon tissue, as well as in breast tumors as compared to normal breast tissue, and concluded that RhoA subclass proteins were elevated in malignancies. They also assessed these tissues via Western Blot, and used antibodies against RhoA, Rac and Cdc42—however these antibodies were not specific for proteins within these subclasses. While Rac and Cdc42 were elevated in some tissue types but not in others, RhoA subclass protein expression levels were consistently found to be increased in colon, breast, and lung cancers compared to their normal tissue counterparts. Furthermore, ^{32}P—

and therefore RhoA subclass protein expression levels—were found to be higher in grade III breast tumors than in grade I. Taken together, these results suggested a compelling association between RhoA subclass proteins and a variety of human malignancies, as well as highlighted RhoA subclass proteins as a potential marker for cancer aggressiveness[40].

When RhoA subclass proteins were found to be expressed highly in a variety of cancers, the question arose of whether any cancers had RhoA mutations. However, in an analysis of human renal cell carcinoma, lung cancer, breast cancer, colon cancer, and ovarian cancer, no evidence of activating RhoA mutations was found [41]. Characterizing the potentially tumorigenic effects of high non-mutated RhoA subclass expression emerged as the next logical step. And out of the RhoA subclass proteins, RhoC emerged as playing a major role in cancers.

In 2005, Hakem et al. developed RhoC -/- mice to study RhoC's role in embryonic development, specifically in immune cell function, as well as its putative tumorigenicity. When the wild-type and RhoC -/- mice were 6-10 weeks of age, they were assessed for differences in terms of thymocyte numbers, lymph node numbers, splenic lymphocyte numbers, lymphocyte proliferation, thymocyte apoptosis, or thymocyte/T-cell/B-cell/neutrophil migration capacity. No significant difference between the immune systems of the wild-type mice and the RhoC -/- mice was found. However, they did find that under serum starvation, fibroblasts from the RhoC -/- had a more rounded morphology and fewer actin stress fibers than did their wild-type counterparts, which retained a classic elongated shape[42]. These findings pointed to RhoC having a role in cytoskeletal remodeling.

In terms of tumorigenesis, when Hakem et al. crossed polyomavirus middle T (PyV-mT) to transgenic RhoC +/- and RhoC -/- mice, they saw no significant differences in terms of size, number, or timing of primary tumor appearance. However, RhoC +/- PyV-mT mice had

significantly greater numbers of lung metastases at significantly greater sizes than those of RhoC -/- PyV-mT mice. RhoC -/- PyV-mT mice's lung metastases had a greater number of cells positive for cleaved caspase3 than the RhoC +/- control mice, meaning that without functioning RhoC the metastatic cells were more susceptible to apoptosis. Altogether, this work pointed to RhoC having a specific role not in primary tumor formation but in facilitating metastasis, potentially through both cytoskeletal remodeling and through protecting metastatic cells from apoptosis [42]. Indeed, RhoC expression had been linked to the metastatic potential of a variety of other cancers besides breast, including gastric [43], hepatocellular[44], bladder [45], pancreatic [46], and melanoma[47].

Further work on RhoC subsequently focused on characterizing its relationship to metastasis. In an analysis of 801 tissue cores from 280 patients covering a variety of normal and cancerous breast tissue, it was found that RhoC expression increased with increasing breast cancer aggressiveness, and that higher RhoC expression was associated with higher patient mortality. Moreover, high RhoC was a predictor of poor response to standard chemotherapy regimens, increasing the likelihood that patients would experience metastasis and relapse [48]. Knocking down RhoC expression with siRNA in non-IBC cells led to slower cell proliferation, reduced motility and invasive capacity, and significantly less collagen I adherence, as well as decreased α2 and β1 integrin expression compared to wild-type and control scrambled siRNA cells[49].

An attempt to characterize breast cancer stem cells (BCSCs) in the inflammatory breast cancer cell line SUM 149 found that the BCSC population, marked by high aldehyde dehydrogenase (ALDH) expression, of SUM 149s was responsible for a large fraction of the high levels of RhoC expression in SUM149s. Even in SUM 149 RhoC knockdowns and in

normal breast epithelial cells (MCF10A) transfected with constitutively activated overexpressed RhoC (G14V), sorting by ALDH activity uncovered a more stem-like ALDH+ cell population that had higher RhoC expression than ALDH- cells. Furthermore, cells with greater RhoC expression had a more morphologically "disorganized" and metastatic phenotype. *In vivo* orthotopic xenograft experiments in NOD/SCID mice showed that the higher the RhoC expression of the cells, the more lung metastases arose in the mice, consistent with prior work on RhoC. The observation that even ALDH- MCF-10A G14V mice could develop metastases supports the idea that RhoC can promote metastasis independently of BCSC mechanisms, despite their ordinarily close association [50].

Of note, RhoA and RhoC have been shown to have a mutual feedback relationship in breast cancer cells: knocking down RhoA leads to increased RhoC expression, and vice versa, while RhoA knockdown increases cell invasion and RhoC knockdown decreases invasion[51]. It is possible that this feedback relationship is driven by competition to bind to Rho GDP dissociation inhibitor (Rho GDI), which when bound leads to Rho proteins staying inactivated but also protects Rho proteins from degradation[52]. However, constitutively-active RhoA and constitutively-active RhoC both increased the motility and invasiveness of head and neck squamous cell carcinoma cell lines, which could point to RhoA and RhoC having some compensatory functions[53].

Cell Junction Proteins and Interaction with Rho GTPases

There are two categories of epithelial cell junctions: adherens junctions (AJ) and tight junctions (TJ). AJs provide structural support and strong mechanical attachments between cells, and are principally composed of the transmembrane protein E-cadherin and the cytoplasmic

proteins α- and β-catenin, which link AJs to the actin cytoskeleton[54]. TJs regulate the passage of ions and solute between cells, and block the mixing of apical and basolateral integral membrane proteins. The transmembrane TJ proteins include Occludin and the Claudin family, and the main cytoplasmic TJ proteins are the ZO family, which link the transmembrane TJ proteins to the actin cytoskeleton. ZO proteins can also interact with cytoplasmic AJ proteins, linking the signaling of AJs, TJs, and the actin cytoskeleton[55].

Besides their regulation of the actin cytoskeleton that leads to indirect regulation of junction structure and function, members of the Rho family are known to directly interact with multiple components of AJs and TJs—for instance, p120 catenin can bind to both E-cadherin and to RhoA-GDP[55]. It has also been demonstrated that RhoA specifically is important for both the initial formation and the structural maintenance of AJs and TJs[56]. Interestingly, studies using both dominant negative and constitutively active forms of either Rac or RhoA GTPases result in AJ and TJ instability[56,57], suggesting that the stability of epithelial junctions is dependent on balanced activation of Rho GTPases. Amongst the RhoA subclass of GTPases, constitutively active RhoC reduces junction stability more than RhoA does; RhoC also binds more strongly to the Rho-associated protein kinase (ROCK) than RhoA does[58], and inhibiting ROCK leads to decreased cell migration and stable localized expression of ZO-1 and E-cadherin at cell junctions[59]. In this thesis, I will characterize further the relationship between RhoC and cellular junctions in aggressive breast cancers.

Type I Interferon Signaling and Interaction with Junction Proteins and Rho GTPases

The canonical type I interferon signaling pathway consists of type I interferons (i.e. IFN-α and IFN-β) binding to their plasma membrane receptors (IFNAR1/2), leading to cytoplasmic

activation of JAK1 and TYK2, which phosphorylate STAT1/2. Tyrosine-phosphorylated heterodimers of STAT1/2 then bind to IRF9, and the whole complex is known as ISGF3. ISGF3 translocates to the nucleus and binds to IFN-stimulated response elements (ISRE) on IFN-induced genes' (ISGs) promoters and initiates transcription of these genes. *STAT1*, *STAT2*, and *IRF9* are all in fact ISGs[60]. There are also a variety of non-canonical interferon signaling pathways, including transcription initiated by unphosphorylated-ISGF3 (U-ISGF3) and by unphosphorylated STAT2 and IRF9, as STAT1 is not strictly necessary for ISG transcription[61]. U-ISGF3 specifically has been found to drive a prolonged expression of ISGs, occurring over days rather than the few hours of transcription induced by ISGF3[62,63].

In some studies, IFN-α treatment has been demonstrated to reduce epithelial barrier integrity in a dose-dependent fashion while increasing expression of occludin and E-cadherin[64,65]. In another study, IFN-α treatment leads to decreased protein expression of claudin-1 and E-cadherin but no changes in mRNA expression[66]. ISGs have also been linked to junction protein expression—IFI27 knockdown in cholangiocarcinoma cells led to increased E-cadherin expression and decreased cell proliferation and invasion[67], and IFITM1 may bind to occludin and modulate tight junctions in endothelial cells[68].

Interestingly, treating cells with interferon-alpha (IFN-α) also leads to increased RhoA activation[69,70], and RhoA has been linked to enhancing the inflammatory response[71]. In this thesis, I will highlight the novel finding of a relationship between RhoC expression, type I interferon response, and cell junction behavior.

E-cadherin and Other Junction Proteins in Cancer

The classical association of E-cadherin and cancer is in the context of epithelial-mesenchymal transition (EMT), the proposed process whereby cells from primary tumors gain the ability to metastasize. EMT was canonically marked by loss of E-cadherin expression and gain of N-cadherin expression. However, recent studies indicate that hybrid epithelial-mesenchymal cells exist that retain expression of some epithelial markers and some mesenchymal markers; these cells have increased stemness and also enhanced motility along with ability to adhere to other tumor cells, meaning that these hybrid epithelial-mesenchymal cells are more likely to migrate in clusters than as single cells[72]. EMT is also broadly associated with loss of tight junctions, although recent studies demonstrate that tight junctions are not uniformly lost in metastatic cells and instead behave in context-dependent manners based on cancer type. A variety of mislocalized claudins, including claudin-1 and claudin-7, have been found to be upregulated in some colorectal, pancreatic, and breast cancers and have been additionally found to promote EMT and metastasis in these contexts[73].

Multiple studies of diverse cancer types demonstrate a loss of junctional markers in malignant vs. normal tissue; however, these studies differ on the prognostic value derived from the loss of junction proteins. For instance, Martin et al. find that the mRNA expression of ZO-1 decreases with increasing breast cancer tumor stage[74], and Hoover et al. report that 74% of their infiltrating ductal breast carcinoma samples had reduced or negative ZO-1 expression and ZO-1 expression decreased as tumor dysplasia increased, whereas 100% of their ductal carcinoma in situ samples retained ZO-1 expression[75]. On the other hand, Bornholdt et al. found no correlation between the level of claudin-7 mRNA expression and the stage of colorectal carcinoma or the severity of dysplasia in colorectal adenomas[76]. Kaihara et al. found that

decreased E-cadherin and ZO-1 staining in primary tumor samples from colorectal cancers predicted which tumors went on to have liver metastases[77]. These results point to the fact that E-cadherin's expression and localization are highly context dependent in cancers.

Interferon Signaling in Cancer

IFN-α has been used clinically as an anti-tumor agent for decades, having first been recognized as anti-tumorigenic in 1970[78]. Type I interferons have been shown to activate dendritic cells and thereby increase anti-tumor immune response. Recent studies also demonstrate that IFN-α treatment reduces the number and size of lung cancer metastases and melanoma metastases in *in vivo* models[79,80]. High-dose IFN-α (>1000 IU/ml) is FDA-approved as monotherapy for Kaposi's sarcoma, follicular non-Hodgkin lymphoma, melanoma, and hairy-cell leukemia, and for adjuvant therapy of melanoma; but overall clinical response rates are modest, and high-dose IFN-α toxicity is high, thus oncological use has diminished in recent times[81]. A clinical study of IFN-α treatment in combination with chemo for patients with resected prostate cancer demonstrated no benefit to event-free survival, and proposed that this was due to the observed activation of both anti-tumor immune cells and immunosuppressive cells[82]. On the other hand, IFN-α is also used clinically as an anti-viral agent, and achieves sustained anti-virologic responses for significant populations of Hepatitis B and C patients[83]. Some of the variation in clinical efficacy of IFN-α can be attributed to differing ISG induction at differing concentrations of IFN-α; low-dose IFN- α tends to induce anti-viral ISGs, whereas high-dose induces proliferation and inflammation-related ISGs[80].

Despite the clinical functions of IFN-α treatment, studies show that a variety of IFN-signaling proteins are overexpressed in cancers. IRF9 is overexpressed in a majority of breast

and uterine tumor samples, and furthermore overexpression of IRF9 contributes to resistance to antimicrotubule agents[84]. IFITM1 is also overexpressed in a variety of cancers, including colorectal cancer and non-small cell lung cancer, and is further overexpressed in metastases compared to primary tumors[68]. IFI27 is increased in cholangiocarcinoma, and higher expression correlated with decreased survival[67]. Breast cancer tumors with high IFN signaling expression are almost twice as likely to metastasize and to be fatal compared to tumors with low IFN signaling expression[85].

IFN-β mRNA has been found to be more highly expressed in invasive ductal carcinoma than in normal breast tissue, and higher IFN-β target gene expression correlated with improved recurrence-free survival in TNBC specifically. More granularly, it was found that prognosis is better in "immune-responsive" TNBC, where tumor-infiltrating lymphocytes (TILs) and IFN/STAT signaling is present; "immune-repressed" TNBCs do not have TILs and suppress IFN/STAT signaling, and are more refractory to chemotherapy and likely to recur. "Immune-repressed" TNBCs also have cancer stem cell (CSC)-like qualities[86]. In progesterone-receptor (PR)-positive breast cancer cells, co-treatment with IFN-α and the PR ligand led to decreased TYK2 phosphorylation, decreased STAT1 phosphorylation, and decreased binding of STAT2 and STAT1 compared to treatment with IFN-α alone. PR-positive cells also had smaller increases in the ISGs IFIT1, IFIT2, IFIT3, OAS1, and ISG15 when treated with IFN-α compared to PR-null cells. This may indicate that PR-positivity offers breast cancers a mechanism of immune evasion through downregulation of interferon response, which is not available to TNBCs[87].

CONCLUSION

IBC is a highly metastatic disease with poor prognosis, no clinically-used molecular markers, and no targeted therapies. A variety of putative molecular markers, namely RhoC, E-cadherin, and IFN-α, have been experimentally demonstrated to be associated with IBC, but studies linking these markers in the context of breast cancer are lacking. There is an urgent need to understand the epidemiology of IBC based on standardized diagnostic definitions, as well as to understand the molecular mechanisms that promote IBC metastasis. In this dissertation work we demonstrate that, using a clinically-relevant definition of IBC in the US, IBC incidence has not changed significantly over the past several decades, while IBC survival has doubled during that time, though racial disparities in survival have persisted. We also demonstrate that in aggressive breast cancers, RhoC modulates both cell junction behavior as well as IFN response. The results of these studies may lead to improvements in IBC care and future development of targeted therapies to reduce metastases in IBC.

FIGURES

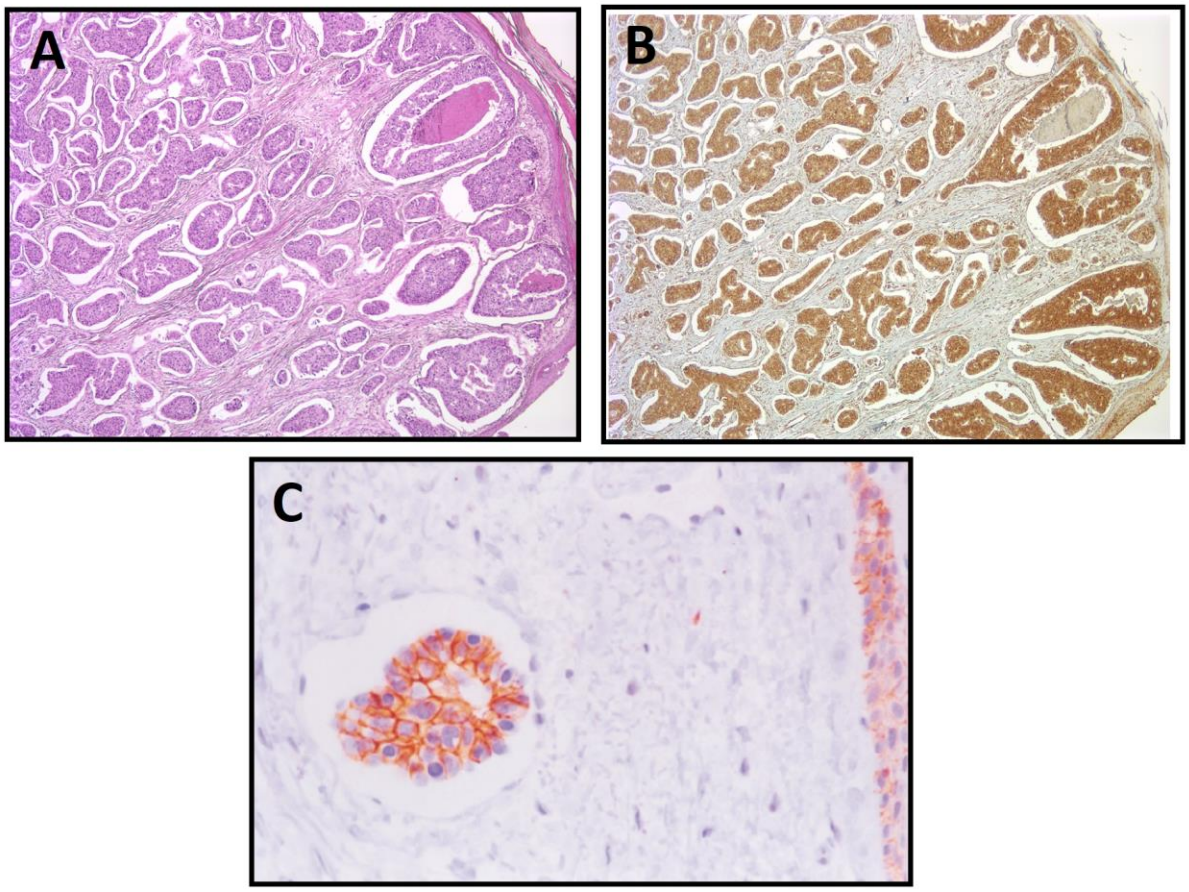

Figure 1.1 IBC molecular marker expression. (A) H&E stain of IBC, depicting tumor emboli in the dermal lymphatics of this section of breast tissue. **(B)** Expression of RhoC in IBC sample. **(C)** Expression of E-cadherin in IBC tumor emboli. Adapted from Kleer et al. 2001[34].

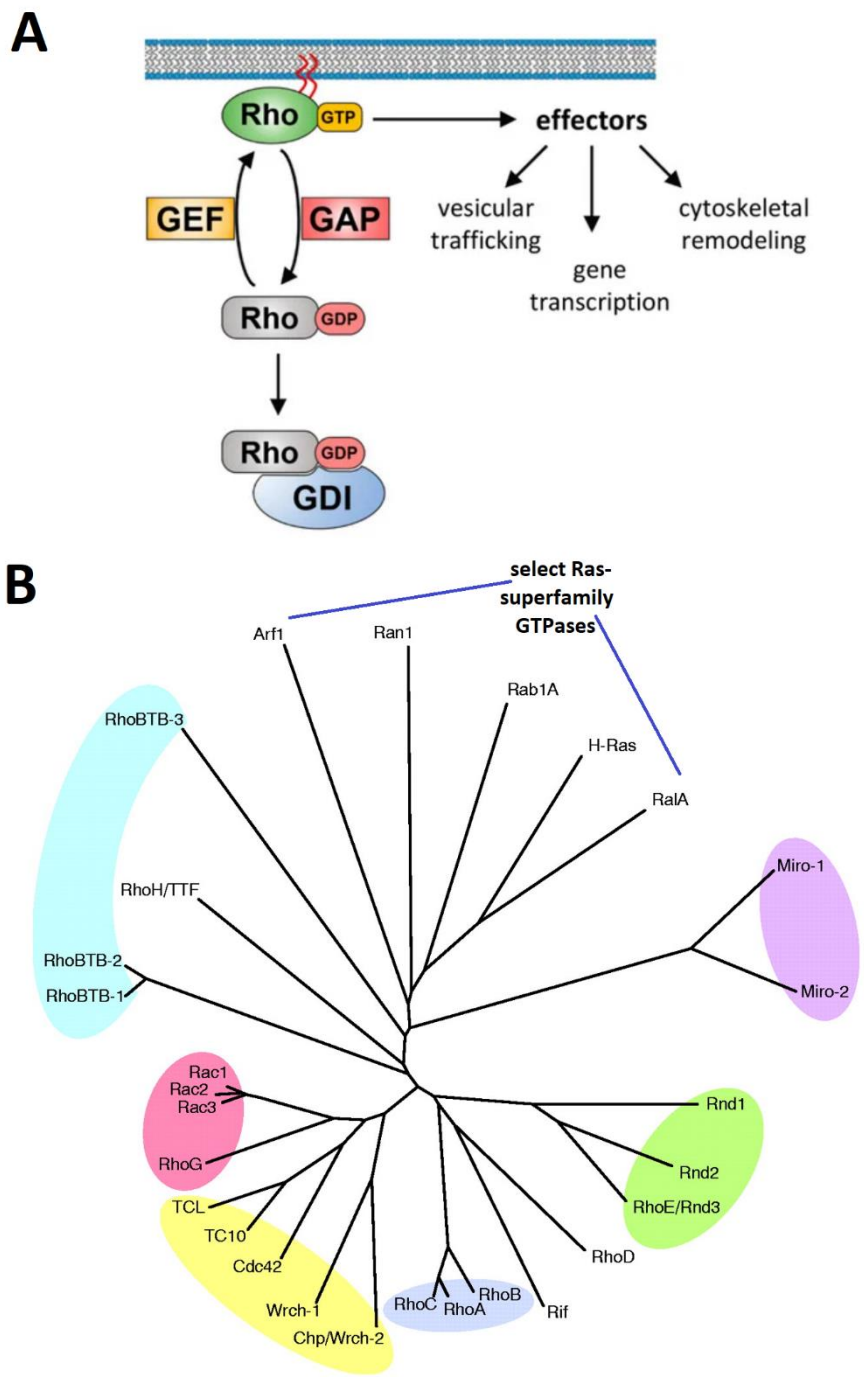

Figure 1.2 Rho GTPase signaling and family. (A) Rho GTPase signaling cycle. Guanine exchange factors (GEFs) activate Rho proteins to a GTP-bound state, allowing them to interact with effector molecules and facilitate downstream signaling. GTPase-activating proteins (GAPs) inactivate Rho proteins by inducing GTP hydrolysis, leaving Rho proteins GDP-bound. GDP dissociation inhibitors (GDIs) bind Rho-GDP and hold them in the cytoplasm to prevent Rho degradation by ubiquitination. Adapted from Olayioye et al. 2019[88] **(B)** Rho family GTPases, arranged in a phylogenetic tree with other Ras family GTPases depicted as well. Of the 22 Rho family GTPases, 19 can be grouped into one of six subfamilies: RhoBTBs (cyan), Rac-related (pink), CDC42-related (yellow), RhoA-related (light blue), Rnds (green), and Miros (purple). Adapted from Wennerberg et al. 2004[89].

REFERENCES

1. Levine PH, Steinhorn SC, Ries LG, Aron JL. Inflammatory Breast Cancer: The Experience of the Surveillance, Epidemiology, and End Results (SEER) Program. *JNCI J Natl Cancer Inst*. 1985. doi:10.1093/jnci/74.2.291
2. Yang WT, Le-Petross HT, Macapinlac H, et al. Inflammatory breast cancer: PET/CT, MRI, mammography, and sonography findings. *Breast Cancer Res Treat*. 2008;109(3):417-426. doi:10.1007/s10549-007-9671-z
3. Fouad TM, Kogawa T, Liu DD, et al. Overall survival differences between patients with inflammatory and noninflammatory breast cancer presenting with distant metastasis at diagnosis. *Breast Cancer Res Treat*. 2015;152(2):407-416. doi:10.1007/s10549-015-3436-x
4. Hance KW, Anderson WF, Devesa SS, Young HA, Levine PH. Trends in inflammatory breast carcinoma incidence and survival: The surveillance, epidemiology, and end results program at the National Cancer Institute. *J Natl Cancer Inst*. 2005. doi:10.1093/jnci/dji172
5. Soliman AS, Banerjee M, Lo A-C, et al. High proportion of inflammatory breast cancer in the population-based cancer registry of gharbiah, Egypt. *Breast J*. 2009;15(4):432-434. https://www.ncbi.nlm.nih.gov/pmc/articles/PMC4276027/. Accessed April 2, 2021.
6. Li J, Gonzalez-Angulo AM, Allen PK, et al. Triple-Negative Subtype Predicts Poor Overall Survival and High Locoregional Relapse in Inflammatory Breast Cancer. *Oncologist*. 2011. doi:10.1634/theoncologist.2011-0196
7. Chaher N, Arias-Pulido H, Terki N, et al. Molecular and epidemiological characteristics of inflammatory breast cancer in Algerian patients. *Breast Cancer Res Treat*. 2012. doi:10.1007/s10549-011-1422-5
8. Li J, Xia Y, Wu Q, et al. Outcomes of patients with inflammatory breast cancer by hormone receptor- and HER2-defined molecular subtypes: A population-based study from the SEER program. *Oncotarget*. 2017. doi:10.18632/oncotarget.17217
9. American Cancer Society. *Breast Cancer Facts & Figures 2019-2020*. Atlanta; 2020. https://www.cancer.org/content/dam/cancer-org/research/cancer-facts-and-statistics/breast-cancer-facts-and-figures/breast-cancer-facts-and-figures-2019-2020.pdf. Accessed April 2, 2021.
10. van Uden DJP, van Laarhoven HWM, Westenberg AH, de Wilt JHW, Blanken-Peeters CFJM. Inflammatory breast cancer: An overview. *Crit Rev Oncol Hematol*. 2015. doi:10.1016/j.critrevonc.2014.09.003
11. Vergés R, Felip E, Alastuey I, et al. Combined chemotherapy, radiotherapy and surgery in inflammatory breast carcinoma. *Acta Oncol (Madr)*. 1995;34(1):123-124. doi:10.3109/02841869509093650
12. Merajver SD, Weber BL, Cody R, et al. Breast conservation and prolonged chemotherapy for locally advanced breast cancer: The University of Michigan experience. *J Clin Oncol*. 1997;15(8):2873-2881. doi:10.1200/JCO.1997.15.8.2873
13. Low JA, Berman AW, Steinberg SM, Danforth DN, Lippman ME, Swain SM. Long-term

follow-up for locally advanced and inflammatory breast cancer patients treated with multimodality therapy. *J Clin Oncol*. 2004;22(20):4067-4074. doi:10.1200/JCO.2004.04.068
14. Droulias CA, Sewell CW, McSweeney MB, Powell RW. Inflammatory carcinoma of the breast: a correlation of clinical, radiologic and pathologic findings. *Ann Surg*. 1976;184(2):217-222.
15. van Uden DJP, Bretveld R, Siesling S, de Wilt JHW, Blanken-Peeters CFJM. Inflammatory breast cancer in the Netherlands; improved survival over the last decades. *Breast Cancer Res Treat*. 2017;162(2):365-374. doi:10.1007/s10549-017-4119-6
16. Ueno NT, Espinosa Fernandez JR, Cristofanilli M, et al. International consensus on the clinical management of Inflammatory Breast Cancer from the Morgan Welch Inflammatory Breast Cancer research program 10th anniversary conference. *J Cancer*. 2018;9(8):1437-1447. doi:10.7150/jca.23969
17. Uematsu T. MRI findings of inflammatory breast cancer, locally advanced breast cancer, and acute mastitis: T2-weighted images can increase the specificity of inflammatory breast cancer. *Breast Cancer*. 2012;19(4):289-294. doi:10.1007/s12282-012-0346-1
18. Dawood S, Merajver SD, Viens P, et al. International expert panel on inflammatory breast cancer: Consensus statement for standardized diagnosis and treatment. *Ann Oncol*. 2011. doi:10.1093/annonc/mdq345
19. Schairer C, Hablas A, Eldein IABS, et al. Clinico-pathologic and mammographic characteristics of inflammatory and non-inflammatory breast cancer at six centers in North Africa. *Breast Cancer Res Treat*. 2019;176(2):407-417. doi:10.1007/s10549-019-05237-5
20. Partain N, Postlewait LM, Teshome M, et al. The Role of Mastectomy in De Novo Stage IV Inflammatory Breast Cancer. *Ann Surg Oncol*. 2021. doi:10.1245/s10434-020-09392-8
21. Taylor GW, Meltzer A. "Inflammatory Carcinoma" of the Breast. *Am J Cancer*. 1938;33(1):33-49. doi:10.1158/ajc.1938.33
22. Kim T, Lau J, Erban J. Lack of uniform diagnostic criteria for inflammatory breast cancer limits interpretation of treament outcomes: A systematic review (Clinical Breast Cancer (2006) 7, (386-395)). *Clin Breast Cancer*. 2006;7(5):386-395. doi:10.3816/CBC.2006.n.055
23. Hirko KA, Soliman AS, Banerjee M, et al. A comparison of criteria to identify inflammatory breast cancer cases from medical records and the surveillance, epidemiology and end results data base, 2007-2009. *Breast J*. 2014. doi:10.1111/tbj.12234
24. Amin MB, Edge S, Greene F, et al., eds. *AJCC Cancer Staging Manual*. 8th ed. Springer International Publishing; 2017.
25. Woodward WA, Krishnamurthy S, Yamauchi H, et al. Genomic and expression analysis of microdissected inflammatory breast cancer. *Breast Cancer Res Treat*. 2013. doi:10.1007/s10549-013-2501-6
26. Van Laere SJ, Ueno NT, Finetti P, et al. Uncovering the molecular secrets of inflammatory breast cancer biology: An integrated analysis of three distinct affymetrix gene expression datasets. *Clin Cancer Res*. 2013. doi:10.1158/1078-0432.CCR-12-2549
27. van Golen KL, Wu ZF, Qiao XT, Bao L, Merajver SD. RhoC GTPase overexpression modulates induction of angiogenic factors in breast cells. *Neoplasia*. 2000;2(5):418-425. doi:http://dx.doi.org/10.1038/sj.neo.7900115
28. Kleer CG, Van Golen KL, Zhang Y, Wu ZF, Rubin MA, Merajver SD. Characterization of RhoC expression in benign and malignant breast disease: A potential new marker for

small breast carcinomas with metastatic ability. *Am J Pathol*. 2002. doi:10.1016/S0002-9440(10)64877-8
29. Van den Eynden GG, Van der Auwera I, Van Laere S, et al. Validation of a tissue microarray to study differential protein expression in inflammatory and non-inflammatory breast cancer. *Breast Cancer Res Treat*. 2004;85(1):13-22. doi:10.1023/B:BREA.0000021028.33926.a8
30. van Golen KL, Wu ZF, Qiao XT, Bao LW, Merajver SD. RhoC GTPase, a novel transforming oncogene for human mammary epithelial cells that partially recapitulates the inflammatory breast cancer phenotype. *Cancer Res*. 2000;60(20):5832-5838. http://www.ncbi.nlm.nih.gov/pubmed/11059780.
31. Lehman HL, Van Laere SJ, van Golen CM, Vermeulen PB, Dirix LY, van Golen KL. Regulation of inflammatory breast cancer cell invasion through Akt1/PKBα phosphorylation of RhoC GTPase. *Mol Cancer Res*. 2012;10(10):1306-1318. doi:10.1158/1541-7786.MCR-12-0173
32. Oglekar M, Elbazanti WO, Weitzman MD, Lehman HL, Van Golen KL. Caveolin-1 mediates inflammatory breast cancer cell invasion via the Akt1 pathway and RhoC GTPase. *J Cell Biochem*. 2015;116(6):923-933. doi:10.1002/jcb.25025
33. Levine PH, Portera CC, Hoffman HJ, et al. Evaluation of lymphangiogenic factors, vascular endothelial growth factor D and E-cadherin in distinguishing inflammatory from locally advanced breast cancer. *Clin Breast Cancer*. 2012. doi:10.1016/j.clbc.2012.04.005
34. Kleer CG, Van Golen KL, Braun T, Merajver SD. Persistent E-cadherin expression in inflammatory breast cancer. *Mod Pathol*. 2001;14(5):458-464. doi:10.1038/modpathol.3880334
35. Ye Y, Tellez JD, Durazo M, Belcher M, Yearsley K, Barsky SH. E-cadherin accumulation within the lymphovascular embolus of inflammatory breast cancer is due to altered trafficking. *Anticancer Res*. 2010.
36. Ogony J, Choi HJ, Lui A, Cristofanilli M, Lewis-Wambi J. Interferon-induced transmembrane protein 1 (IFITM1) overexpression enhances the aggressive phenotype of SUM149 inflammatory breast cancer cells in a signal transducer and activator of transcription 2 (STAT2)-dependent manner. *Breast Cancer Res*. 2016;18(1). doi:10.1186/s13058-016-0683-7
37. Etienne-Manneville S, Hall A. Rho GTPases in cell biology. *Nature*. 2002;420(6916):629-635. doi:10.1038/nature01148
38. Ridley AJ. RhoA, RhoB and RhoC have different roles in cancer cell migration. *J Microsc*. 2013;251(3):242-249. doi:10.1111/jmi.12025
39. Madaule P, Axel R. A novel ras-related gene family. *Cell*. 1985;41(1):31-40. doi:10.1016/0092-8674(85)90058-3
40. Fritz G, Just I, Kaina B. Rho GTPases are over-expressed in human tumors. *Int J Cancer*. 1999;81(5):682-687. doi:10.1002/(SICI)1097-0215(19990531)81:5<682::AID-IJC2>3.0.CO;2-B
41. Moscow JA, He R, Gnarra JR, et al. Examination of human tumors for rhoA mutations. *Oncogene*. 1994;9(1).
42. Hakem A, Sanchez-Sweatman O, You-Ten A, et al. RhoC is dispensable for embryogenesis and tumor initiation but essential for metastasis. *Genes Dev*. 2005;19(17):1974-1979. doi:10.1101/gad.1310805
43. Kondo T, Sentani K, Oue N, Yoshida K, Nakayama H, Yasui W. Expression of RhoC is

associated with metastasis of gastric carcinomas. *Pathobiology*. 2004;71(1):19-25. doi:10.1159/000072958
44. Wang W, Yang LY, Yang ZL, Huang GW, Lu WQ. Expression and significance of RhoC gene in hepatocellular carcinoma. *World J Gastroenterol*. 2003;9(9):1950-1953.
45. Kamai T, Tsujii T, Arai K, et al. Significant association of Rho/ROCK pathway with invasion and metastasis of bladder cancer. *Clin Cancer Res*. 2003;9(7):2632-2641. doi:10.1126/science.279.5350.509
46. Suwa H, Ohshio G, Imamura T, et al. Overexpression of the rhoC gene correlates with progression of ductal adenocarcinoma of the pancreas. *Br J Cancer*. 1998;77(1):147-152. doi:10.1038/bjc.1998.23
47. Clark E a, Golub TR, Lander ES, Hynes RO. Genomic Analysis of metastasis reveals an essential role for RhoC. *Nature*. 2000;406(6793):532-535. doi:10.1038/35018520
48. Kleer CG, Griffith KA, Sabel MS, et al. RhoC-GTPase is a novel tissue biomarker associated with biologically aggressive carcinomas of the breast. *Breast Cancer Res Treat*. 2005;93(2):101-110. doi:10.1007/s10549-005-4170-6
49. Wu M, Wu ZF, Rosenthal DT, Rhee EM, Merajver SD. Characterization of the roles of RHOC and RHOA GTPases in invasion, motility, and matrix adhesion in inflammatory and aggressive breast cancers. In: *Cancer*. Vol 116. ; 2010:2768-2782. doi:10.1002/cncr.25181
50. Rosenthal DT, Zhang J, Bao L, et al. RhoC impacts the metastatic potential and abundance of breast cancer stem cells. *PLoS One*. 2012;7(7). doi:10.1371/journal.pone.0040979
51. Simpson KJ, Dugan AS, Mercurio AM. Functional analysis of the contribution of RhoA and RhoC GTPases to invasive breast carcinoma. *Cancer Res*. 2004;64(23):8694-8701. doi:10.1158/0008-5472.CAN-04-2247
52. Nethe M, Hordijk PL. The role of ubiquitylation and degradation in RhoGTPase signalling. *J Cell Sci*. 2010;123(23):4011-4018. doi:10.1242/jcs.078360
53. Pan Q, Bao LW, Teknos TN, Merajver SD. Targeted disruption of protein kinase Cε reduces cell invasion and motility through inactivation of RhoA and RhoC GTPases in head and neck squamous cell carcinoma. *Cancer Res*. 2006;66(19):9379-9384. doi:10.1158/0008-5472.CAN-06-2646
54. Knust E. Composition and Formation of Intercellular Junctions in Epithelial Cells. *Science (80-)*. 2002;298(5600):1955-1959. doi:10.1126/science.1072161
55. Hartsock A, Nelson WJ. Adherens and tight junctions: Structure, function and connections to the actin cytoskeleton. *Biochim Biophys Acta - Biomembr*. 2008;1778(3):660-669. doi:10.1016/j.bbamem.2007.07.012
56. Citi S, Guerrera D, Spadaro D, Shah J. Epithelial junctions and Rho family GTPases: The zonular signalosome. *Small GTPases*. 2014. doi:10.4161/21541248.2014.973760
57. Harris TJC, Tepass U. Adherens junctions: from molecules to morphogenesis. *Nat Rev Mol Cell Biol*. 2010;11(7):502-514. doi:10.1038/nrm2927
58. Sahai E, Marshall CJ. ROCK and Dia have opposing effects on adherens junctions downstream of Rho. *Nat Cell Biol*. 2002;4(6):408-415. doi:10.1038/ncb796
59. Kim M, Shewan AM, Ewald AJ, Werb Z, Mostov KE. p114RhoGEF governs cell motility and lumen formation during tubulogenesis through a ROCK-myosin-II pathway. *J Cell Sci*. 2015. doi:10.1242/jcs.172361
60. Nan J, Wang Y, Yang J, Stark GR. IRF9 and unphosphorylated STAT2 cooperate with

NF-κB to drive IL6 expression. *Proc Natl Acad Sci U S A*. 2018. doi:10.1073/pnas.1714102115
61. Blaszczyk K, Nowicka H, Kostyrko K, Antonczyk A, Wesoly J, Bluyssen HAR. The unique role of STAT2 in constitutive and IFN-induced transcription and antiviral responses. *Cytokine Growth Factor Rev*. 2016. doi:10.1016/j.cytogfr.2016.02.010
62. Cheon H, Holvey-Bates EG, Schoggins JW, et al. IFNβ-dependent increases in STAT1, STAT2, and IRF9 mediate resistance to viruses and DNA damage. *EMBO J*. 2013. doi:10.1038/emboj.2013.203
63. Wang W, Yin Y, Xu L, et al. Unphosphorylated ISGF3 drives constitutive expression of interferon-stimulated genes to protect against viral infections. *Sci Signal*. 2017;10(476). doi:10.1126/scisignal.aah4248
64. Lechner J, Krall M, Netzer A, Radmayr C, Ryan MP, Pfaller W. Effects of interferon α-2b on barrier function and junctional complexes of renal proximal tubular LLC-PK1 cells. *Kidney Int*. 1999. doi:10.1046/j.1523-1755.1999.00487.x
65. Lechner J, Pfaller W. Interferon α2b increases paracellular permeability of renal proximal tubular LLC-PK1 cells via a mitogen activated protein kinase signaling pathway. In: *Renal Failure*. ; 2001. doi:10.1081/JDI-100104739
66. Rendón-Huerta EP, Torres-Martínez A, Charles-Niño C, et al. Pegylated interferon-α2b and ribavirin decrease claudin-1 and E-cadherin expression in HepG2 and Huh-7.5 cells. *Ann Hepatol*. 2013. doi:10.1016/s1665-2681(19)31346-8
67. Chiang KC, Huang ST, Wu RC, et al. Interferon α-inducible protein 27 is an oncogene and highly expressed in cholangiocarcinoma patients with poor survival. *Cancer Manag Res*. 2019. doi:10.2147/CMAR.S196485
68. Liang R, Li X, Zhu X. Deciphering the Roles of IFITM1 in Tumors. *Mol Diagnosis Ther*. 2020. doi:10.1007/s40291-020-00469-4
69. Chaigne-Delalande B, Deuve L, Reuzeau E, et al. RhoGTPases and p53 are involved in the morphological appearance and interferon-α response of hairy cells. *Am J Pathol*. 2006. doi:10.2353/ajpath.2006.050345
70. Badr G, Saad H, Waly H, et al. Type I interferon (IFN-α/β) rescues B-lymphocytes from apoptosis via PI3Kδ/Akt, Rho-A, NFκB and Bcl-2/BclXL. *Cell Immunol*. 2010. doi:10.1016/j.cellimm.2010.02.012
71. Fang K, Law IKM, Padua D, et al. MicroRNA-31-3p Is Involved in Substance P (SP)-Associated Inflammation in Human Colonic Epithelial Cells and Experimental Colitis. *Am J Pathol*. 2018. doi:10.1016/j.ajpath.2017.10.023
72. Sinha D, Saha P, Samanta A, Bishayee A. Emerging concepts of hybrid epithelial-to-mesenchymal transition in cancer progression. *Biomolecules*. 2020;10(11):1-22. doi:10.3390/biom10111561
73. Kyuno D, Takasawa A, Kikuchi S, Takemasa I, Osanai M, Kojima T. Role of tight junctions in the epithelial-to-mesenchymal transition of cancer cells. *Biochim Biophys Acta - Biomembr*. 2021;1863(3). doi:10.1016/j.bbamem.2020.183503
74. Martin TA, Watkins G, Mansel RE, Jiang WG. Loss of tight junction plaque molecules in breast cancer tissues is associated with a poor prognosis in patients with breast cancer. *Eur J Cancer*. 2004. doi:10.1016/j.ejca.2004.08.008
75. Hoover KB, Liao SY, Bryant PJ. Loss of the tight junction MAGUK ZO-1 in breast cancer: Relationship to glandular differentiation and loss of heterozygosity. *Am J Pathol*. 1998. doi:10.1016/S0002-9440(10)65691-X

76. Bornholdt J, Friis S, Godiksen S, et al. The level of claudin-7 is reduced as an early event in colorectal carcinogenesis. *BMC Cancer*. 2011. doi:10.1186/1471-2407-11-65
77. Kaihara T, Kusaka T, Nishi M, et al. Dedifferentiation and decreased expression of adhesion molecules, E-cadherin and ZO-1, in colorectal cancer are closely related to liver metastasis. *J Exp Clin Cancer Res*. 2003.
78. Gresser I, Brouty-Boyé D, Thomas MT, Macieira-Coelho A. Interferon and cell division. Ii. influence of various experimental conditions on the inhibition of l1zl0 cell multiplication in vitro by interferon preparations12. *J Natl Cancer Inst*. 1970. doi:10.1093/jnci/45.6.1145
79. Zhuang PY, Shen J, Zhu XD, et al. Direct Transformation of Lung Microenvironment by Interferon-α Treatment Counteracts Growth of Lung Metastasis of Hepatocellular Carcinoma. *PLoS One*. 2013. doi:10.1371/journal.pone.0058913
80. Medrano RFV, Hunger A, Mendonça SA, Barbuto JAM, Strauss BE. Immunomodulatory and antitumor effects of type I interferons and their application in cancer therapy. *Oncotarget*. 2017. doi:10.18632/oncotarget.19531
81. Berraondo P, Sanmamed MF, Ochoa MC, et al. Cytokines in clinical cancer immunotherapy. *Br J Cancer*. 2019. doi:10.1038/s41416-018-0328-y
82. Karakhanova S, Mosl B, Harig S, et al. Influence of interferon-alpha combined with chemo (radio) therapy on immunological parameters in pancreatic adenocarcinoma. *Int J Mol Sci*. 2014. doi:10.3390/ijms15034104
83. Caraglia M, Dicitore A, Marra M, et al. Type I Interferons: Ancient Peptides with Still Under-Discovered Anti-Cancer Properties. *Protein Pept Lett*. 2013. doi:10.2174/092986613805290372
84. Luker KE, Pica CM, Schreiber RD, Piwnica-Worms D. Overexpression of IRF9 confers resistance to antimicrotubule agents in breast cancer cells. *Cancer Res*. 2001.
85. Buess M, Nuyten DSA, Hastie T, Nielsen T, Pesich R, Brown PO. Characterization of heterotypic interaction effects in vitro to deconvolute global gene expression profiles in cancer. *Genome Biol*. 2007. doi:10.1186/gb-2007-8-9-r191
86. Doherty MR, Cheon HJ, Junk DJ, et al. Interferon-beta represses cancer stem cell properties in triple-negative breast cancer. *Proc Natl Acad Sci U S A*. 2017. doi:10.1073/pnas.1713728114
87. Goodman ML, Trinca GM, Walter KR, et al. Progesterone Receptor Attenuates STAT1-Mediated IFN Signaling in Breast Cancer. *J Immunol*. 2019. doi:10.4049/jimmunol.1801152
88. Olayioye MA, Noll B, Hausser A. Spatiotemporal Control of Intracellular Membrane Trafficking by Rho GTPases. *Cells*. 2019;8(12):1478. doi:10.3390/cells8121478
89. Wennerberg K, Der CJ. Rho-family GTPases: It's not only Rac and Rho (and i like it). *J Cell Sci*. 2004;117(8):1301-1312. doi:10.1242/jcs.01118

Chapter 2 : Incidence and Survival of Inflammatory Breast Cancer between 1973-2015 in the United States[1]

SUMMARY

Inflammatory breast cancer (IBC) is an aggressive variant characterized by erythema, edema, and "peau d'orange" of the skin progressing within six months. As IBC is a rare cancer and diagnosis relies on clinical presentation (not standardized molecular markers), it is difficult to identify and extract data on IBC cases in cancer databases, and as such the epidemiology of IBC is infrequently analyzed. The National Cancer Institute's Surveillance, Epidemiology, and End Results (SEER) program hosts the most comprehensive databases of cancer cases in the United States; no reports on IBC survival based on the SEER database had been published in the literature for patients diagnosed after 2008, almost a decade before we began this analysis. We therefore determined to assess the incidence and survival of IBC in the US over four decades, comparing historical results to the most recent data available. Using SEER*Stat, a case list of IBC patients diagnosed between 1973-2015 in the US (n = 29,718) was extracted from SEER 18

---

[1] **Hannah G. Abraham[1,2], Yaoxuan Xia[3], Bhramar Mukherjee[3], Sofia D. Merajver[1,2,3].**

Incidence and Survival of Inflammatory Breast Cancer between 1973-2015 in the SEER Database. *Breast Cancer Res Treat* ***185(1)***, (2021)

1. University of Michigan Medical School, Ann Arbor, MI
2. University of Michigan Rogel Cancer Center, Ann Arbor, MI
3. University of Michigan School of Public Health, Ann Arbor, MI

registries by using a combination of morphology, stage, and extent of disease criteria, M1 and M0 patients included. Age-adjusted incidence rates, relative survival rates, and mean survival time were calculated. Significance was determined as non-overlapping 95% confidence intervals. The overall incidence of IBC from 1973 – 2015 is 2.76 (2.73, 2.79) cases per 100,000 people, with white patients having an incidence rate of 2.63 (2.60, 2.67), black patients 4.52 (4.39, 4.65), and patients of other race 1.84 (1.76, 1.93). The overall IBC relative 5-year survival rate is 40.5% (39.0%, 42.0%), 42.5% (40.7%, 44.3%) and 29.9% (26.6%, 33.3%) for white patients and black patients respectively. Patients diagnosed in 1978-1982 have a mean survival time of 62.3 (52.0, 72.6) months, while those diagnosed in 2008-2012 have mean survival time of 99.4 (96.4, 102.4) months. There is no significant difference in survival time between T4D patients and patients with other T staging and Extent of Disease coding consistent with clinical IBC presentation. Overall, IBC survival has increased over four decades, but despite the improvement in survival for all racial groups, a persistent survival disparity that has not narrowed over two decades remains between white and black patients.

INTRODUCTION

Inflammatory breast cancer (IBC) is a rare and aggressive variant of stage IIID breast cancer, with increased likelihood of metastasis upon diagnosis relative to non-inflammatory breast cancer. Patients presenting with IBC experience diffuse or localized erythema and swelling of the breast, often with a “peau d’orange” appearance of the skin, that evolves and progresses within six months[1].

The literature on IBC examining survival using the National Cancer Institute’s Surveillance, Epidemiology, and End Results (SEER) program has assessed patients diagnosed

before 2008[2–5]. Studies with more recent patient data used pathological instead of clinical definitions of IBC, resulting in smaller patient cohorts as IBC is inconsistently noted on pathology reports[6], since the diagnosis of IBC relies on clinical presentation and history of the disease progression. There was therefore concern that the current literature on IBC survival was not capturing all patients who in fact have IBC. Nevertheless, a consistent observation across previous studies is that IBC incidence is higher in blacks than in whites, and that survival in IBC and other advanced breast cancers is worse in blacks than in whites[2–5,7–9].

This study aimed to achieve a comprehensive view of the clinical and epidemiological evolution of IBC in the United States over the past four decades. Major global advocacy and education efforts[10] are hypothesized to have produced greater awareness and more timely diagnosis and implementation of multimodality treatments in IBC. We combine pathological and clinical definitions of IBC to capture most or all patients with a true clinical diagnosis of IBC, and we assess incidence and survival of IBC patients by race from 1973 – 2015 using SEER 18.

MATERIALS AND METHODS

Data Source and Case Definitions

We used SEER*Stat software version 8.3.5 to extract case lists of IBC patients from the November 2017 submission of SEER 18 registries for all cases diagnosed between 1973 – 2015. SEER 18 represents 27.8% of the US population, based on the 2010 census.

The original SEER coding guidelines for IBC dictated that a case be defined as IBC, through the code ICD-O 8530, only if "IBC" itself or "dermal lymphatic invasion" were specifically noted in the pathological report. By 1988, the American Joint Committee on Cancer (AJCC) clinical staging categories were also being used to code patients for SEER, and T4d

became the recommended coding for clinically presenting IBC. In the following decades the recommended coding for IBC has fluctuated between emphasizing that clinical signs must be occurring in a majority of the breast to be IBC and not specifying a threshold amount of coverage. Previous studies have noted the importance of the trifecta of clinical signs—rapidly-progressing erythema, edema, and "peau d'orange"—in accurately diagnosing IBC, no matter what percentage of the breast is covered, since it is widely acknowledged by experienced clinicians to be almost impossible on physical exam to accurately ascertain what amount of skin represents a specified fraction, such as 1/3 or 1/2, of the breast.

Therefore, in order to capture the most accurate subset of breast cancer patients with IBC, and in accordance with the consensus of the IBC International Consortium[10], we chose to coalesce the previously used categories (**Table 2.1**). We first defined IBC patients as all female breast cancer patients coded with the ICD-O-3 code 8530 (IBC specifically noted on pathology report) or with the AJCC 6th edition code T4d (erythema and edema involving more than half the breast), resulting in an initial cohort of 15,670 patients with stringently-defined IBC which we used to assess what ICD-O-3, AJCC, and extent of disease codes were associated with these cases. We then expanded our cohort in a clinically-relevant fashion by defining IBC patients as all female breast cancer patients coded with 8530, T4d, or the extent of disease collaborative staging extension codes 510 - 750 (describe erythema, edema, and "peau d'orange" to varying extents—codes further expanded upon in **Table 2.2**). This results in a cohort of 29,718 IBC patients diagnosed between 1973–2015, which we used for all further analyses.

Incidence Analyses

Different SEER registries began contributing data at different times, so our case list extraction represents a varying fraction of the US population sampled over time, as follows: 1973 – 1991, 9.4%; 1992 - 1999, 13.4%; and 2000–2015, 27.8%. In order to compare IBC case count to an appropriate healthy population, case count and healthy population count were extracted using SEER*Stat software package version 8.3.5 from the November 2017 submissions of SEER 9 for all patients diagnosed between 1973 - 1991, SEER 13 for 1992 - 1999, and SEER 18 for 2000 - 2015. Age-adjusted incidence rates were calculated for all races for women with IBC, with age-adjustment based on the 2000 U.S. standard population and 95% confidence intervals (CI) calculated using the Tiwari et al modification[11], and p values were reported as significance tests for the difference between incidence rates.

Receptor Status Analyses

We sought to assess the proportion of IBC patients with hormone receptor (HR)+/HER2- cancer, HR-/HER2+ cancer, and triple-negative breast cancer, given that prior studies focused mainly on single institution cohorts, with the exception of the recent study by Aurit et al[12]. In our overall cohort of 29,718 IBC patients, 7,799 patients (26.2%) had at least one HR and HER2 status known. Using this smaller cohort, we assessed the proportion of IBC patients with each receptor status, and investigated the contribution of race to mean age at diagnosis of IBC, by receptor status. Based on the 2010 Collaborative Stage coding guidelines, we include receptor status coded as "borderline" (formerly defined as 1-9% cells stained) as "positive" (currently defined as $\geq$ 1% of cells stained). Significance was determined as non-overlapping 95% CI of the

mean ages for comparative groups, with 95% CI calculated as per Kaye et al[13], and p values were reported as significance tests for the difference between mean age of diagnosis.

Survival Analyses

Comparison of Relative Survival Rates over Calendar Time

Relative survival rates are the ratio of the proportion of observed survivors in a cohort of cancer patients to the proportion of expected survivors in a comparable healthy population, thus representing cancer survival apart from other causes of death. We calculated 5-, 10-, 15-, and 20-year relative survival rates using Survival Sessions on SEER*Stat software version 8.3.6 and the November 2015 submission of SEER 18 registries for cases diagnosed between 1973 – 2013, on a cohort of patients defined to have IBC using the coding from **Table 2.1**. We used this database because it had the broadest range of years of diagnosis available in a SEER*Stat Survival Session, although it did not include patients from 2013-2015, as does our incidence analysis. Using this database yields a cohort of 23,130 IBC patients diagnosed between 1973 – 2013. We estimated relative survival rates stratified by race using the Ederer II method[14], and 95% CI were calculated using the Greenwood Method[15]. P values were reported as significance tests for the difference between relative survival rates.

We use two methods of calculating relative survival rates: cohort analysis and period analysis. A schematic layout of patients included in these analyses is presented in **Figure 2.1**. Period survival analysis betters predicts the survival of more recently diagnosed patients than does traditional cohort analysis[16], so we compare period analysis rates to cohort analysis rates to assess difference in survival between recently-diagnosed and historically-diagnosed patients.

Comparison of Mean Survival over Calendar Time

Although period analysis assesses the survival of recently-diagnosed patients, it does not compare survival of patients diagnosed in each calendar year[17]. In order to calculate this, we use the recorded survival in months in our case listing of IBC patients from the November 2017 submission of SEER 18 registries for all cases diagnosed between 1973 – 2015, defining IBC as in **Table 2.1**. To make a cohort comparable to the one used for calculating relative survival rates, we once again restricted the cases to those diagnosed between 1973 – 2012, excluding cases diagnosed by autopsy or death certificate only, cases whose "cause-specific death classification" was listed as "N/A not first tumor", and cases listed as "Alive" whose survival months = 0. These exclusions are the recommended filters from the SEER*Stat program in order to best represent survival of a specific cancer. Applying these exclusions results in a cohort of 21,933 IBC patients with active follow-up who were diagnosed between 1973–2012, out of a previous total cohort of 25,494 IBC patients diagnosed in the same period. The average rate of loss-to-follow-up over 1973–2012 was 12.6% (see **Table 2.3**).

To account for unobserved survival information for patients alive at the end of our selected time period, we impute their survival times by pseudo observations. We assume that patients born in similar years have similar survival dynamics and residual survival. Based on this assumption, we divided patients into cohorts based on birth year. Birth cohorts were created as follows: patients born from 1880 to 1910 were grouped into one birth cohort. From 1910 to 1980, patients born in every 10-year interval were grouped into a birth cohort: e.g., patients born in 1910-1920 were grouped together, and so on. Patients born after 1980 were grouped into a

birth cohort. Pseudo survival times (the time from diagnosis to death) for censored patients were imputed using survival models for each birth cohort.

In order to obtain the survival rates used for imputation, we fit a separate Cox proportional hazards regression model for overall survival for patients in each birth cohort, where patients alive in 2012 were listed as censored at the corresponding follow-up time. For this regression model, we considered formulas adjusting for (1) age at diagnosis and (2) age at diagnosis and race as follows:

$$\lambda_{1c}(u) = \lambda_{0c}(u)\, e^{\beta_1 \cdot Age} \qquad (1)$$

$$\lambda_{2c}(u) = \lambda_{0c}(u)\, e^{\beta_1 \cdot Age + \beta_2 I(African\ American) + \beta_3 I(Other\ Race)} \qquad (2)$$

where c indexes the birth cohort where $\lambda_{*c}(u)$ is the instantaneous rate of death at follow-up time u for cohort c.

For each patient with unknown survival time in birth cohort c, we impute the corresponding survival time conditionally on having survived until the censoring time t* by the inverse transformation as follows:

$$\text{imputed survival} = S_{*c}^{-1}\left(U \times S_{*c}(t^*)\right)$$

where $\widehat{S_{*c}}(k) = e^{-\int_0^k \widehat{\lambda_{*c}}(u)du}$ and U is a random number generated from a uniform[0,1].

Mean survival time in months was calculated based on the survival months for uncensored patients and imputed survival time for censored patients in a five-year diagnosis cohort (1973-1977, 1978-1982, etc.). Empirical bootstrap method was used to calculate the confidence interval of the mean survival time for each diagnosis cohort. To investigate the survival difference between African American and White patients, we calculated the mean survival time separately for African American and White patients using the pseudo survival time

imputed from *Formula 2*. Empirical bootstrap method was used to calculate the confidence interval of the mean survival time for each diagnosis cohort, separately for the two populations.

To obtain a more accurate estimate of survival time, we used multiple imputation. Specifically, we drew 10 survival times for each censored patient using 10 different random numbers *U*. We calculated the mean survival months and confidence interval for patients in a 5-year period using each imputed dataset, and used Rubin's combining rules to combine parameter estimates and standard errors across imputed datasets to give the final estimates. The race differences in the mean survival time post-imputation were also combined using Rubin's rule to arrive at a p-value.

RESULTS

Most Common Coding for IBC Cases in the SEER Database

In our stringently-defined IBC cohort of 15,670 patients diagnosed between 1973 – 2015, we assessed which ICD-O-3, AJCC, and extent of disease collaborative staging extension (EoD-CS-Ext) codes were entered for each case, and sought to identify any common patterns in coding, especially in the EoD-CS-Ext codes as the current literature has not studied what EoD-CS-Ext codes are used in practice to define IBC cases. As **Figure 2.2** demonstrates, there are a discrete number of codes consistently used for the majority of IBC cases. 55% of the cohort was given the ICD-O-3 code of "8530" for inflammatory carcinoma, while 35% of the cohort had the ICD-O-3 code "8500" for infiltrating duct carcinoma. For AJCC codes, 81% of the cohort was coded "T4d" for inflammatory carcinoma and 11% was coded "Any T, Mets" denoting cancer with distant metastases. EoD-CS-Ext codes were only added in 2004, so unsurprisingly 51% of the cohort did not have EoD-CS-Ext coding. Of the remaining 7,642 cases, 37% were coded

"710", 35% were coded "750", and 18% were coded "730", all of which code for "diagnosis of inflammatory carcinoma with a clinical description of inflammation, erythema, edema, peau d'orange, etc" involving varying percentages of the breast (see **Table 2.2** for code descriptions). Thus, after defining a cohort using the ICD-O-3 and AJCC codes for IBC, this cohort was consistently coded with the codes recommended for IBC in all three coding methods (ICD-O-3, AJCC, and EoD-CS-Ext).

Our second IBC case cohort sought to be defined by the presence of clinical signs of IBC as much as the pathological. IBC cases were defined as all female breast cancer patients coded with ICD-O-3 8530, AJCC T4d, or EoD-CS-Ext 510 - 750 (describe erythema, edema, and "peau d'orange" to varying extents—codes further expanded upon in **Table 2.2**). This resulted in a cohort of 29,718 IBC patients diagnosed between 1973–2015. The coding distribution of this cohort is displayed in **Figure 2.3**. Once again the ICD-O-3 codes were divided primarily between 8530 for inflammatory carcinoma (29%) and 8500 for infiltrating duct carcinoma (52%). The AJCC coding distribution for this cohort was 43% T4d for inflammatory carcinoma, 27% Any T Mets for cancer with distant metastases, and 23% T4b denoting "edema (including peau d'orange) or ulceration of the skin of the breast, or satellite skin nodules confined to the same breast". T4b is also the catchall code for any case that only has "T4" in the record. The EoD-CS-Ext coding for this cohort was more varied—27% of the cohort did not have EoD-CS-Ext codes, but of the remaining 21,727 cases, 28% were coded "510", 8% were "520", 8% were "580", 16% were "710", 9% were "730", and 16% were "750". While the latter three codes describe the clinical signs of IBC occurring along with a stated diagnosis of IBC, the codes 510, 520, and 580 describe the same clinical signs occurring without an explicit identification of IBC (see **Table 2.2**). We consider that this cohort best represents all possible cases of clinically-

relevant IBC in the SEER database between 1973-2015, and utilize this cohort in the following analyses of incidence, age at diagnosis, and survival.

Overall Incidence of IBC Over 4 Decades

As displayed in **Figure 2.4**, the incidence of IBC as captured by the SEER program has changed over time. From 1973 – 1987, IBC incidence is relatively constant at 0.56 cases per 100,000 people, but from 1988 – 2003 the incidence of IBC rises to 2.03 cases per 100,000 people, followed by a sharp increase to 4.90 cases per 100,000 in 2004-2009, and then a near-return to previous levels of incidence with 2.80 cases per 100,000 in 2010-2015. The overall incidence of IBC from 1973 – 2015 is 2.76 cases per 100,000 people (**Table 2.4**). Interestingly, the major changes in IBC incidence coincide with changes in SEER coding guidelines for IBC, i.e. the introduction of the "T4d" AJCC code in 1988 and the introduction of Extent of Disease Collaborative Staging codes in 2004. Notably, the larger increases in incidence that occur in 1988 and 2004 are followed by plateauing incidence rates in all races (**Figure 2.4B**), suggesting that the increases are likely due to changes in SEER coding guidelines for IBC, rather than to underlying biological variations, an idea that has also been proposed in previous literature[7].

Racial Disparities in IBC Incidence

The overall age-adjusted incidence of IBC from 1973 – 2015 when stratified by race is 2.63 cases per 100,000 people for white patients, 4.52 for black patients, and 1.84 for patients of other races (Asian, Pacific Islander, Native American, etc.) (**Table 2.5**). This pattern of black patients having significantly higher IBC incidence than white patients ($p < 0.00001$) and of patients of other races having lower IBC incidence than white patients ($p < 0.00001$) has been

consistent throughout the history of SEER, becoming more pronounced as more registries contributed larger numbers of minority patients to the data in 1992 and 2000.

Receptor Status and Age-at-Diagnosis for Subtypes of IBC

In our cohort of 7,799 IBC patients with at least one HR and HER2 status known, 3,464 (44.4%) were HR+/HER2-, 1,133 (14.5%) were HR-/HER2+, and 1,702 (21.8%) had triple-negative IBC (**Table 2.6**). We find that across races, non-white patients are diagnosed with IBC at significantly younger ages than white patients (mean age at diagnosis for white patients = 61.8 years, for black patients = 57.8 years ($p < 0.00001$), and for patients of other race = 57.5 years ($p < 0.00001$)) (**Table 2.6**). Furthermore, for HR+/HER2-, HR-/HER2+, and triple-negative IBC, black patients are diagnosed significantly younger than white patients, by about 4 years ($p < 0.00001$, $p = 0.00004$, and $p < 0.00001$, respectively). Both white and black patients with IBC are diagnosed with HR-/HER2+ IBC at significantly younger ages than with HR+/HER2- IBC ($p < 0.00001$ for white patients, $p = 0.00236$ for black patients), concordant with the age distribution for all breast cancers. For all races, mean age at diagnosis for triple-negative IBC is not significantly different from mean age at diagnosis for IBC overall ($p = 0.391$, $p= 0.396$, $p = 0.396$ for white, black, and other patients respectively).

5-, 10-, 15-, and 20-year Relative Survival Rates of IBC Patients

The comparison of relative survival rate estimates using cohort analysis and period analysis, stratified by race, is presented in **Table 2.7**. The 20- year relative survival rate calculated by period survival analysis for patients with IBC is 21.5% for all patients, 22.1% for white patients, 16.2% for black patients, and 26.9% for patients of other races, representing rates

higher than those calculated by cohort-based analysis. Black patients have significantly lower relative survival rates for both cohort and period-based analysis compared with white patients: using period analysis, the 5-year relative survival rate of black patients is 29.9% and that of white patients is 42.5% ($p < 0.00001$), while the10-year relative survival rate of black patients is 18.4% and that of white patients is 30.7% ($p < 0.00001$).

The comparison of 20-year period-based estimates and 5-, 10-, 15-, 20-year cohort-based estimates of relative survival rates is presented in **Figure 2.5**. Relative 5-year survival rate of all patients using cohort-based analysis is 41.9%, 10-year is 28.0%, 15-year is 21.3%, and 20-year is 15.6%. In comparison, the period-based relative 20-year survival rate is 21.5%. The difference between cohort- and period-based survival is significant at $\alpha=0.05$ for the 20-year survival rates of all patients ($p = 0.0158$).

Racial Disparities in Mean Survival Months of IBC Patients

After multiple imputation using one Cox proportional hazard model with age of diagnosis as the only covariate, and another Cox proportional hazard model with age of diagnosis and race as covariates, the mean survival months of patients for each 5-year period of diagnosis from 1973 to 2012 are presented in **Table 2.8**. The mean survival months calculated using both Cox models are similar, validating the obtained results—for patients diagnosed between 1973 to 1977, both models give mean survival of 48.0 months; mean survival steadily increases to 99.4 months in the double-covariate model for patients diagnosed between 2008-2012 ($p < 0.00001$) (see **Figure 2.6A**).

Mean survival months for patients of different races are shown in **Table 2.9** and **Figure 2.6B**. The mean survival time for white patients is 81.9 months from diagnosis year 1988 to

1992, rising to 101.9 months from diagnosis year 2008 to 2012 ($p = 0.177$). The mean survival time for black patients is 48.5 months from diagnosis year 1988 to 1992, rising to 84.3 months from diagnosis year 2008 to 2012 ($p < 0.00001$). For both these time increments, white patients' mean survival time is significantly higher than black patients' ($p = 0.0157$ and $p = 0.00626$ for 1988-1992 and 2008-2012, respectively).

The results of the linear model with number of survival months as the outcome (imputed using the Cox proportional hazard model with age of diagnosis and race as covariates) and race and year of diagnosis as the main effects are seen in **Table 2.10**: the effect of race on survival time is 26.05 (95% CI 21.8, 30.2), indicating that white patients have increased survival time compared to black patients, while the effect of year of diagnosis on survival time is 1.64 (95% CI 1.13, 2.15), indicating that patients diagnosed after the year 2000 have approximately 64% increased survival time compared to patients diagnosed prior to 2000. The interaction between race and year of diagnosis was not significant.

IBC Survival By AJCC Stage

The comparison of mean survival months between patients coded with stage T4d, patients with stage "Any T with Mets", and patients with all other T stages is presented in **Figure 2.7A**, and the breakdown of this data by race is presented in **Figure 2.7B**. Patients with metastases have significantly lower survival than patients without metastases—in 2008-2012 the mean survival time for "Any T, Mets" patients is 62.4 months, for T4d patients 108.2 months ($p < 0.00001$) and for Other T patients 98.9 months ($p < 0.00001$). T4d patients and Other T patients consistently have no significant differences in survival, with mean survival time in 2003-2007 101.6 months for T4d patients and 102.6 months for Other T patients ($p = 0.374$), and in

1988-1992 75.5 months for T4d patients and 70.4 months for Other T patients (p = 0.301). For patients with and without metastases, white patients' mean survival time is consistently higher than black patients' (see **Table 2.11, 2.12**).

DISCUSSION

Our calculated age-adjusted incidence rates of IBC are higher than those reported in recent literature, although our incidence rates by race are consistent with previously reported trends. We propose that this is due to our coding definition of IBC, which emphasizes the importance of clinical signs like diffuse erythema, edema and "peau d'orange"—the defining characteristics of IBC—in the absence of a specifically stated pathologic or clinical diagnosis of IBC in the tumor registry record[18,19]. We employed a specific definition that leverages the existing data on SEER that is pertinent to IBC and, importantly, that aligns with IBC diagnosis in the clinic—IBC is unique amongst solid tumor categories in that the diagnosis is primarily driven by clinical presentation and not by identification from the pathology report. This method of coding IBC cases might rarely capture cases of locally advanced non-IBC. However, as IBC incidence has historically been underreported due to lack of consensus about coding and diagnosis, our approach sought to assess all possible cases of IBC in the SEER databases, including cases that may have been misclassified under previous analyses. By using the SEER databases' coding variables relevant to the clinical diagnosis of IBC, this study is the most comprehensive assessment of incident cases and of survival reported to date. Our results demonstrate that patients coded as T4D and patients with other T staging who we identified as IBC patients based on EoD-CS-Ext criteria have no significant difference in mean survival

(**Figure 2.7A)**, validating that the EoD-CS-Ext codes 510-750 are useful in capturing IBC patients who may not have been previously studied.

Recent studies have further suggested that IBC incidence is declining across the USA[12]. We propose that perception of a decline in IBC incidence may be due to the increase in IBC cases registered between 2004–2009 under newly implemented coding criteria in 2004, compared to cases coded in 2010–2015 (**Figure 2.4, Table 2.4**), after the criteria had been in use and coding-related additional prevalent cases had already been captured. The apparent downward trend in incidence is possibly then an artefact of new coding method adoption, rather than a real biological phenomenon. Regarding the trends in IBC incidence from 1973–2015, our analysis suggests that true IBC incidence has remained relatively constant over the past 4 decades, based on the plateauing incidence rates observed following the major IBC coding changes of 1988 and 2004. Indeed, our calculated IBC incidence rates are concordant with IBC incidence reports spanning two decades in prior publications[3,7,8].

Investigating the relationship between mean age at diagnosis of IBC and receptor status revealed, unexpectedly, no significant difference between mean age at diagnosis of triple-negative IBC compared to IBC overall, unlike the trend seen in non-IBC cases, where triple negative breast cancer is diagnosed at younger average age for all races. Furthermore, there was no significant difference between any receptor status and mean age at diagnosis that was robust across different races. However, these findings are limited by the relatively small sample size of our cohort with HR and HER2 status known (26.2% of our total cohort).

Our study demonstrates that black patients, regardless of receptor status, are diagnosed with IBC on average about 4 years younger than white patients. These results are concordant with the median age of diagnosis trends for breast cancer overall—we find that for IBC white

patients' median age of diagnosis is 61.8 years compared to 57.8 for black IBC patients, whereas it has been shown that for all breast cancer white patients' median age of diagnosis is 63 and black patients' is 59[20]. Moreover, while white patients have a higher incidence of breast cancer than black patients (2008-2012 incidence in white patients was 130.1 per 100,000 compared to 126.5 per 100,000 for black patients[21]), in 2006-2015 breast cancer incidence rates increased by 0.9% per year in black patients compared to 0.4% per year in white patients[22]. In IBC, on the other hand, we find that black patients consistently have higher incidence than patients of other races, and we also see a larger rate of increase in black IBC incidence compared to white IBC incidence over the past decade (see **Figure 2.4B**).

Besides a higher incidence and younger median age at diagnosis of IBC, we also observe persistently lower survival for black patients with IBC compared to white patients. The period-based 5- and 10-year relative survival rates of black patients are about 12% lower than the rates of white patients, and although this gap narrows to about 6% lower for the 20-year relative survival rates, that is likely more reflective of the still-sobering survival rates of IBC as a disease rather than of a survival benefit to black patients. Furthermore, as depicted in **Table 2.10**, the relationship between race and year of diagnosis is insignificant, indicating that the survival gap between white patients and black patients as measured in mean survival months has not significantly narrowed over recent decades. To understand the etiology of the IBC survival gap between blacks and whites, it will be important to measure potential contributions to lower black IBC survival from differences in biology, access to prompt diagnostic studies at presentation, awareness of the signs and symptoms of IBC amongst black patients, timely initiation of appropriate multimodality treatments and follow up, and survivorship care.

Importantly, this study finds that IBC survival overall has improved significantly over recent decades. As measured in mean survival months, IBC survival improved significantly between 1973-1977 and 1988-1992 and 1998-2002, approximately doubling over 30 years (1973-2003), and has continued to steadily increase since then. The difference in means between cohort-based and period-based relative rates of IBC survival also point to IBC survival having improved for all races over the years.

Our calculations of IBC mean survival months are possibly somewhat obscured by the wide confidence intervals that result from the multiple imputations we performed in order to conservatively estimate the survival of patients who had been diagnosed too recently to have more than 60 accrued months of post-diagnosis survival. Possibly a less conservative imputation method would still accurately estimate the survival of censored patients, and certainly a larger cohort of patients over a longer time period would provide a better picture of IBC survival differences between races. This would be especially helpful in comparing patients of non-white and non-black race (Asian, Pacific Islander, Native American, etc.), as the relatively low numbers of these patients compelled us to exclude them from the mean survival months analysis. However, our work here comprises the largest US cohort on which IBC survival has ever been reported.

Our results suggest that while actual IBC incidence has remained stable over time, IBC survival has moderately increased in recent years, for all races. However, despite the overall improvement in survival, there remains a persistent disparity in survival between white patients and black patients that has not narrowed over two decades. Further research is urgently needed to assess and address the root causes of this survival disparity.

FIGURES

Calendar Year of diagnosis	Calendar Year of follow up							
	2005	2006	2007	2008	2009	2010	2011	2012
2005	1	1-2	2-3	3-4	4-5	5		
2006		1	1-2	2-3	3-4	4-5	5	
2007			1	1-2	2-3	3-4	4-5	5
2008				1	1-2	2-3	3-4	4-5
2009					1	1-2	2-3	3-4
2010						1	1-2	2-3
2011							1	1-2
2012								1

Figure 2.1 Comparison of cohort-based vs period-based calculation of relative survival. Patients included and their years of follow-up for traditional cohort analysis are selected within the hollow box, while the patients and years of follow-up for period analysis are selected within the shaded box; in this example, 5-year relative survival is being calculated. 1-5 indicates the years of follow-up since the patient's diagnosis. Specifically, to calculate, for example, 5-year relative survival rates using cohort analysis, we included patients diagnosed between 2005-2007, with a period of follow-up from 1 to 5 years (the hollow frame). To calculate 5-year relative survival rates using period analysis, we included patients diagnosed between 2005-2012 and surviving until 2010-2012. The study population is left truncated at the beginning of the period of interest (beginning of 2010), and right censored at its end (the end of 2012). The year of follow-up for period analysis is also from 1 to 5 years (the shaded box).

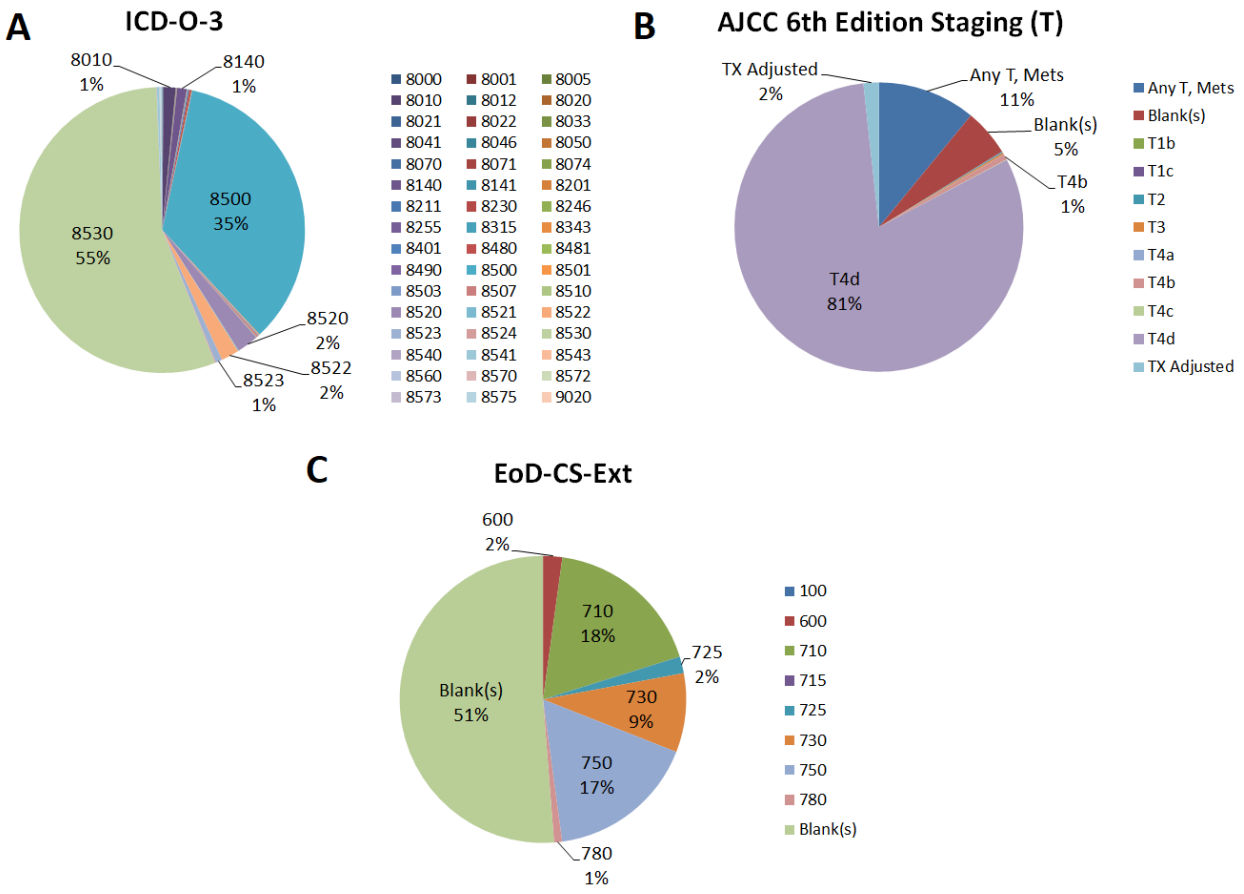

Figure 2.2 Coding distribution for IBC cohort defined by currently recommended IBC codes. IBC cases were defined as all female breast cancer patients with ICD-O-3 code 8530 (pathologically-defined IBC) or AJCC 6th Edition Staging T code T4d (IBC with clinical signs) diagnosed between 1973 – 2015. The distribution of **A)** ICD-O-3 codes, **B)** AJCC codes, and **C)** EoD-CS-Ext codes in this cohort are depicted. Codes described in **Table 2.2**.

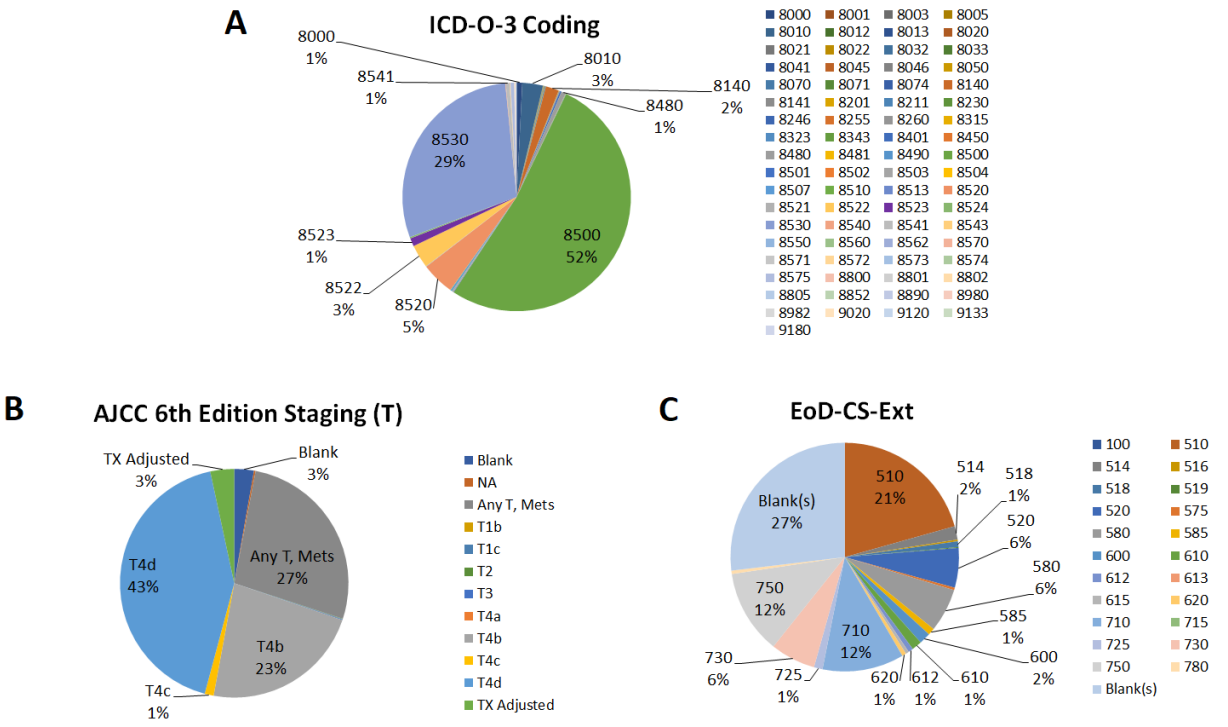

Figure 2.3 Coding distribution for IBC cohort defined by clinically-relevant updated coding criteria. IBC cases were defined as all female breast cancer patients with ICD-O-3 code 8530 (pathologically-defined IBC) or AJCC 6th Edition Staging T code T4d (IBC with clinical signs) or extent of disease collaborative staging extension codes 510-750 (clinical signs consistent with IBC) diagnosed between 1973 – 2015. The distribution of **A)** ICD-O-3 codes, **B)** AJCC codes, and **C)** EoD-CS-Ext codes in this cohort are depicted. Codes described in **Table 2.2**.

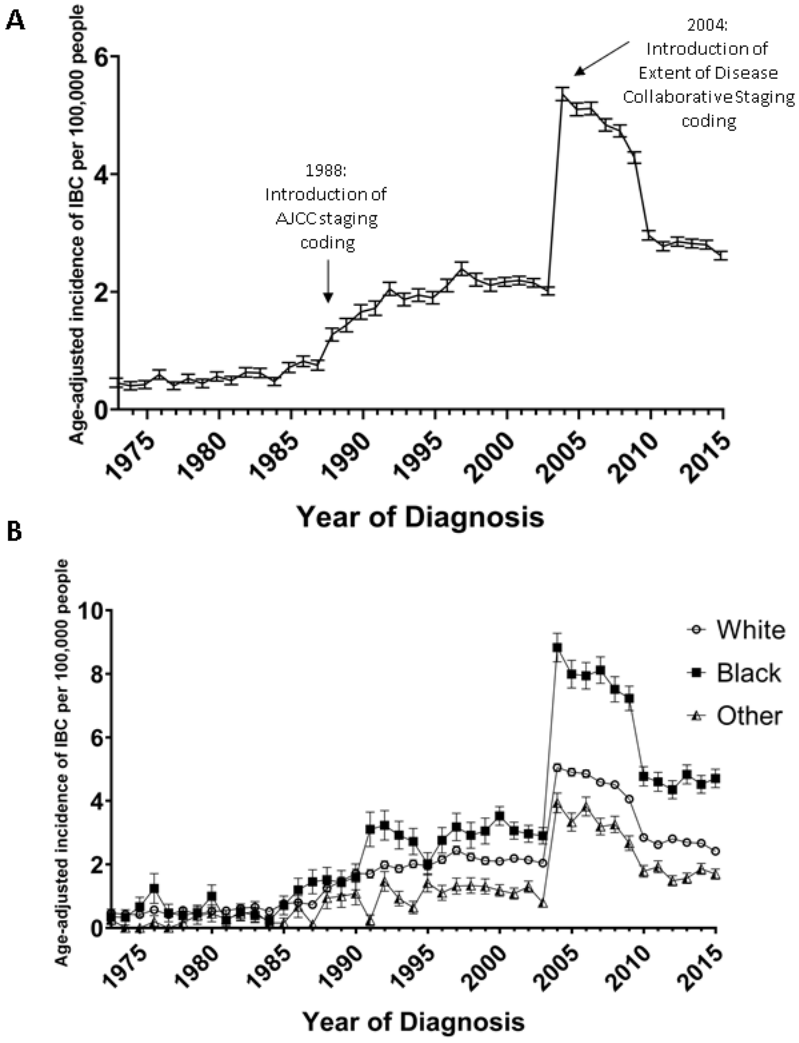

Figure 2.4 Incidence of IBC between 1973-2015. IBC cases defined as all female breast cancer patients coded as ICD-O-3 8530, AJCC 6th edition T4d, or EoD CS-Extension 510 – 750. **A)** Age-adjusted incidence rates for inflammatory breast cancer per 100,000 people from 1973 – 2015, with bars representing standard error. IBC incidence increases in years when key coding changes were added to SEER (1988, 2004) and subsequently plateaus. **B)** Age-adjusted incidence rates for IBC per 100,000 people from 1973 – 2015, by race, with bars representing standard error. Open circles: white patients; solid squares: black patients; open triangles: patients of other race. Black patients consistently have higher incidence of IBC than white patients, who consistently have higher incidence of IBC than patients of other race.

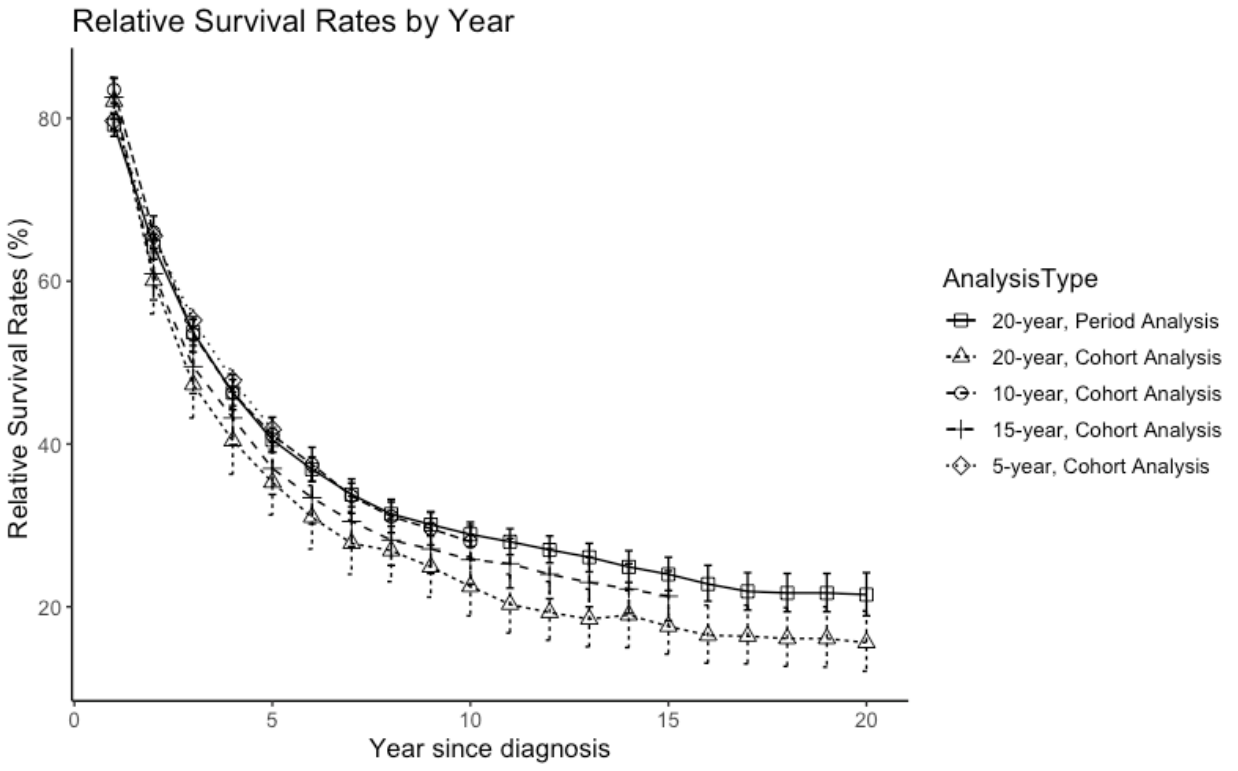

Figure 2.5 5-, 10-, 15-, 20-year relative survival of IBC. 20-year period-based and 5-year, 10-year, 15-year, and 20-year cohort-based relative survival curves for patients with IBC, with bars representing 95% CI. Open squares: 20-year period-based curve; open diamonds: 5-year cohort-based curve; open circles: 10-year cohort-based curve; dashed lines: 15-year cohort-based curve; open triangles: 20-year cohort-based curve. There is substantial separation between the 20-year period-based relative survival curve and the 20-year cohort-based relative survival curve, indicating an improvement in IBC survival in recent years compared to historical patients.

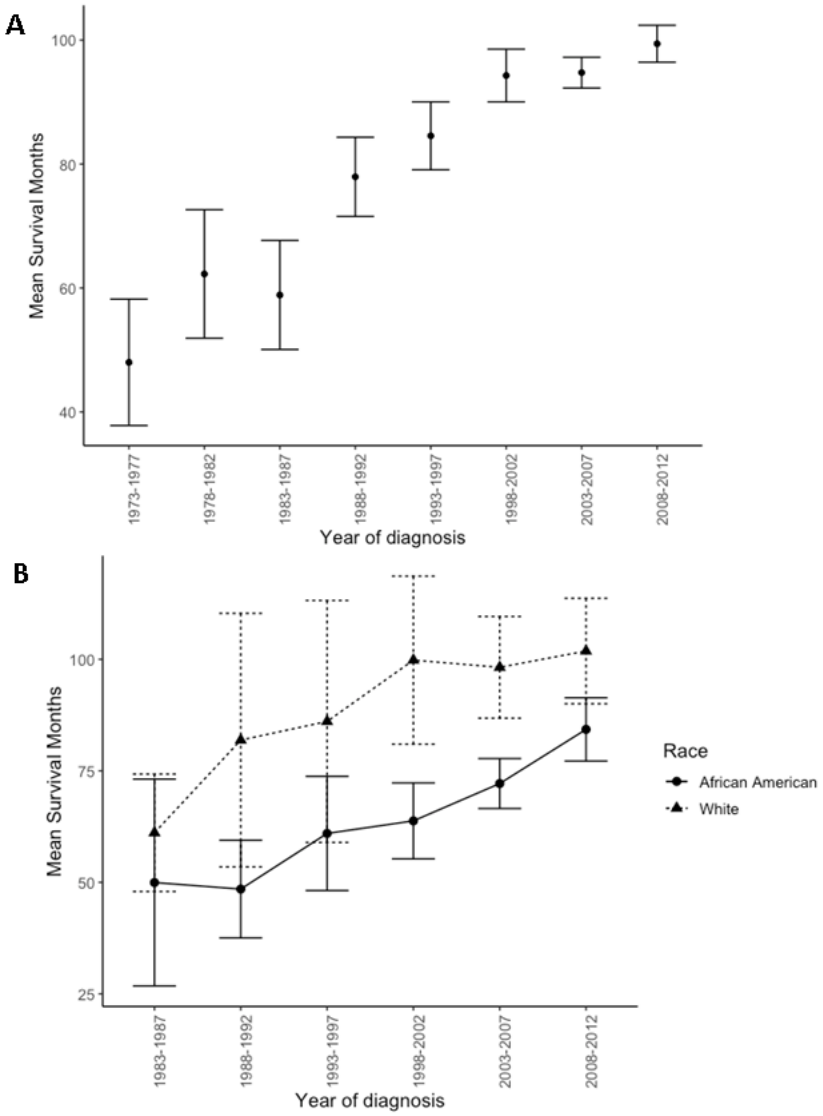

Figure 2.6 Mean survival months of IBC have increased over several decades. A) Adjusted mean survival time (in months) by year of diagnosis of IBC from 1973-2012, with bars representing 95% CI. Mean survival time increases significantly from 48 months for patients diagnosed between 1973 – 1977 to 99 months for patients diagnosed between 2008 – 2012. **B)** Adjusted mean survival time (in months) by year of diagnosis stratified by race, using Cox proportional hazard model adjusting for age of diagnosis and race, with bars representing 95% CI. Solid circles: African American patients; solid triangles: white patients. While mean survival time increases for both races, white patients consistently have about 25 months more survival time in a given year of diagnosis than do African American patients.

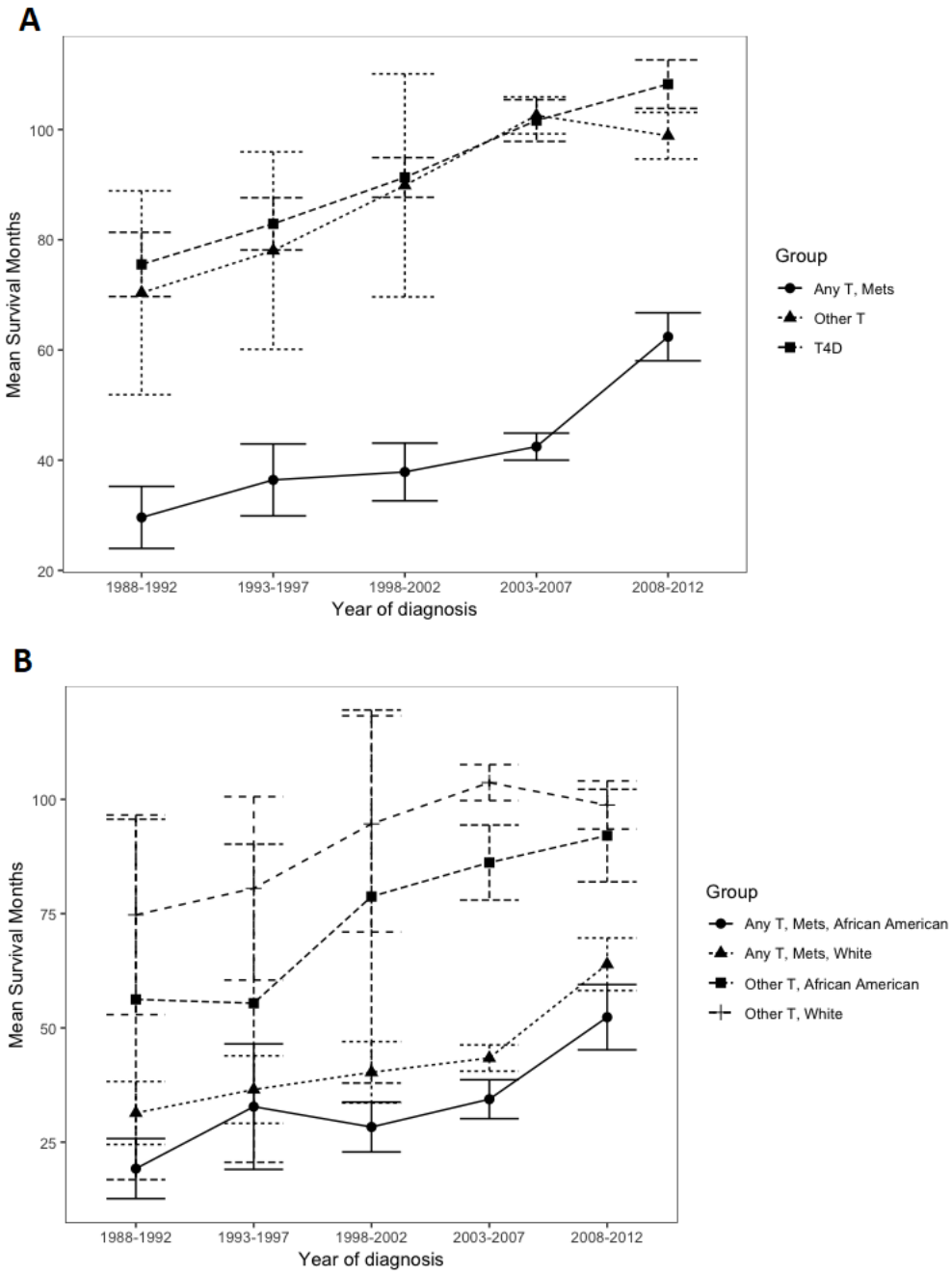

Figure 2.7 Mean survival months by T coding in IBC. A) Adjusted mean survival time (in months) by stage T coding of IBC patients diagnosed between 1988-2012, with bars representing 95% CI. While survival increases for all groups over time, T4D (solid circles) and other T patients (solid triangles) without metastases have consistently similar survival, which is significantly higher than the survival time of Any T, Mets patients (solid squares). **B)** Adjusted mean survival time (in months) by stage T coding stratified by race, using Cox proportional hazard model adjusting for age of diagnosis and race, with bars representing 95% CI. Solid circles: Any T, Mets African American patients; solid triangles: Any T, Mets white patients; solid squares: Other T African American patients; dashed line: Other T white patients. While mean survival time increases for both races, white patients consistently have higher survival in a given year of diagnosis than do African American patients.

TABLES

Table 2.1 SEER coding definitions for IBC patients. The original SEER coding guidelines for IBC dictated that a case be defined as IBC, through the code ICD-O 8530, only if "IBC" itself or "dermal lymphatic invasion" were specifically noted in the pathological report. By 1988, the American Joint Committee on Cancer (AJCC) clinical staging categories were also being used to code patients for SEER, and T4d became the recommended coding for clinically presenting IBC. In the following decades the recommended coding for IBC has fluctuated between emphasizing that clinical signs must be occurring in a majority of the breast to be IBC and not specifying a threshold amount of coverage. Previous studies have noted the importance of the trifecta of clinical signs—rapidly-progressing erythema, edema, and "peau d'orange"—in accurately diagnosing IBC, no matter what percentage of the breast is covered, since it is widely acknowledged by experienced clinicians to be almost impossible on physical exam to accurately ascertain what amount of skin represents a specified fraction, such as 1/3 or 1/2, of the breast. Therefore, in order to capture the most accurate subset of breast cancer patients with IBC, we chose to coalesce the previously used categories, using the coding in the following table.

Code Type	Value to define IBC
Sex	Female
And Morphology – Site recode	Breast
And Morphology – Histologic Type ICD-O-3	8530 ("Inflammatory Carcinoma")
Or Stage – Adjusted AJCC 6th edition T	T4d ("Inflammatory Carcinoma")
Or Extent of Disease – Collaborative Staging Extension	510 - 750

Table 2.2 SEER Extent of Disease Collaborative Staging Extension coding descriptions. Descriptions for EoD-CS-Ext codes we used to define IBC. Obtained from https://staging.seer.cancer.gov/cs/input/02.05.50/breast/extension/?breadcrumbs=(~schema_list~),(~view_schema~,~breast~)

CS Extension value	Description
510	"Extensive skin involvement, including: Satellite nodule(s) in skin of primary breast, ulceration of skin of breast, any of the following conditions described as involving not more than 50% of the breast, or amount or percent of involvement not stated: Edema of skin, En cuirasse, Erythema, Inflammation of skin, Peau d'orange ('pigskin')"
514	"Any of the following conditions described as involving less than one-third (33%) of the breast WITHOUT a stated diagnosis of inflammatory carcinoma WITH or WITHOUT dermal lymphatic infiltration: Edema of skin, En cuirasse, Erythema, Inflammation of skin, Peau d'orange ('pigskin')"
516	"514 + Extensive skin involvement, including: Satellite nodule(s) in skin of primary breast, Ulceration of skin of breast"

518	“Any of the following conditions described as involving one third (33%) or more but less than or equal to half (50%) of the breast WITHOUT a stated diagnosis of inflammatory carcinoma WITH or WITHOUT dermal lymphatic infiltration: Edema of skin, En cuirasse, Erythema, Inflammation of skin, Peau d'orange (‘pigskin’)”
519	“518 + Extensive skin involvement, including: Satellite nodule(s) in skin of primary breast, Ulceration of skin of breast”
520	“Any of the following conditions described as involving more than 50% of the breast WITHOUT a stated diagnosis of inflammatory carcinoma WITH or WITHOUT dermal lymphatic infiltration: Edema of skin, En cuirasse, Erythema, Inflammation of skin, Peau d'orange (‘pigskin’)”
575	“520 + Extensive skin involvement, including: Satellite nodule(s) in skin of primary breast, Ulceration of skin of breast”
580	“Any of the following conditions with amount or percent of breast involvement not stated and WITHOUT a stated diagnosis of inflammatory carcinoma WITH or WITHOUT dermal lymphatic infiltration: Edema of skin, En cuirasse, Erythema, Inflammation of skin, Peau d'orange (‘pigskin’)”
585	“580 + Extensive skin involvement, including: Satellite nodule(s) in skin of primary breast, Ulceration of skin of breast”
600	“Diagnosis of inflammatory carcinoma WITH a clinical description of inflammation, erythema, edema, peau d'orange, etc., involving less than one-third (33%) of the skin of the breast, WITH or WITHOUT dermal lymphatic infiltration”
610	“510 + Invasion of (or fixation to): Chest wall, Intercostal or serratus anterior muscle(s), Rib(s)”
612	“514 or 516 + Invasion of (or fixation to): Chest wall, Intercostal or serratus anterior muscle(s), Rib(s)”
613	“518 or 519 + Invasion of (or fixation to): Chest wall, Intercostal or serratus anterior muscle(s), Rib(s)”
615	“520, 575, 580 or 585 + Invasion of (or fixation to): Chest wall, Intercostal or serratus anterior muscle(s), Rib(s)”
620	“520 + Invasion of (or fixation to): Chest wall, Intercostal or serratus anterior muscle(s), Rib(s)”
710	“Diagnosis of inflammatory carcinoma WITH a clinical description of inflammation, erythema, edema, peau d'orange, etc., involving not more than 50% of the skin of the breast, WITH or WITHOUT dermal lymphatic infiltration”
715	“Diagnosis of inflammatory carcinoma WITH a clinical description of inflammation, erythema, edema, peau d'orange, etc., involving not more than one-third (33%) of the skin of the breast, WITH or WITHOUT dermal lymphatic infiltration”
720	“Diagnosis of inflammatory carcinoma WITH a clinical diagnosis of inflammation, erythema, edema, peau d'orange, etc., of not more than 50% of the breast, WITH or WITHOUT dermal lymphatic infiltration”
725	“Diagnosis of inflammatory carcinoma WITH a clinical description of inflammation, erythema, edema, peau d'orange, etc., involving one-third (33%) or more but less than or equal to one-half (50%) of

	the skin of the breast, WITH or WITHOUT dermal lymphatic infiltration"
730	"Diagnosis of inflammatory carcinoma WITH a clinical description of inflammation, erythema, edema, peau d'orange, etc., involving more than one-half (50%) of the skin of the breast, WITH or WITHOUT dermal lymphatic infiltration"
750	"Diagnosis of inflammatory carcinoma WITH a clinical description of inflammation, erythema, edema, peau d'orange, etc., but percent of involvement not stated, WITH or WITHOUT dermal lymphatic infiltration."

Table 2.3 Rate of lost-to-follow-up of IBC patients. Calculated according to standard SEER*Stat survival session exclusions.

Year of Diagnosis	Case Count	Autopsy/DCO cases	N/A not first tumor	Alive w/0 survival months	Case Count after exclusions	% Lost to follow-up
1973	35	0	2	0	33	5.714285714
1974	34	0	1	0	33	2.941176471
1975	40	0	4	0	36	10
1976	57	0	4	0	53	7.01754386
1977	38	1	4	0	33	13.15789474
1978	50	0	6	0	44	12
1979	41	0	4	0	37	9.756097561
1980	54	0	5	0	49	9.259259259
1981	51	0	5	0	46	9.803921569
1982	66	0	16	1	49	25.75757576
1983	65	0	3	0	62	4.615384615
1984	51	1	7	0	43	15.68627451
1985	74	0	6	0	68	8.108108108
1986	88	0	7	0	81	7.954545455
1987	80	0	13	0	67	16.25
1988	138	0	16	0	122	11.5942029
1989	164	0	20	0	144	12.19512195
1990	184	0	27	0	157	14.67391304
1991	200	0	30	0	170	15
1992	341	0	41	0	300	12.02346041
1993	319	0	37	0	282	11.59874608
1994	333	0	43	0	290	12.91291291
1995	337	0	44	0	293	13.05637982
1996	381	0	50	0	331	13.12335958
1997	437	0	67	0	370	15.33180778
1998	415	0	73	0	342	17.59036145
1999	404	0	57	0	347	14.10891089

2000	868	1	102	1	764	11.98156682
2001	893	1	135	0	757	15.22956327
2002	897	3	108	1	785	12.48606466
2003	856	0	130	0	726	15.18691589
2004	2332	5	322	3	2002	14.1509434
2005	2200	5	300	4	1892	14
2006	2299	1	281	5	2012	12.48368856
2007	2218	9	319	3	1887	14.92335437
2008	2212	2	327	2	1881	14.96383363
2009	2041	0	283	1	1757	13.91474767
2010	1429	1	204	5	1219	14.69559132
2011	1353	0	182	4	1167	13.74722838
2012	1419	2	211	4	1202	15.29245948
2013	1418	0	197	7	1215	14.31593794
2014	1439	1	215	10	1214	15.63585823
2015	1367	1	214	105	1066	22.01901975

Table 2.4 Incidence of IBC from 1973-2015. Case count and age-adjusted incidence rates for inflammatory breast cancer per 100,000 people in time periods from 1973 – 2015 (95% confidence intervals). Confidence intervals calculated using Tiwari et al. modification[11].

	Total	
Year of Diagnosis	Cases	Rate
1973 - 2015	29718	2.76 (2.73, 2.79)
1973 - 1987	824	0.56 (0.52, 0.60)
1988 - 2003	7167	2.03 (1.98, 2.08)
2004 - 2009	13302	4.90 (4.81, 4.98)
2010 - 2015	8425	2.80 (2.74, 2.86)

Table 2.5 Incidence of IBC by year and by race from 1973-2015. Case count and age-adjusted incidence rates for inflammatory breast cancer per 100,000 people by year from 1973 – 2015 (95% confidence intervals). Confidence intervals calculated using Tiwari et al. modification[11].

	Total		**White**		**Black**		**Other**	
Year of Diagnosis	Cases	Rate	Cases	Rate	Cases	Rate	Cases	Rate
1973	35	0.45 (0.31, 0.63)	32	0.47 (0.32, 0.67)	2	0.35 (0.02, 1.31)	1	0.26 (0, 1.44)
1974	34	0.40 (0.27, 0.56)	32	0.43 (0.29, 0.60)	2	0.33 (0.02, 1.22)	0	0 (0, 0.76)
1975	40	0.42 (0.30, 0.57)	35	0.42 (0.29, 0.58)	5	0.67 (0.18, 1.56)	0	0 (0, 0.70)
1976	57	0.59 (0.44, 0.77)	48	0.57 (0.41, 0.75)	8	1.24 (0.50, 2.41)	1	0.19 (0, 1.06)
1977	38	0.40 (0.28, 0.55)	35	0.42 (0.29, 0.59)	3	0.47 (0.07, 1.31)	0	0 (0, 0.60)
1978	50	0.52 (0.38, 0.69)	46	0.55 (0.40, 0.74)	3	0.39 (0.05, 1.09)	1	0.17 (0, 0.93)
1979	41	0.44 (0.31, 0.60)	35	0.44 (0.30, 0.61)	4	0.48 (0.10, 1.21)	2	0.39 (0.02, 1.31)

1980	54	0.56 (0.41, 0.73)	43	0.52 (0.37, 0.71)	8	1.00 (0.40, 1.94)	3	0.46 (0.06, 1.33)
1981	51	0.49 (0.36, 0.65)	48	0.54 (0.39, 0.72)	2	0.24 (0.02, 0.88)	1	0.28 (0, 1.15)
1982	66	0.63 (0.48, 0.80)	56	0.62 (0.47, 0.81)	4	0.50 (0.11, 1.20)	4	0.45 (0.10, 1.17)
1983	65	0.62 (0.47, 0.79)	59	0.65 (0.49, 0.85)	3	0.40 (0.06, 1.04)	3	0.51 (0.08, 1.38)
1984	51	0.48 (0.35, 0.62)	48	0.52 (0.38, 0.69)	2	0.23 (0.01, 0.74)	1	0.16 (0, 0.75)
1985	74	0.71 (0.56, 0.90)	67	0.76 (0.59, 0.97)	6	0.71 (0.24, 1.52)	1	0.16 (0, 0.72)
1986	88	0.82 (0.65, 1.01)	73	0.80 (0.62, 1.01)	11	1.20 (0.55, 2.09)	4	0.67 (0.15, 1.65)
1987	80	0.75 (0.59, 0.94)	64	0.73 (0.56, 0.93)	15	1.45 (0.77, 2.36)	1	0.12 (0, 0.59)
1988	138	1.27 (1.06, 1.50)	113	1.24 (1.02, 1.50)	16	1.52 (0.83, 2.45)	8	0.94 (0.38, 1.83)
1989	164	1.43 (1.22, 1.67)	140	1.48 (1.24, 1.75)	15	1.43 (0.76, 2.33)	9	1.00 (0.42, 1.93)
1990	184	1.66 (1.42, 1.91)	158	1.71 (1.45, 2.00)	16	1.61 (0.88, 2.59)	10	1.08 (0.48, 1.98)
1991	200	1.72 (1.48, 1.97)	164	1.71 (1.45, 1.99)	34	3.10 (2.11, 4.34)	2	0.24 (0.01, 0.76)
1992	341	2.05 (1.83, 2.28)	268	1.99 (1.75, 2.24)	50	3.23 (2.37, 4.26)	23	1.47 (0.91, 2.19)
1993	319	1.87 (1.67, 2.09)	257	1.86 (1.64, 2.10)	46	2.92 (2.11, 3.88)	16	0.92 (0.51, 1.49)
1994	333	1.94 (1.74, 2.16)	277	2.02 (1.78, 2.27)	45	2.72 (1.97, 3.64)	11	0.64 (0.30, 1.12)
1995	337	1.90 (1.70, 2.11)	277	1.95 (1.73, 2.20)	34	2.02 (1.39, 2.79)	26	1.42 (0.92, 2.06)
1996	381	2.11 (1.90, 2.33)	310	2.15 (1.92, 2.41)	48	2.76 (2.02, 3.64)	23	1.11 (0.69, 1.66)
1997	437	2.40 (2.17, 2.63)	353	2.44 (2.19, 2.71)	56	3.18 (2.38, 4.12)	27	1.32 (0.86, 1.91)
1998	415	2.21 (2.00, 2.43)	331	2.23 (2.00, 2.49)	53	2.92 (2.17, 3.79)	31	1.34 (0.89, 1.88)
1999	404	2.11 (1.91, 2.33)	317	2.12 (1.89, 2.36)	57	3.05 (2.30, 3.95)	30	1.31 (0.88, 1.87)
2000	868	2.17 (2.03, 2.32)	678	2.10 (1.94, 2.26)	147	3.52 (2.97, 4.13)	43	1.18 (0.84, 1.59)
2001	893	2.19 (2.05, 2.34)	720	2.19 (2.03, 2.36)	133	3.06 (2.55, 3.62)	40	1.08 (0.77, 1.48)
2002	897	2.15 (2.01, 2.30)	715	2.14 (1.99, 2.31)	128	2.96 (2.46, 3.52)	52	1.30 (0.96, 1.70)
2003	856	2.01 (1.88, 2.15)	694	2.04 (1.89, 2.20)	130	2.90 (2.41, 3.44)	32	0.79 (0.53, 1.11)
2004	2332	5.36 (5.14, 5.58)	1772	5.05 (4.81, 5.29)	394	8.83 (7.96, 9.75)	164	3.94 (3.35, 4.59)
2005	2200	5.10 (4.89, 5.32)	1705	4.90 (4.67, 5.14)	348	7.99 (7.15, 8.88)	141	3.33 (2.80, 3.94)
2006	2299	5.12 (4.91, 5.33)	1746	4.86 (4.63, 5.09)	375	7.94 (7.13, 8.79)	172	3.82 (3.26, 4.44)
2007	2218	4.84 (4.64, 5.04)	1673	4.59 (4.37, 4.81)	388	8.12 (7.31, 8.97)	153	3.19 (2.70, 3.74)
2008	2212	4.74 (4.54, 4.94)	1675	4.51 (4.30, 4.74)	371	7.51 (6.75, 8.33)	161	3.26 (2.76, 3.80)
2009	2041	4.28 (4.10, 4.47)	1528	4.06 (3.85, 4.27)	369	7.23 (6.50, 8.02)	138	2.67 (2.23, 3.15)
2010	1429	2.96 (2.81, 3.12)	1073	2.85 (2.67, 3.02)	254	4.77 (4.19, 5.41)	98	1.78 (1.44, 2.17)
2011	1353	2.77 (2.62, 2.93)	993	2.62 (2.45, 2.79)	247	4.60 (4.03, 5.22)	109	1.93 (1.57, 2.32)
2012	1419	2.85 (2.70, 3.01)	1084	2.81 (2.64, 2.99)	245	4.35 (3.81, 4.94)	87	1.48 (1.18, 1.83)
2013	1418	2.82 (2.67, 2.98)	1041	2.69 (2.53, 2.87)	274	4.83 (4.26, 5.45)	95	1.56 (1.26, 1.92)
2014	1439	2.80 (2.65, 2.95)	1057	2.67 (2.50, 2.84)	262	4.52 (3.97, 5.11)	116	1.86 (1.53, 2.23)
2015	1367	2.62 (2.48, 2.76)	969	2.41 (2.26, 2.58)	276	4.71 (4.15, 5.31)	110	1.69 (1.38, 2.04)
1973-2015	29718	2.76 (2.73, 2.79)	22809	2.63 (2.60, 2.67)	4889	4.52 (4.39, 4.65)	1950	1.84 (1.76, 1.93)

Table 2.6 IBC receptor status by race and mean age at diagnosis. Age measured in years. Significance relative to white patients, determined by non-overlapping 95% CI calculated as per Kaye et al[13] and demonstrated by *.

	Total IBC with known receptors			at least one HR+ and HER2-			ER-, PR-, HER2+			ER-, PR-, HER2-		
Race	Count	Mean Age	95% CI	Count (% total)	Mean Age	95% CI	Count (% total)	Mean Age	95% CI	Count (% total)	Mean Age	95% CI
White	5736	61.8	(61.4, 62.2)	2600 (45.3)	63.4	(62.8, 63.9)	835 (14.6)	59.9	(59.0, 60.9)	1164 (20.3)	61.7	(60.8, 62.6)
Black	1453	57.8*	(57.1, 58.6)	585 (40.3)	59.2*	(58.1, 60.4)	195 (13.4)	55.5*	(53.6, 57.5)	435 (29.9)	57.7*	(56.4, 59.1)
Other	581	57.5*	(56.3, 58.6)	268 (46.1)	58.3*	(56.7, 60.1)	97 (16.7)	58.0	(55.4, 60.7)	97 (16.7)	57.3	(54.2, 60.3)
Unknown	29	56.1*	(51.9, 60.2)	11 (37.9)	57.9	(49.4, 66.4)	6 (20.7)	50.3*	(42.8, 57.9)	6 (20.7)	53.2*	(49.5, 56.9)

Table 2.7 Relative survival rates for IBC by race, % (95% CI). "Cohort": cohort analysis, "Period": period analysis. Significance relative to black patients, determined by non-overlapping 95% CI calculated via the Greenwood method[15] and demonstrated by * for cohort and $^{+}$ for period analysis.

		5-year	10-year	15-year	20-year
Black	Cohort	29.8 (26.7, 32.9)	14.8 (10.9, 19.4)	10.4 (5.0, 18.1)	3.7 (0.7, 11.2)
	Period	29.9 (26.6, 33.3)	18.4 (15.2, 21.8)	16.7 (12.9, 20.9)	16.2 (9.1, 25.1)
White	Cohort	44.0* (42.4, 45.7)	30.6* (28.2, 33.0)	22.1* (18.8, 25.6)	17.5* (13.4, 22.0)
	Period	42.5^{+} (40.7, 44.3)	30.7^{+} (28.9, 32.5)	25.1^{+} (22.7, 27.5)	22.1 (19.2, 25.2)
Other	Cohort	46.8* (41.5, 51.8)	26.3 (18.5, 34.7)	19.1 (10.3, 29.9)	14.1 (3.8, 31.0)
	Period	43.6^{+} (38.0, 49 .0)	32.6^{+} (26.7, 38.7)	30.5 (22.8, 38.6)	26.9 (18.3, 36.3)
All	Cohort	41.9* (40.5, 43.3)	28.0* (25.9, 30.0)	21.3* (18.3, 24.4)	15.6* (12.1, 19.5)
	Period	40.5^{+} (39.0, 42.0)	28.9^{+} (27.4, 30.4)	24.0^{+} (22.0, 26.1)	21.5 (18.9, 24.2)

Table 2.8 Mean survival months of IBC. Before and after imputation of censored patients (95% CI).

	Mean Survival Time (Months)		
Year	Unadjusted	Cox Model, adjusted for age	Cox Model, adjusted for race and age
1973-1977	47.0 (37.4, 56.6)	48.0 (37.8, 58.2)	48.0 (37.9, 58.2)
1978-1982	61.9 (52.0, 71.9)	62.3 (51.9, 72.6)	62.3 (52.0, 72.6)
1983-1987	55.7 (48.3, 63.1)	58.9 (50.1, 67.7)	58.9 (50.1, 67.6)
1988-1992	68.5 (63.7, 73.3)	77.9 (71.5, 84.3)	77.9 (71.6, 84.3)
1993-1997	66.5 (63.4, 69.7)	84.5 (79.1, 90.2)	84.6 (79.1, 90.0)
1998-2002	62.2 (60.5, 63.8)	94.5 (90.2, 98.7)	94.3 (90.0, 98.5)
2003-2007	48.6 (47.9, 49.2)	95.1 (92.7, 97.6)	94.8 (92.3, 97.2)
2008-2012	28.2 (27.9, 28.6)	100.2 (97.2, 103.2)	99.4 (96.4, 102.4)

Table 2.9 Mean survival months of IBC by race. Before and after imputation using Cox Model Adjusted for Age and Race (95% CI). Significance relative to white patients, determined by non-overlapping 95% CI and demonstrated by *.

	Mean Survival Time (Months)			
	African American		White	
Year	Unadjusted	Adjusted	Unadjusted	Adjusted
1988-1992	46.4* (37.4, 55.4)	48.5 (37.5, 59.4)	71.3 (65.9, 76.7)	81.9 (53.5, 110.3)
1993-1996	49.1* (41.8, 56.4)	61.0 (48.2, 73.8)	68.1 (64.6, 71.6)	86.1 (59.0, 113.2)
1997-2002	47.4* (43.7, 51.2)	63.8* (55.3, 72.3)	64.8 (62.9, 66.7)	99.8 (81.0, 118.7)
2003-2007	41.0* (39.5, 42.5)	72.1* (66.6, 77.7)	49.9 (49.1, 50.6)	98.2 (86.8, 109.6)
2008-2012	25.7* (24.8, 26.4)	84.3 (77.2, 91.4)	28.7 (28.2, 29.1)	101.9 (90.0, 113.7)

Table 2.10 Effect of Race and Year of Diagnosis on survival time. Year of diagnosis is scaled to the left by 2000, and black patients are the reference for race. The outcome, survival time, is imputed from the Cox model adjusting for age and race, and the linear coefficient estimates are subsequently reported here. Significance is determined by 95% CI > 0, and is depicted by *.

	Cox Model, adjusting for age and race	
Variables	$\hat{\beta}$	95% CI
Race	26.05*	(21.8, 30.2)
Year of diagnosis	1.64*	(1.13, 2.15)
Race & Year of diagnosis interaction	-0.40	(-0.94, 0.15)

Table 2.11 Mean survival months by T stage of IBC patients. Using Cox Model Adjusted for Age and Race (95% CI). Significance (*) relative to Any T, Mets, determined by non-overlapping 95% CI.

	Mean Survival Time (Months)		
Year	T4D	Other T	Any T, Mets
1988-1992	75.5* (69.7, 81.4)	70.4* (51.9, 88.8)	29.6 (24.0, 35.2)
1993-1997	82.9* (78.1, 87.6)	78.0* (60.0, 96.0)	36.4 (29.9, 42.9)
1998-2002	91.3* (87.7, 94.9)	89.9* (69.7, 110.0)	37.9 (32.6, 43.1)
2003-2007	101.6* (97.9, 105.4)	102.6* (99.2, 105.9)	42.5 (40.0, 44.9)
2008-2012	108.2* (103.8, 112.6)	98.9* (94.7, 103.1)	62.4 (58.0, 66.7)

Table 2.12 Mean survival months by race and T stage of IBC patients. Cox Model Adjusted for Age and Race (95% CI). Significance (*) relative to white patients, determined by non-overlapping 95% CI.

	Mean Survival Time (Months)					
	African American			White		
Year	T4D	Other T	Any T, Mets	T4D	Other T	Any T, Mets
1988-1992	49.8* (38.9, 60.6)	56.2 (16.8, 95.7)	19.2 (12.6, 25.8)	78.4 (71.8, 85.0)	74.7 (52.9, 96.6)	31.4 (24.5, 38.3)
1993-1997	61.5* (49.3, 73.7)	55.4 (20.6, 90.2)	32.8 (19.0, 46.5)	84.0 (78.8, 89.2)	80.5 (60.5, 100.6)	36.5 (29.1, 43.9)
1998-2002	64.0* (56.3, 71.8)	78.7 (37.9, 119.5)	28.3 (22.9, 33.8)	95.8 (91.7, 99.9)	94.6 (71.0, 118.3)	40.3 (33.6, 37.0)
2003-2007	78.7* (70.2, 87.2)	86.2* (78.0, 94.4)	34.4* (30.1, 38.7)	105.4 (101.0, 109.7)	103.7 (99.7, 107.6)	43.4 (40.5, 46.3)
2008-2012	94.9 (84.6, 105.2)	92.1 (82.0, 102.2)	52.3 (45.2, 59.5)	109.9 (104.5, 115.2)	98.8 (93.5, 104.0)	63.9 (58.2, 69.7)

REFERENCES

1. van Uden DJP, van Laarhoven HWM, Westenberg AH, de Wilt JHW, Blanken-Peeters CFJM. Inflammatory breast cancer: An overview. *Crit Rev Oncol Hematol*. 2015. doi:10.1016/j.critrevonc.2014.09.003
2. Chang S, Parker SL, Pham T, Buzdar AU, Hursting SD. Inflammatory breast carcinoma incidence and survival: The Surveillance, Epidemiology, and End Results program of the National Cancer Institute, 1975- 1992. *Cancer*. 1998. doi:10.1002/(SICI)1097-0142(19980615)82:12<2366::AID-CNCR10>3.0.CO;2-N
3. Hance KW, Anderson WF, Devesa SS, Young HA, Levine PH. Trends in inflammatory breast carcinoma incidence and survival: The surveillance, epidemiology, and end results program at the National Cancer Institute. *J Natl Cancer Inst*. 2005. doi:10.1093/jnci/dji172
4. Schlichting JA, Soliman AS, Schairer C, Schottenfeld D, Merajver SD. Inflammatory and non-inflammatory breast cancer survival by socioeconomic position in the Surveillance, Epidemiology, and End Results database, 1990-2008. *Breast Cancer Res Treat*. 2012. doi:10.1007/s10549-012-2133-2
5. Schinkel JK, Zahm SH, Jatoi I, et al. Racial/ethnic differences in breast cancer survival by inflammatory status and hormonal receptor status: An analysis of the Surveillance, Epidemiology, and End Results data. *Cancer Causes Control*. 2014. doi:10.1007/s10552-014-0395-1
6. Li J, Xia Y, Wu Q, et al. Outcomes of patients with inflammatory breast cancer by hormone receptor- and HER2-defined molecular subtypes: A population-based study from the SEER program. *Oncotarget*. 2017. doi:10.18632/oncotarget.17217
7. Goldner B, Behrendt CE, Schoellhammer HF, Lee B, Chen SL. Incidence of inflammatory breast cancer in women, 1992-2009, United States. *Ann Surg Oncol*. 2014. doi:10.1245/s10434-013-3439-y
8. Il'yasova D, Siamakpour-Reihani S, Akushevich I, Akushevich L, Spector N, Schildkraut J. What can we learn from the age- and race/ethnicity- specific rates of inflammatory breast carcinoma? *Breast Cancer Res Treat*. 2011. doi:10.1007/s10549-011-1719-4
9. Levine PH, Steinhorn SC, Ries LG, Aron JL. Inflammatory Breast Cancer: The Experience of the Surveillance, Epidemiology, and End Results (SEER) Program. *JNCI J Natl Cancer Inst*. 1985. doi:10.1093/jnci/74.2.291
10. Dawood S, Merajver SD, Viens P, et al. International expert panel on inflammatory breast cancer: Consensus statement for standardized diagnosis and treatment. *Ann Oncol*. 2011. doi:10.1093/annonc/mdq345
11. Tiwari RC, Clegg LX, Zou Z. Efficient interval estimation for age-adjusted cancer rates. *Stat Methods Med Res*. 2006. doi:10.1177/0962280206070621
12. Aurit SJ, Devesa SS, Soliman AS, Schairer C. Inflammatory and other breast cancer incidence rate trends by estrogen receptor status in the Surveillance, Epidemiology, and End Results database (2001–2015). *Breast Cancer Res Treat*. 2019. doi:10.1007/s10549-019-05193-0
13. Kaye DH, Freedman D a. Reference Guide on Statistics. *Ref Man Sci Evid*. 2011.
14. Ederer F, Heise H. *Instructions to IBM 650 Programmers in Processing Survival Computations. Methodological Note No.10. End Results Evaluation Section.* Bethesda, MD; 1959.

15. Greenwood M. A Report on the Natural Duration of Cancer. Reports on Public Health and Medical Subjects. Ministry of Health. *London H M S O*. 1926.
16. Brenner H, Gefeller O. An alternative approach to monitoring cancer patient survival. *Cancer*. 1996. doi:10.1002/(SICI)1097-0142(19961101)78:9<2004::AID-CNCR23>3.0.CO;2-#
17. Efron B. Bootstrap Methods: Another Look at the Jackknife. *Ann Stat*. 1979. doi:10.1214/aos/1176344552
18. Hirko KA, Soliman AS, Banerjee M, et al. A comparison of criteria to identify inflammatory breast cancer cases from medical records and the surveillance, epidemiology and end results data base, 2007-2009. *Breast J*. 2014. doi:10.1111/tbj.12234
19. Levine PH, Zolfaghari L, Young H, et al. What is inflammatory breast cancer? revisiting the case definition. *Cancers (Basel)*. 2010. doi:10.3390/cancers2010143
20. Noone A, Howlader N, Krapcho M, et al. SEER Cancer Statistics Review, 1975-2015. National Cancer Institute. Bethesda, MD.
21. DeSantis C, Miller K, Sauer AG, Jemal A, Siegel R. Cancer statistics for African Americans, 2019. *CA Cancer J Clin*. 2019;69(3):211-233. doi:https://doi.org/10.3322/caac.21555
22. DeSantis CE, Fedewa SA, Goding Sauer A, Kramer JL, Smith RA, Jemal A. Breast cancer statistics, 2015: Convergence of incidence rates between black and white women. *CA Cancer J Clin*. 2016. doi:10.3322/caac.21320

Chapter 3 : RhoC Modulates Cell Junctions and Type I Interferon Response in Aggressive Breast Cancers[2]

SUMMARY

Metastases are the leading cause of death in cancer patients. RhoC, a member of the Rho GTPase family, has been shown to facilitate metastasis of aggressive breast cancer cells by influencing motility, invasion, and chemokine secretion, but as yet there is no integrated model of the precise mechanism of how RhoC promotes metastasis. A common phenotypic characteristic of metastatic cells influenced by these mechanisms is dysregulation of cell-cell junctions. Thus, we set out to study how RhoA- and RhoC-GTPase influence the cell-cell junctions in aggressive breast cancers. We demonstrate that CRISPR-Cas9 knockout of RhoC in SUM 149 and MDA 231 breast cancer cells results in increased junction protein expression and colocalization at cell membranes. In functional assessments of junction stability, RhoC knockout cells have increased barrier integrity and increased cell-cell adhesion compared to wild-type cells. Whole exome RNA sequencing and targeted gene expression profiling demonstrate decreased expression of Type I interferon-stimulated genes in RhoC knockout cells compared to wild-type. Treatment of wild-type cells with interferon-alpha resulted in significant increases in

---

[2] Hannah G. Abraham[1], Peter J. Ulintz[1,2], Laura Goo[1], Joel A. Yates[1], Andrew C. Little[1,3], Li Wei Bao[1], Zhifen Wu[1], Sofia D. Merajver[1]. RhoC modulates cell junctions and Type I interferon response in aggressive breast cancers. (2021) *Manuscript submitted for publication*.
[1]Department of Internal Medicine, University of Michigan, Ann Arbor, MI, USA
[2]Now at Diamond Age Data Science, Somerville, MA, USA
[3]Now at Boehringer Ingelheim Oncology, Ridgefield, CT, USA

adhesion and decreases in invasiveness, whereas RhoC knockout cells exhibited a dampened response to interferon-alpha stimulation with respect to adhesion and invasiveness. We delineate a key role of RhoC-GTPase in modulation of cell-cell junctions and response to interferon, which supports inhibition of RhoC as a potential anti-invasion therapeutic strategy.

INTRODUCTION

Cancer metastases are the leading cause of death in cancer patients, and yet details of the cellular processes that drive the early metastases in aggressive cancers are not fully understood. RhoC, a member of the Rho GTPase family, has been linked to the metastatic potential of a variety of cancers including inflammatory breast cancer, pancreatic cancer, and melanoma[1–5]. In breast cancer, RhoC expression correlates with increasing breast cancer stage and grade (as a histologic surrogate for aggressiveness), and higher RhoC expression was associated with higher patient mortality in a cohort of 280 breast cancer patients[6]. Moreover, in this cohort high RhoC expression was a predictor of poor response to standard chemotherapy regimens, increasing the likelihood that patients would experience metastasis and relapse[6]. RhoC is overexpressed in the majority of cases of inflammatory breast cancer, the most aggressive and metastatic form of breast cancer[7]. Animal and *in vitro* studies demonstrated that RhoC is necessary specifically for facilitating metastasis[8], primarily through protecting metastatic cells from apoptosis, modulating cell motility, and influencing chemokine secretion [8,9].

These studies led us to postulate that a possible cellular effect of RhoC-driven metastatic progression is through modulation of cell junctions that would facilitate increased cellular motility. The Rho family GTPases regulate actin cytoskeleton organization[10], and thereby interact directly or indirectly with components of adherens junctions (AJs) and tight junctions

(TJs)[11]. RhoA, whose amino acid sequence is 90% homologous to RhoC[12], specifically is important for both the initial formation and the structural maintenance of AJs and TJs[13]. Indeed, studies using both dominant negative and constitutively active forms of RhoA result in AJ and TJ instability[13,14], suggesting that the stability of epithelial junctions is dependent on balanced activation of Rho GTPases.

When considering pathological settings of junction instability, the metastatic process itself is a prime example. Multiple studies of diverse cancer types demonstrate a loss of junction markers in malignant vs normal tissue; however, these studies differ on the prognostic value derived from the loss or dysregulation of junction components [15,16]. In a study of colorectal cancers, decreased E-cadherin (AJ transmembrane protein) and ZO-1 (TJ cytoplasmic linker protein) expression in primary tumors predicted which tumors went on to have liver metastases[17]. In addition to the observed dysregulation of cell-cell junctions in the metastatic process, junction proteins are also known to be downregulated in settings of increased inflammatory interferon signaling[18,19]. Treating cells with interferon-alpha (IFN-α) leads to increased RhoA activation[20,21]. Furthermore, breast cancer tumors with high interferon signaling pathway expression are nearly twice as likely to metastasize compared to tumors with low levels of expression[22].

This study aims to investigate the role of RhoC in regulating cell-cell junction stability and interferon signaling in aggressive breast cancer cell lines. We assess the hypothesis that RhoC amplifies interferon signaling and thereby increases junction dysregulation, consequently promoting cancer cells' motility and invasiveness. This work supports inhibition of RhoC as a potential therapeutic strategy in aggressive cancers.

MATERIALS AND METHODS

Cell Culture and Reagents

MDA-MB 231 (MDA 231) cells were acquired from ATCC and maintained in Gibco RPMI-1640 (+) L-glutamine, 10% fetal bovine serum (FBS), 5 μg/mL gentamycin, and 1X anti-anti. VARI068 cells, sourced from a patient-derived xenograft[23], were maintained the same way. SUM 149 cells and SUM 190 cells were provided by Dr. Steve Ethier and were maintained in Gibco Ham's F12 (+) L-glutamine, 0.5% penicillin-streptomycin, 2.5 μg/mL Amphotericin B, 5 μg/mL gentamycin, 5 μg/mL insulin, and 1 μg/mL hydrocortisone. SUM 149 cells were additionally supplemented with 5% FBS, while SUM 190 cells were supplemented with 0.1% bovine serum albumin. MCF7 cells were acquired from ATCC and maintained in DMEM, 10% FBS, 5 μg/mL gentamycin, and 1X anti-anti. MCF10A cells were acquired from ATCC and maintained in 50:50 DMEM:F12, 5% horse serum, 10 μg/mL insulin, 0.02 μg/mL epidermal growth factor, 0.5 μg/mL hydrocortisone, 0.1 μg/mL cholera toxin, 5 μg/mL gentamycin, and 1X anti-anti. All cells were maintained at 5% CO_2, except for SUM 149 and SUM 190 which were maintained at 10% CO_2. Interferon-alpha 2a (IFN-α) was obtained from GenScript (# Z03003-1), reconstituted in ddH_2O, and used to treat cells at either 100 IU/ml or 1000 IU/ml.

Generation of CRISPR-Cas9 Knockout Cells

As described in Allen et al[24], SUM 149, MDA 231, VARI068, MCF7, MCF10A, and SUM 190 cells were transfected with pSpCas9(BB)-2A-GFP (PX458), provided by Feng Zhang (Addgene plasmid # 48138), containing the sequence GCCCTGATAGTTTAGGTGAG targeting RhoA for RhoA knockout lines or the sequence AGGAAGACTATGATCGACTG targeting RhoC for the RhoC knockout lines. Transfection was accomplished using the Nucleofactor II

system (Lonza). 48 hours post-transfection, single cells were sorted by GFP expression and seeded into 96-well plates, and clonal expansion was carried out. Genomic DNA was then harvested from clones and screened for RhoA or RhoC mutations via SURVEYOR reactions (IDT) with the primer pair Forward-GTTTTAGACCGTCTGCCATTTC and Reverse-AATCTCCACCTACCAGGTTCAA for RhoA and Forward-CTGTCTTTGCTTCATTCTCCCT and Reverse-CCAGAGCAGTCTTAGAAGCCAT for RhoC. Clones that screened positive were subsequently sequenced to characterize their RhoA or RhoC mutations and were also immunoblotted for RhoA and RhoC.

Antibodies

The following primary antibodies were used: anti-E-cadherin rabbit polyclonal antibody (ThermoFisher #PA5-32178) at 1:500 dilution, anti-β-catenin mouse monoclonal antibody (Invitrogen #MA1-300) at 1:500 dilution, anti-ZO-1 mouse monoclonal antibody (Invitrogen #33-9100) at 1:150 dilution for immunofluorescent staining and 1:200 for Western Blot, anti-Occludin rabbit polyclonal antibody (Zymed #71-1500) at 1:300 dilution for immunofluorescent staining and Western Blot, anti-p-STAT1 rabbit monoclonal antibody (CST #9167) at 1:1000 dilution, anti-STAT1 rabbit monoclonal antibody (CST #9172) at 1:1000 dilution, anti-p-STAT2 rabbit antibody (CST #4441) at 1:500 dilution, anti-STAT2 rabbit antibody (CST #4594) at 1:500 dilution, anti-IRF9 rabbit monoclonal antibody (CST #76684) at 1:500 dilution, anti-IFI27 rabbit polyclonal antibody (ThermoFisher #PA5-68038) at 1:1000 dilution, anti-IFITM1 mouse monoclonal antibody (Proteintech #60074-1-IG) at 1:20,000 dilution, anti-MX1 rabbit polyclonal antibody (Proteintech #13750-1-AP) at 1:1000, anti-ISG15 rabbit polyclonal antibody (Proteintech #15981-1-AP) at 1:1000, and anti-actin antibody (Sigma #A3854) at 1:15,000 dilution. The following secondary antibodies were used: Alexa Fluor 488-conjugated anti-mouse

secondary antibody (Molecular Probes) at 1:1000 for immunofluorescent staining, Alexa Fluor 647-conjugated anti-rabbit secondary antibody (Molecular Probes) at 1:1000 for immunofluorescent staining, HRP-conjugated anti-mouse secondary antibody (Santa Cruz) at 1:4000 for Western Blot, and HRP-conjugated anti-rabbit secondary antibody (CST) at 1:2500 for Western Blot.

Immunofluorescent Staining

Cells were seeded on 4-well chamber slides and grown to a confluent monolayer. Slides were fixed in 4% paraformaldehyde for 10 minutes at room temperature, washed with 100 mM PBS-glycine for 10 minutes at room temperature, then permeabilized in 0.1% Triton X-100 in PBS for 10 minutes at 4°C. Samples were washed thrice with 100mM PBS-glycine, then incubated in blocking solution containing IF Buffer (0.2% Triton X-100, 0.05% Tween-20, 0.1% BSA, 7.7mM NaN_3 in PBS) and 10% goat serum for 1.5 hr at room temperature. Subsequently, samples were incubated in a primary antibody solution overnight at 4°C. The samples were then washed four times in IF Buffer for 15 minutes each at room temperature, then incubated in a secondary antibody solution (all secondary antibodies used at 1:1000 dilution), followed by one wash with IF Buffer for 20 minutes and two washes with PBS for 10 minutes each, at room temperature. Slides were mounted in Prolonged Gold Antifade reagent with DAPI (4′,6-diamidino-2-phenylindole) for nuclear counterstaining (Molecular Probes). Images were acquired on a Nikon A1B confocal microscope at 40X magnification.

Western Blot

Protein lysates were mixed with loading dye and boiled at 95°C, then loaded into a 4-15% polyacrylamide gel and run at 130-160 V for about 90 minutes. For blotting proteins smaller than 90 kDa, gel was subsequently removed from chamber and soaked in 20% methanol at RT for 5 minutes, then transferred to a PVDF membrane using the iBlot 2 Dry Blotting System. For proteins larger than 90 kDA, gel was removed from chamber and soaked in 20% methanol transfer buffer for 5 minutes, then transferred to a PVDF membrane using a BioRad Wet Transfer chamber running at 80 V for 75 minutes. After transfer, the membrane was blocked in 5% milk/TBST at RT for 1 hr, rinsed with TBST thrice for 5 minutes each, then incubated in primary antibody solution at 4°C overnight on shaker. The next day, the membrane was again rinsed with TBST, then incubated in secondary antibody solution (in 5% milk-TBST) at RT for 1 hr. Once again, the membrane was rinsed with TBST, and then incubated in developing reagent at RT for 2 minutes. Finally the membrane was placed in a chemilluminescence reader and the blot was recorded.

FITC-Dextran Assay

Cells were seeded into Transwell plates and grown for 36 hours, until they reached confluency. FITC-Dextran solution was prepared at 1mg/ml, and 0.5ml of this solution was added to the apical chambers of the Transwells, with normal media in the basal chambers. After 24 hours, 50ul was removed from the basal chambers and transferred to a 96-well plate, then fluorescence was measured in a fluorescent plate reader. The ratio of fluorescence from the apical chamber to the basal chamber was recorded.

Centrifugation Adhesion Assay

Adapted from Weetall et al[25]. V-bottom 96-well plates were seeded with 2 x 10^4 cells/well and left in 37°C overnight. Calcein-AM-labeled cells (2uM Calcein-DMSO solution, Invitrogen #C3100MP) were subsequently seeded at 1.5 x 10^4 cells/well to the plate (negative control: wells with overnight-seeded cells but no Calcein-labeled cells; positive control: empty wells with Calcein-labeled cells added). Plates were incubated at 37°C for 2 hours, then centrifuged at 75 g for 10 minutes. Nonadherent cells accumulated at the bottom of the wells and fluorescence at the bottom of the well was quantified. Log fold change in fluorescence between test wells and positive control wells was recorded. Assay was repeated with media containing 100 IU/ml IFN-α; overnight-seeded cells were treated with IFN-α for 48 hours prior to seeding in v-bottom plates, then were seeded in media with IFN-α for 24 hours, while Calcein-labeled cells were treated with IFN-α for 72 hours prior to Calcein labeling, seeding, and incubation in v-bottom plate for 2 hours (they were also seeded in media containing IFN-α).

siRNA Knockdown of Junction Proteins

siTJP1 (ZO-1) and non-targeting control siRNA were ordered from Dharmacon (siTJP1 5 nmol #L-0077-46-00-0005) and transfected in SUM 149s using 5.2 µl DharmaFECT 2/well in 6-well plates, while in MDA 231s transfection used 2 µl DharmaFECT 4/well in 6-well plates (Dharmacon). Protein was harvested from cells 2-5 days after transfection and immunoblotted for ZO-1 to confirm transient knockdown.

Transwell Invasion Assay

100,000 cells/well were seeded into Matrigel Transwell Invasion chambers (Corning #354480) in serum-free media, with serum-containing media in bottom chambers. Cells were incubated at 37°C for 24 hours, then the top chambers were scrubbed to remove cells that had not invaded. Chambers were then fixed in 70% ethanol for 10 minutes, stained in 0.2% Crystal Violet for 10 minutes, and left to dry overnight. Brightfield images of each insert were acquired at 2X magnification on an Olympus IX51, and the ImageJ Color Inspector 3D plugin was used to quantify the percent coverage of purple pixels per insert image. Assays were performed in technical triplicate and biological triplicate. Multiple comparisons ANOVA was conducted on the data in GraphPad Prism 9. For assays with siRNA-treated cells, cells were seeded into chambers 48 hours post-transfection. For assays with IFN-α-treated cells, cells were seeded into chambers either with no prior IFN-α treatment or with 48 hours pre-treatment with IFN-α, and were seeded in serum-free media containing 100 IU/ml of IFN-α.

RNAseq

Four biological replicates of SUM 149, MDA 231, VARI068, MCF7, MCF10A, and SUM 190 cells, wild-type and RhoC knockouts, were incubated at 37°C overnight. Normal growth media for each cell line was replaced with DMEM for 24 hrs, and RNA was harvested. RNA was sequenced via the Illumina HiSeq 4000 as paired 51bp reads to a targeted depth of 75M paired reads per sample. Read data in FASTQ format were quality assessed with FastQC/MultiQC (v.0.11.3) and contamination checked with fastq_screen (v.0.11.1). Reads were adapter-trimmed using CutAdapt (v.1.8.1) and aligned to the GRCh37 hg19 human genome using Tophat/Bowtie2 (v.2.0.13/v.2.2.1, options –b2_very_sensitive and the default max intron

length of 500000). Raw read counts were extracted for each gene using HTSeq (v.0.6.0). DESeq2 (v1.14.1), run within the R (v.3.3.3) Bioconductor package (Biobase v.2.34) was used to model differential expression in genes between modeled conditions. The main factors used in the model were cell line and CRISPR knockout status (cRhoC or WT). DESeq2 utilizes generalized linear models for each gene and infers a log2 fold change between conditions using maximum likelihood estimation and (by default) a Wald test for significance. Default parameters for DESeq2 were used, specifying a standardized normal prior on the non-intercept coefficients (betaPrior=TRUE). QC plotting was performed in R using ggplot. Genes were annotated with NCBI Entrez GeneIDs and text descriptions.

In the crRhoC vs WT dataset, 1293 differentially expressed genes were identified out of a total of 20,978 with detected expression based on an adjusted p-value threshold of 0.05 and a minimum absolute log2 fold change of 0.585. Gene set enrichment was performed on these data using the commercial iPathwayGuide software (Advaita Bioinformatics, Ann Arbor, MI). iPathwayGuide (iPG) scores pathways using a custom enrichment method[26–28] that is composed of two primary sub-methods: i) the over-representation of differentially expressed (DE) genes in a given pathway, and ii) the perturbation of that pathway computed by propagating the measured expression changes across the pathway topology. These two sub-methods each produce p-values (pORA and pAcc, respectively) that are combined using Fisher's method into a pathway-specific p-value, which is then corrected for multiple comparisons using an FDR correction. The tool searched KEGG pathways (Release 90.0+/05-29, May 19) utilizing directional information in gene-relationships[29]. An enrichment against GO terms[30,31] was also performed, utilizing the ORA method (i) above.

In addition to classic enrichment, a prediction of upstream regulators was also performed by iPG based on the differentially expressed gene set and a network of regulatory (activation/inhibition) interactions from a proprietary knowledge base compiled from StringDB[32] (Version 11.0. Jan 19th, 2019) and BioGrid[33] (v3.5.171. March 25th, 2019) data. The activation/inhibition network is polled using gene expression information to consider hypotheses that upstream regulators of genes are either activated or inhibited. A z-score for each upstream regulator is computed by iterating over connected downstream genes and their incoming edges, as well as a p-value corresponding to the z-score as the one-tailed area under the probability density function for a normal distribution, N(0,1). An over-representation approach is also used to compute the statistical significance of observing at least a given number of consistent DE genes, with an associated p-value computed using the hypergeometric distribution[34]. Finally, these two p-values are combined using the Fisher's method to rank the upstream regulators and test the hypothesis that the upstream regulators are predicted as activated or inhibited in the experimental condition (crRhoC vs WT).

Targeted Gene Expression Profiling

Three biological replicates of MDA 231 and SUM 149 wild-type, RhoA knockout, and RhoC knockout cells were treated with 100 IU/ml IFN-α for 72 hours, then RNA was harvested and run on nanoString Pan Cancer Immune Profiling panels (nanoString Technologies, Inc.). The expression of 730 immune-related genes and 40 housekeeping genes was measured, and the nSolver 4.0 software (nanoString Technologies, Inc.) was used to normalize expression values and conduct differential expression analysis. Genes were considered differentially expressed between treated and untreated cells if they had FDR-adjusted p-value < 0.05. To compare the

change in expression with IFN-α treatment in wild-type, RhoA knockout, and RhoC knockout cells, p-values were calculated as per Kaye et al[35].

RESULTS

Loss of RhoA and RhoC Expression in Breast Cancer Cells Results in Significant Morphological Changes

In order to investigate the effect of RhoC expression on cell-cell junctions, we created MDA 231 and SUM 149 cell lines where RhoA and RhoC had been independently knocked-out via CRISPR-Cas9 (cell lines denoted crRhoA and crRhoC, respectively). Both the MDA 231 and SUM 149 cell lines are triple-negative breast cancer cells with high expression of RhoC in wild-type cells; SUM 149 is an inflammatory breast cancer cell line, while MDA 231 is a non-inflammatory breast cancer cell line. We found that the crRhoC cells exhibited compensatory increases in RhoA expression (**Figure 3.1A**). Furthermore, the crRhoA cells assumed a more spindlelike shape compared to their wild-type counterparts, and the crRhoC cells were more cuboidal compared to wild-type (**Figure 3.1B**).

RhoA and RhoC Expression Modulate Junctional Protein Expression and Colocalization

We sought to characterize the role of RhoC and RhoA in epithelial junctions in these breast cancer cell lines. We first assessed total protein levels of key cell-cell junctions proteins: the tight junction proteins ZO-1 and Occludin, and the adherens junction proteins E-cadherin and β-catenin. We found that crRhoA cells demonstrated a trend towards decreased expression of junction proteins as compared to wild-type via Western Blot. In contrast, crRhoC cells exhibited a trend towards increased junction protein expression compared to wild-type (**Figure 3.2**). Out of

the four junction proteins, this pattern of Rho-modulated expression was most evident in ZO-1, both in SUM 149 and in MDA 231 cells. Immunofluorescent staining for junction proteins (**Figure 3.3A**) highlighted an increase in the amount of junction proteins localizing to areas of cell-cell contact in the crRhoC cells, as well as increased colocalization of junction markers in crRhoC cells. Moreover, the SUM 149 crRhoA cells consistently assembled in loose or disordered clusters, characterized by variable spaces between cells, and had decreased tight junctions and cell-cell projections compared to both wild-type and crRhoC cells (**Figure 3.3B,C**).

RhoA and RhoC Expression Modulate Cell-Cell Adhesion and Barrier Function

Having observed a qualitative change in junction protein expression and localization, we sought to determine whether this change translated into functional differences in adhesion between wild-type and crRhoC cells. We measured cell-cell adhesion using a fluorometric centrifugation assay, wherein fluorescently-labeled cells were added to wells with previously-seeded cells of the same type, incubated for 2 hours, and then subjected to centrifugal shear stress in order to measure the perturbation of adhesion between different cell types. Positive controls for the assay were wells containing only fluorescently-labeled cells. Both crRhoC SUM 149 and crRhoC MDA 231 cells had a greater reduction in fluorescent signal compared to their positive controls than did wild-type cells, suggesting a functionally stronger cell-cell adhesion when RhoC is knocked out (**Figure 3.4A**). To further assess the functional significance of the junction changes induced by reducing RhoA and RhoC expression, we undertook a FITC-Dextran barrier integrity assay to determine the effectiveness of the tight junctions in these cells. In both crRhoC SUM 149 and crRhoC MDA 231 cells, there was a significant increase in the barrier integrity of the cell monolayer compared to wild-type, and in crRhoA SUM 149 and

crRhoA MDA 231 there was a significant decrease in the barrier integrity of the cell monolayer compared to wild-type (**Figure 3.4B**). These changes imply that barrier integrity increases with RhoC knockout, and decreases with RhoA knockout, which is consistent with the changes in tight junction protein colocalization observed via immunofluorescent staining.

RhoC Expression Increases Cell Invasion, But ZO-1 Knockdown Does Not Rescue Invasion in crRhoC Cells

To investigate whether RhoA and RhoC expression affect the invasive potential of breast cancer cells, we conducted transwell invasion assays. Compared to wild-type and crRhoA cells, crRhoC cells had significantly less transwell invasion (**Figure 3.5A**). To assess whether RhoC's effect on cell invasion is facilitated by RhoC's effect on junction protein expression, we decided to test whether transiently modulating expression of ZO-1 would contribute to invasive capability. Cells were treated with ZO-1 siRNA or scrambled control siRNA for 72 hrs to achieve transient ZO-1 knockdown (**Figure 3.5B**), following which transwell invasion was assessed. ZO-1 knockdown did not significantly change invasiveness in wild-type, crRhoA, or crRhoC cells (**Figure 3.5C,D**).

crRhoC Cells Have Altered Interferon-α Signaling Compared to Wild-type

Seeking to understand the molecular mechanisms of Rho-driven junction regulation, we conducted whole transcriptome RNAseq analysis of SUM 149, MDA 231, VARI068, MCF7, MCF10A, and SUM 190 wild-type and crRhoC cells, using six cell lines in order to increase our analytical power. Analysis detected 1,293 genes differentially expressed between crRhoC cells and wild-type at an adjusted p-value of 0.05 and a minimum log2 fold change threshold of 0.585. A number of interferon-stimulated genes (ISGs) had significantly decreased expression in

crRhoC cells compared to wild-type, and many of these genes were downstream of IRF9 and STAT2, resulting in IRF9 and STAT2 as the predicted most significantly inhibited regulators in crRhoC cells compared to wild-type (**Table 3.1**), with 17 consistent genes each listed as inhibited (out of a total of 38 and 43 target genes, p-values 7.9e-11 and 3.9e-10, respectively) (**Figure 3.6A, Table 3.2**). The expression of IRF9 and STAT2 themselves were not significantly differentially altered between crRhoC cells and wild-type cells.

As type I interferon signaling is known to influence junction protein expression in a context-dependent manner[18,36], we sought to investigate specifically whether the predicted inhibition of type I interferon signaling in crRhoC cells was borne out at the protein level, and whether any changes in junctional behavior would result. SUM 149 and MDA 231 wild-type, crRhoA, and crRhoC cells were subsequently treated with IFN-α at two doses (100 and 1000 IU/ml) for 2 hours and 72 hours, and expression of proteins in the type I interferon signaling pathway was assessed via Western Blot. In response to interferon treatment, we observed that RhoC modified the cells' responses: MDA 231 crRhoC cells had increased STAT2 and IRF9 expression compared to wild type (**Figure 3.6B,C)**, whereas SUM 149 crRhoC cells had trends towards decreased p-STAT2 and total STAT2 expression compared to wild type (**Figure 3.6D,E**). There were no significant differences between the two doses tested. The difference in interferon response expression between crRhoC and wild-type cells were evident at both the 2 hour and 72 hour time points, consistent with the 17 ISGs identified by RNAseq that are downstream of short-term ISGF3-driven signaling as well as long-term U-ISGF3-driven signaling[37–39] (**Figure 3.7**).

RhoC Modulation of Interferon Signaling Leads to Functional Changes in Junction Behavior and Cell Invasiveness

To assess the impact of RhoA and RhoC expression on long-term ISG expression, SUM 149 and MDA 231 wild-type, crRhoA and crRhoC cells were treated with IFN-α at 100 IU/ml for 72 hours, then RNA was harvested and a relevant array of cancer related genes was assessed by the nanoString Pan-Cancer Immune Panel. Out of the genes that were significantly differentially expressed in treated cells compared to untreated controls, the interferon-stimulated gene IFITM1 had decreased expression in both crRhoA and crRhoC cells compared to wild type, and additional interferon-stimulated genes like MX1 and ISG15 were significantly decreased in only the crRhoC cells compared to wild type. IFI27 was the only interferon-stimulated gene that had significantly increased expression in treated crRhoC cells compared to both treated crRhoA cells and treated wild-type (**Figure 3.8A,B**).

In order to determine whether these differences in mRNA expression between crRhoC cells and wild-type cells were borne out at the protein level, cells were again treated with IFN-α at 100 IU/ml for 72 hours, and protein was harvested for Western Blot of MX1, ISG15, IFITM1 and IFI27 (**Figure 3.8C**). There was no expression of these proteins in the untreated SUM 149 cells, whereas in MDA 231 the untreated cells all expressed ISG15 and the untreated crRhoA and crRhoC cells expressed IFI27, with crRhoC cells expressing the highest amount of these two proteins at baseline. The treated cells all had similar protein expression of MX1, ISG15, and IFI27, with MDA 231 cells having slightly increased protein expression compared to SUM 149 cells. However IFN-α treatment elicited higher IFITM1 protein expression in crRhoC cells than in wild-type. SUM 149 crRhoA cells had decreased expression of IFITM1 with IFN-α treatment

compared to wild-type, whereas MDA 231 crRhoA cells had increased expression of IFITM1 with IFN-α treatment compared to wild-type.

We further sought to assess the impact of RhoA and RhoC expression on functional responses to IFN-α treatment. The centrifugation adhesion assay was repeated with media containing IFN-α at 100 IU/ml. 72 hours of IFN-α treatment increased cell-cell adhesion for all cell types. However, the change in adhesion between untreated and IFN-α treated cells was greater in magnitude in wild-type cells compared to crRhoC cells **(Figure 3.9A, Table 3.3)**. Transwell invasion assays were also repeated with media containing IFN-α at 100 IU/ml, with cells treated for 24 or 72 hours. Cells treated for 72 hours had reduced invasion compared to untreated cells and 24-hour-treated cells. In MDA 231, the magnitude of invasion reduction was greater in wild-type and crRhoA cells compared to crRhoC cells, whereas in SUM 149s the reverse was demonstrated—crRhoC cells had a larger reduction in invasion than wild-type or crRhoA cells (**Figure 3.9B,C, Table 3.4**). There were no significant differences in proliferation or viability between treated and untreated or between wild-type and Rho knockout cells (data not shown).

DISCUSSION

In investigating the cellular and molecular basis of the impact of RhoC on metastasis, we demonstrate that RhoC affects both cell-cell junction behavior as well as IFN-α response. Knocking out RhoC results in a trend towards increased tight and adherens junction protein expression (**Figure 3.2**) and membrane localization (**Figure 3.3**) that resembles normal junctions, while also significantly increasing the functionality of these junctions with respect to adhesiveness and impermeability (**Figure 3.4**). crRhoC cells also exhibit decreased cell invasion

(**Figure 3.5A**). Interestingly, low-dose IFN-α treatment has similar effects on wild-type cells as the effect of RhoC knockout—the increased adhesion and decreased invasion induced by 72 hours of IFN-α treatment in wild-type cells (**Figure 3.9**) is comparable in magnitude to the increased adhesion and decreased invasion seen in crRhoC cells compared to wild-type. crRhoC cells treated with IFN-α exhibit a dampened response in terms of changes in adhesion and invasion, compared to treated wild-type cells, but it is important to highlight that IFN-α does increase adhesion and decrease invasion in both crRhoC and wild-type cells. Taken together, these data point to IFN-α and RhoC inhibition as being capable of reducing cancer cell invasion in a cumulative fashion—a potential combination strategy that could be more effective in RhoC driven phenotypes, such as inflammatory breast cancer, as there was clearly a larger effect on adhesion and invasion in SUM 149 crRhoC cells treated with IFN-α compared to MDA 231 crRhoC cells.

A corollary interpretation of these results is that RhoC knockout blunts cellular response to IFN-α overall. This interpretation is further supported by the smaller increase in expression of interferon-stimulated genes in crRhoC cells post-IFN-α treatment compared to wild-type cells, in which IFN-α treatment robustly increased interferon-stimulated gene expression (**Figure 3.8A**). The potential for RhoC contributing to normal IFN-α signaling is a novel finding. Expression of interferon signaling proteins IFI27 and ISG15 was higher in untreated MDA 231 crRhoC cells than in wild-type, and IFITM1 expression was higher in treated crRhoC cells than in wild-type. Expression of IFI27 in some studies is correlated with decreased proliferation and migration[40,41], and in others with increased tumorigenesis and migration and decreased patient survival[42–44]. ISG15 expression is correlated with increased invasion, induction of M2-like macrophages, and decreased patient survival[45,46]. IFITM1 is also correlated with increased tumorigenesis and

invasion[47]. The increased expression of these invasion-associated proteins and the overall decreased ISG expression in crRhoC cells compared to wild-type, in the context of IFN-α treatment reducing cell invasion without significantly affecting cell viability, adds complexity to the understanding of RhoC as primarily a promoter of metastasis.

Previous studies from our lab have found that macrophage-conditioned media, specifically from M2a macrophages, promotes cancer cell invasion, and that functional RhoC is necessary to achieve the full extent of macrophage-promoted invasion[24,48]. Interestingly, IFN-α treatment has been demonstrated to promote a shift in macrophage polarization from M2 to M1[49,50]. Our current study posits that functional RhoC contributes to increased IFN signaling in cancer cells, which would conflict with the logical conclusion from previous studies that RhoC is positively associated with M2 macrophages and M2 macrophages are negatively associated with IFN-α. Further study is therefore necessary to determine why cells with functional high RhoC expression have reduced junction functionality and increased invasion in the absence of IFN-α, and the opposite effect in the presence of IFN-α.

IFN-α has been recognized as an anti-tumor compound since 1970[51]. High-dose IFN-α (>1000 IU/ml) is FDA-approved as monotherapy for Kaposi's sarcoma, follicular non-Hodgkin lymphoma, melanoma, and hairy-cell leukemia, and for adjuvant therapy of melanoma; overall clinical response rates are modest, and high-dose IFN-α toxicity is high, thus oncological use has diminished in recent times[52]. On the other hand, IFN-α is also used clinically as an anti-viral agent, and achieves sustained anti-virologic responses for significant populations of Hepatitis B and C patients[53]. Some of the variation in clinical efficacy of IFN-α can be attributed to differing ISG induction at differing concentrations of IFN-α; low-dose IFN- α tends to induce anti-viral ISGs, whereas high-dose induces proliferation and inflammation-related ISGs[54]. Our findings

that low-dose IFN-α modulates breast cancer invasion and adhesion is notable in that it posits a potential anti-tumor clinical benefit through multiple mechanisms of action, without the morbidity of high-dose treatment.

Higher ISG expression is associated with estrogen receptor negative breast cancers[22]. The cell lines we focused on in this study are both triple-negative breast cancers, and the RNAseq results of decreased ISG expression in RhoC knockout cells compared to wild-type were more significant in our triple-negative breast cancer cell lines than in other breast cancer cell lines (**Table 3.1**). A recent study by Doherty, et. al.[42] also examined the effect of low-dose IFN-α on triple-negative breast cancer and found that chronic, weeks-long exposure to low-dose IFN-α led to increased epithelial morphology, decreased stemness markers, and decreased migration[55]. This is consistent with our results of decreased invasion with 3 days of low-dose IFN-α treatment, and comparable to our results of both increased epithelial morphology and decreased invasion in RhoC knockout cells compared to wild-type. Previous work from our lab has identified RhoC as a modulator of stemness markers in breast cancer cells, and moreover identified RhoC as necessary for lung metastasis from orthotopic xenografts while increased stemness markers modulated the number of metastases[56]. This study suggests that these previously discovered links to epithelial character, stemness and invasion in both IFN-α and RhoC may be, at least in part, related to RhoC's contribution to IFN response.

Our overall hypothesis—that RhoC amplifies interferon signaling and thereby increases junction dysregulation, consequently promoting cancer cells' motility and invasiveness—is borne out insofar as RhoC contributes to Type I interferon cellular response and also contributes to regulation of junction behavior. However, we find that IFN-α signaling itself results in increased cell-cell adhesion and decreased invasion. Our current work supports that the role of

RhoC in metastases of certain aggressive cancers appears to be a result of intrinsic modulation of the cancer cells' junctions and invasiveness, and potential amplification of interferon signaling; other effects on the tumor microenvironment, such as a shift in macrophage population abundance, may cooperate to produce highly aggressive phenotypes. As such, via multiple mechanisms, our data indicate that the inhibition of RhoC in aggressive breast cancers could provide anti-invasion therapeutic benefit.

FIGURES

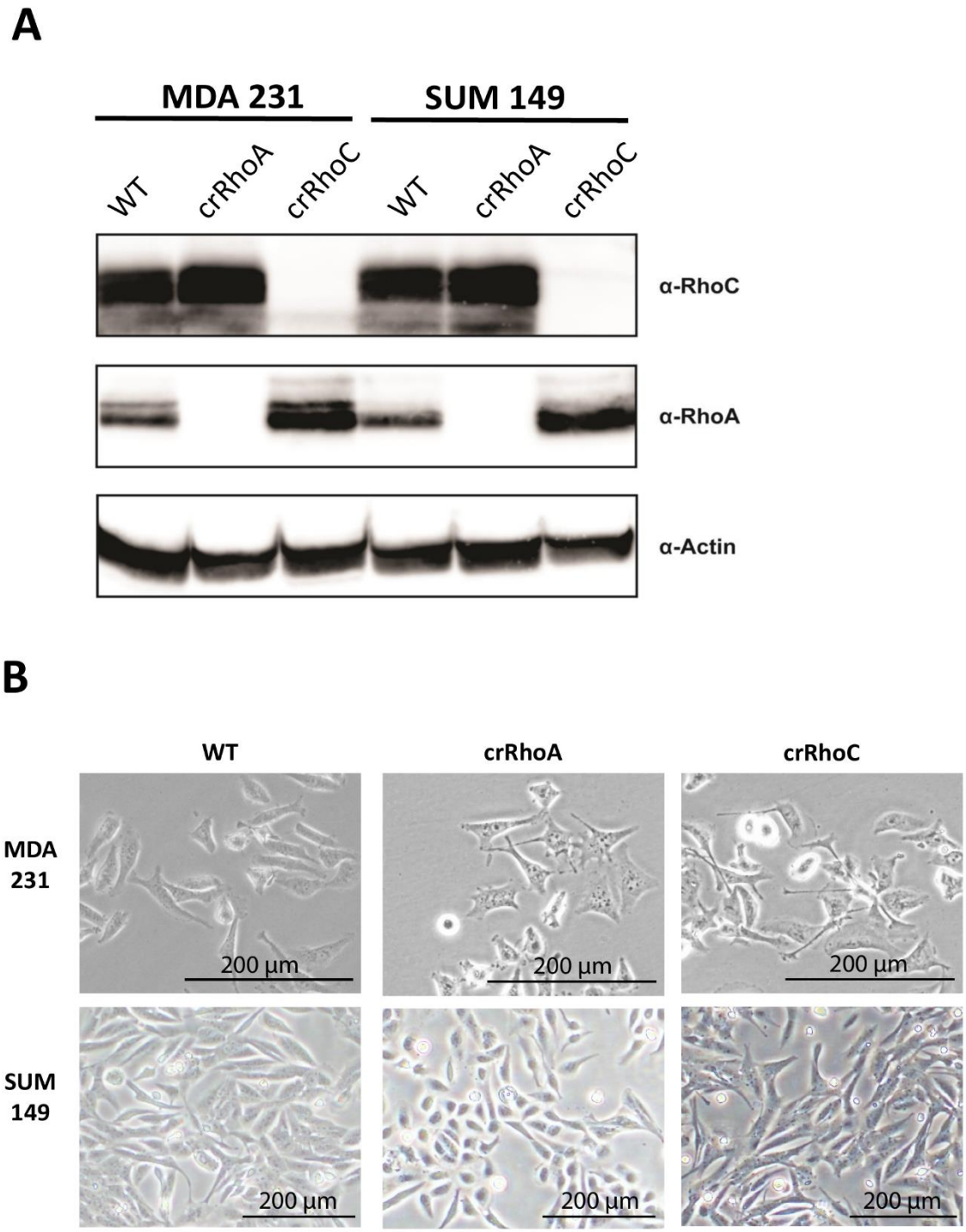

Figure 3.1 Rho knockout changes expression and morphology of cells. (A) Validation of CRISPR-Cas9 knockout of RhoA and RhoC via Western Blot. **(B)** Brightfield images of wild-type, crRhoA, and crRhoC cells. RhoA knockout markedly changes the morphology of both MDA 231 and SUM 149 cells, leading to a consistent "triangle" shape in the MDA 231s and a rounded shape in the SUM 149s. RhoC

knockout changes cell morphology more subtly, leading to a consistent “crescent” shape in the MDA 231s and a more cuboidal shape in the SUM 149s. Scale bars = 200μm.

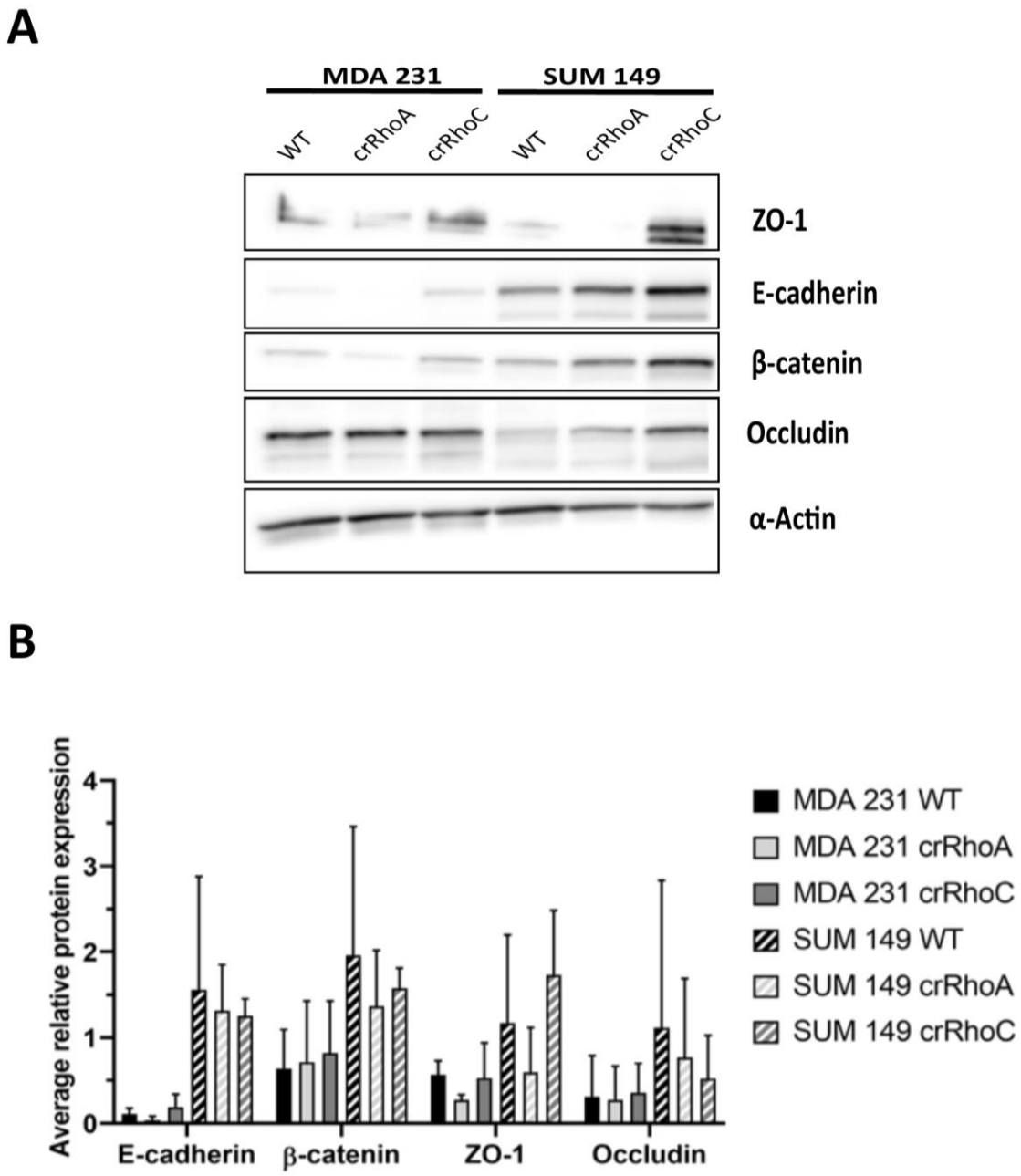

Figure 3.2 Rho knockout changes junction marker expression. (A) Representative Western blot of junction protein expression in wild-type, crRhoA, and crRhoC cells. crRhoC cells trended towards increased expression of junction markers, most notably ZO-1. **(B)** Quantification of Western blots of three biological replicates. No changes in junction expression reached significance. Solid bars are MDA 231, striped bars are SUM 149; black bars are wild-type, light grey bars are crRhoA cells, and dark grey bars are crRhoC cells.

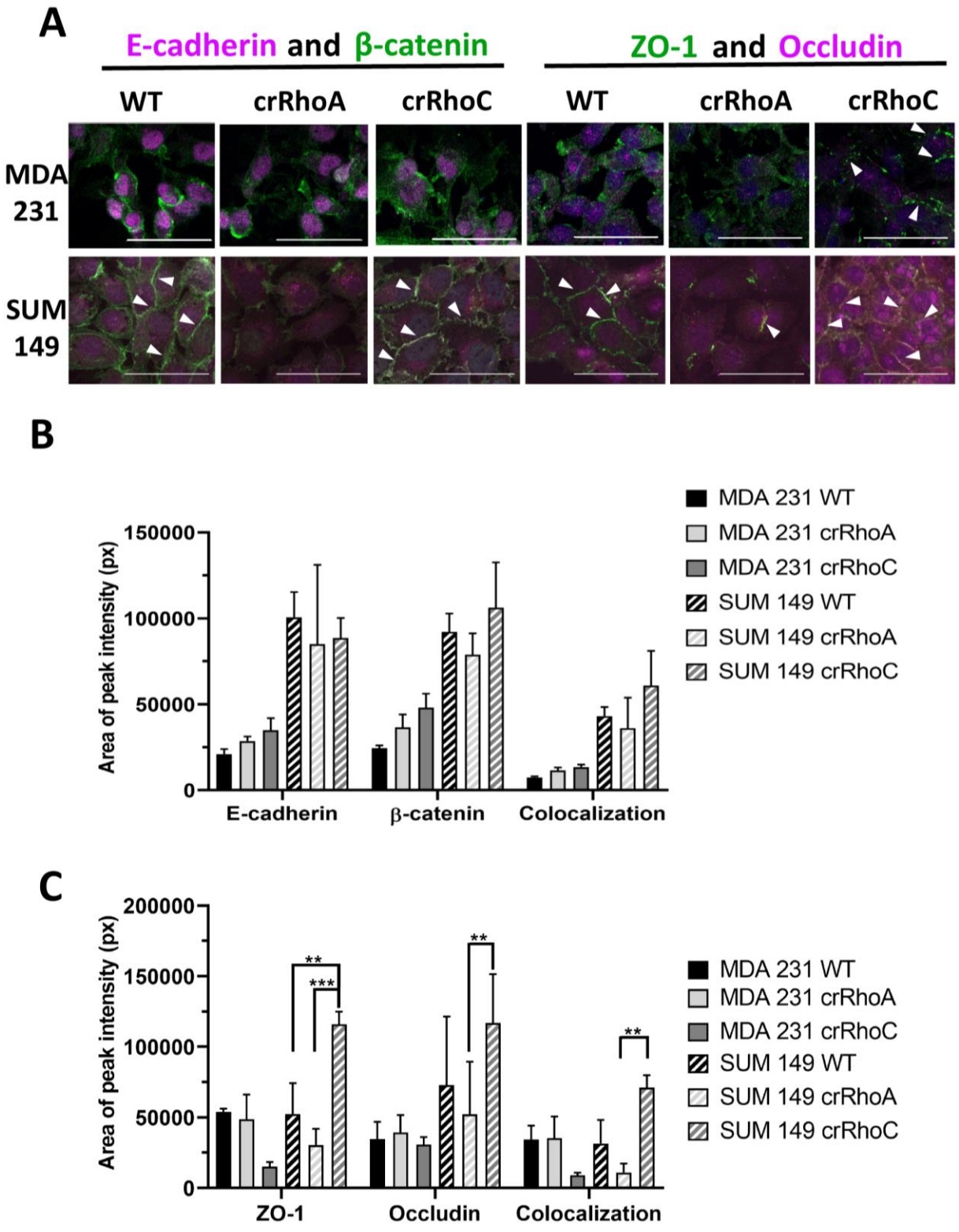

Figure 3.3 Rho expression changes junction marker localization to cell-cell borders. (A) Representative images of immunofluorescence staining of junction markers in wild-type, crRhoA, and crRhoC cells. White arrows point to areas of junction marker localization to cell-cell borders. Scale bars = 50 μm. Quantification from 3 fields of view per cell type of **(B)** adherens junction marker and **(C)** tight

junction marker localization to cell-cell borders in wild-type, crRhoA and crRhoC cells, with area of peak intensity corresponding to areas of cell-cell border localization. Solid bars are MDA 231, striped bars are SUM 149; black bars are wild type, light grey bars are crRhoA cells, and dark grey bars are crRhoC cells. Statistical significance assessed between wild-type, crRhoA and crRhoC cells; **: $p < 0.01$; ***: $p < 0.001$.

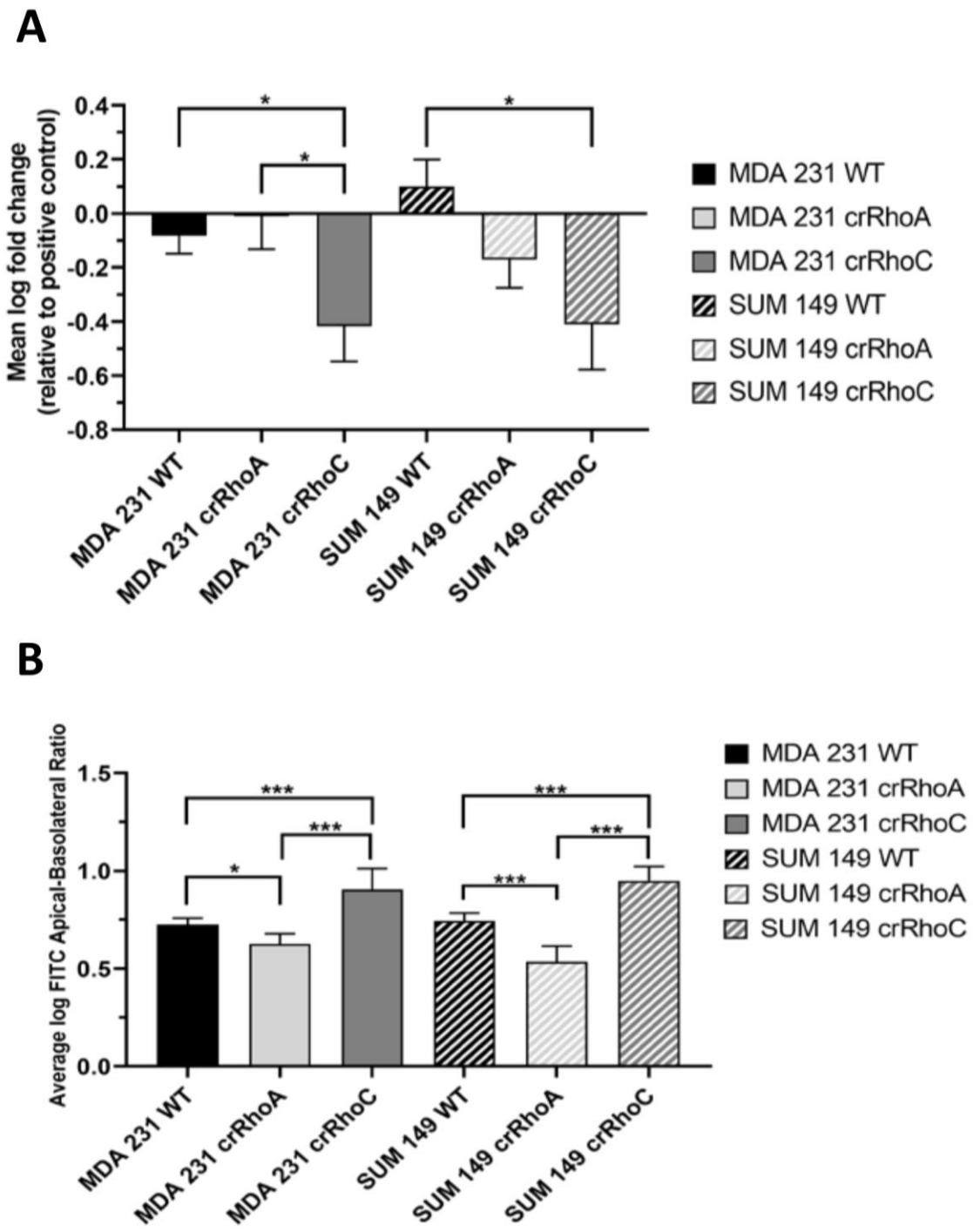

Figure 3.4 Rho expression changes cell-cell adhesiveness and junction stability. A) Quantification of difference in fluorescent intensity between positive control (non-adhering) and test wells in centrifugation adhesion assay (n = 3 biological replicates); decreases in fluorescent intensity correspond to increases in cell-cell adhesiveness. crRhoC cells have significantly increased adhesiveness compared to wild type. **(B)** Quantification of the ratio of fluorescent intensity in apical vs basal chambers in FITC-Dextran barrier permeability assay (n = 3 biological replicates); higher ratio corresponds to increased barrier integrity. crRhoA cells have decreased barrier integrity compared to wild-type, whereas crRhoC cells have

increased barrier integrity. Solid bars are MDA 231, striped bars are SUM 149; black bars are wild-type, light grey bars are crRhoA, and dark grey bars are crRhoC cells. *: $p < 0.05$; **: $p < 0.01$; ***: $p < 0.001$.

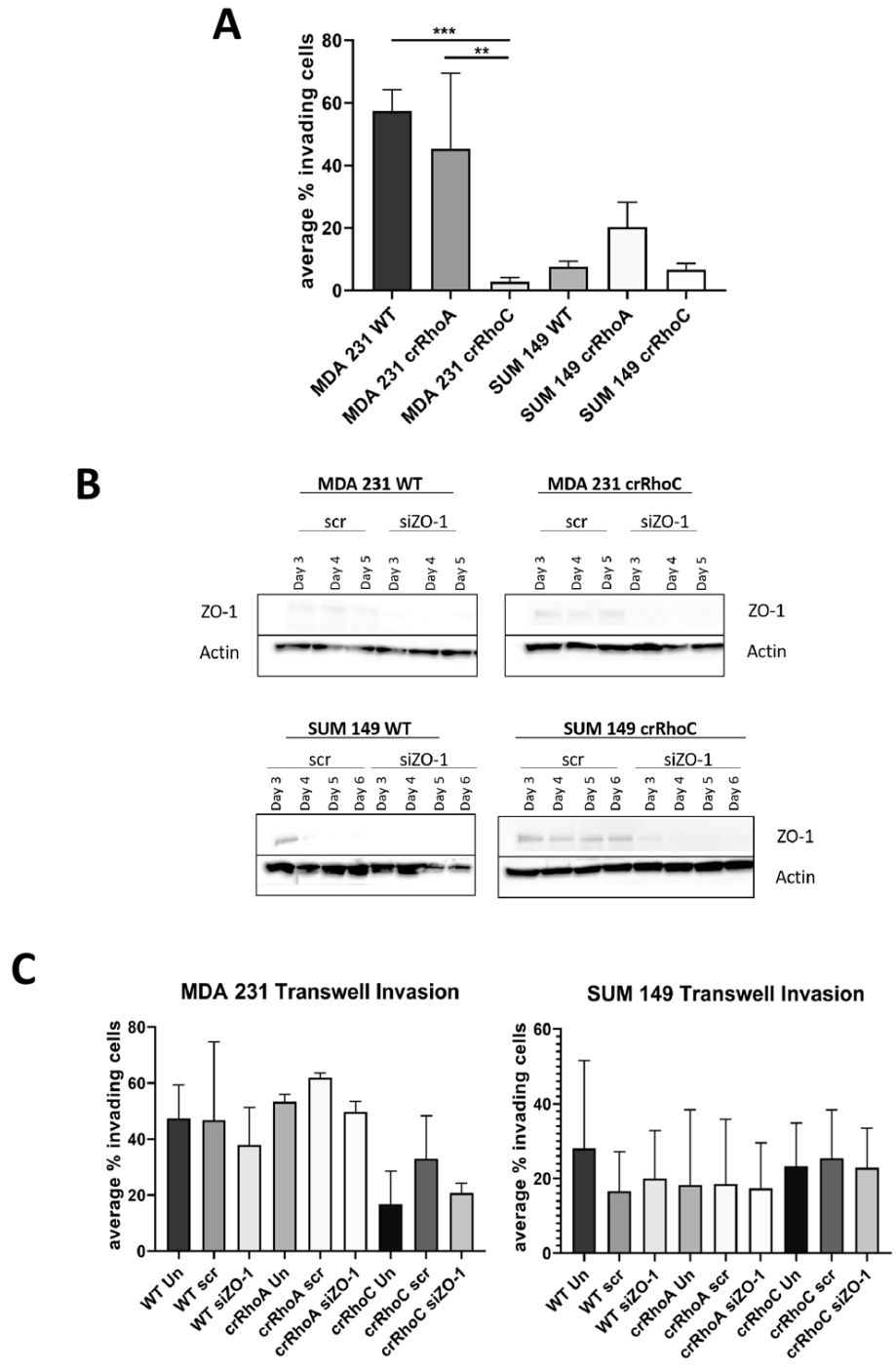

Figure 3.5 RhoC expression significantly changes breast cancer cell invasion, but ZO-1 expression does not. (A) In Matrigel-coated Transwell invasion assays (n = 3 biological replicates), crRhoC cells were less invasive than wild-type cells, most significantly in MDA 231. **: $p < 0.01$; ***: $p < 0.001$. **(B)** Transient siRNA knockdown of ZO-1 was achieved in MDA 231 and SUM 149 WT and crRhoC cells. **(C)** In Matrigel-coated Transwell invasion assays (n = 3 biological replicates), there was no significant difference in invasion between control cells and cells with silenced ZO-1 expression.

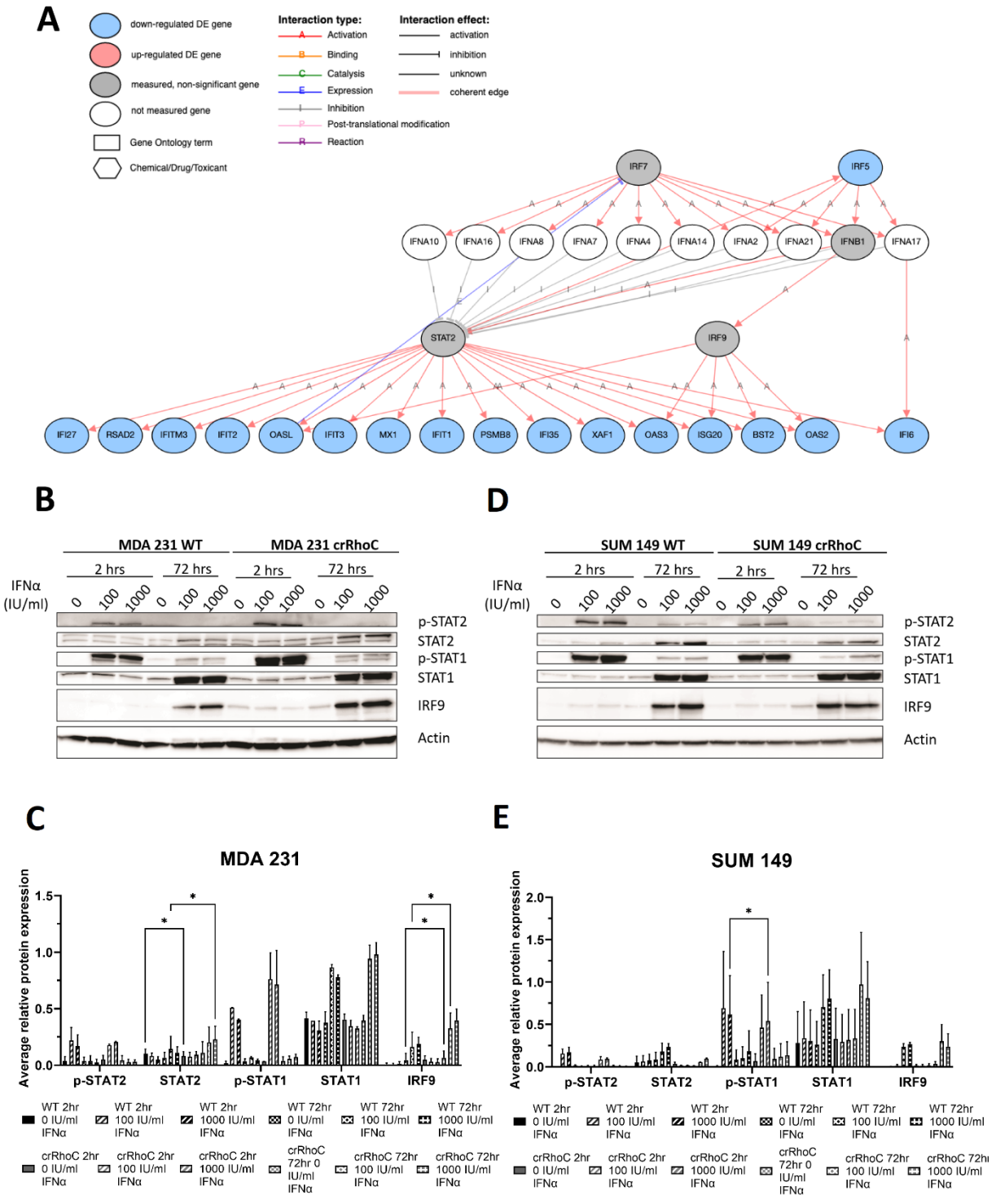

Figure 3.6 RhoC expression influences gene and protein expression of Type I interferon signaling response. (A) Type I interferon signaling pathway and the genes significantly downregulated in crRhoC knockout cells compared to wild-type, as measured in RNAseq. Genes in blue circles were downregulated in crRhoC compared to wild-type; genes in grey circles were not significantly differentially expressed between crRhoC and wild-type. **(B)** Western blot of interferon signaling markers in MDA 231 wild-type

and crRhoC cells—crRhoC cells have increased STAT2 and IRF9 compared to wild type. **(C)** Quantification of two biological replicates of MDA 231 western blots; significance compared between wild-type and crRhoC and reported as *: $p < 0.05$. **(D)** Western blot of interferon signaling markers in SUM 149 wild-type and crRhoC cells—crRhoC cells have decreased p-STAT2 and STAT2 compared to wild type. **(E)** Quantification of two biological replicates of SUM 149 western blots—trends of decreased p-STAT2 and STAT2 did not reach significance. Significance compared between wild-type and crRhoC and reported as *: $p < 0.05$.

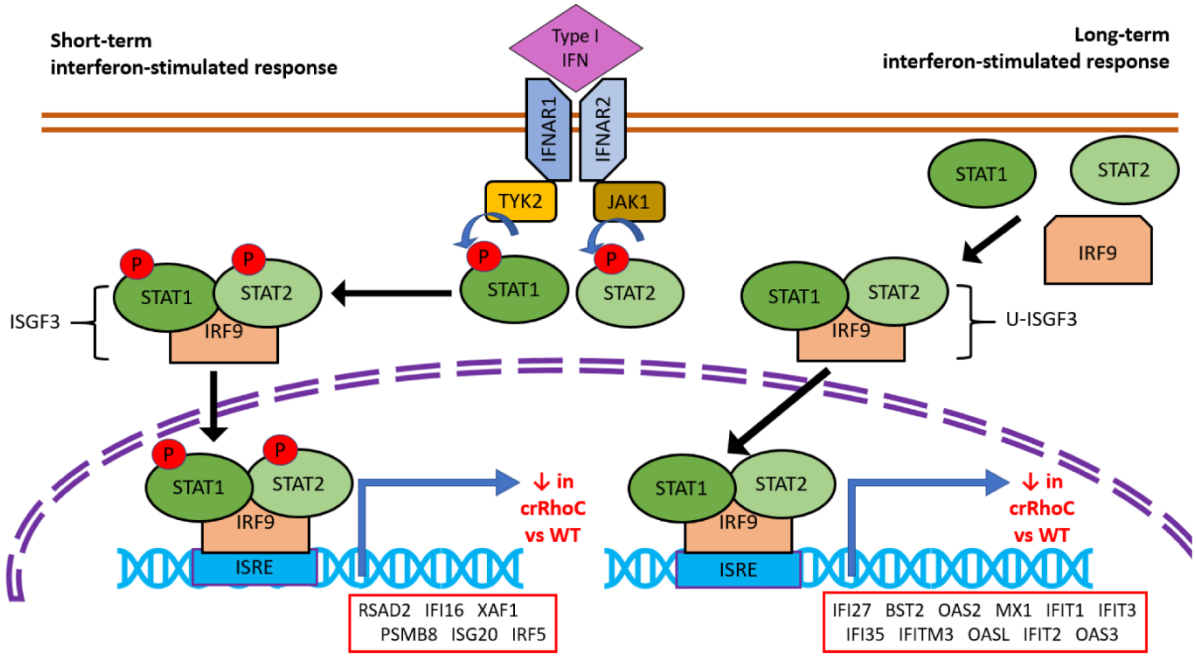

Figure 3.7 IFN signaling and effect of RhoC knockout. Short-term and long-term signaling through type I interferon signaling pathways. Short-term interferon signaling is driven by phosphorylated STAT1 and STAT2 complexed with IRF9 that translocates to the nucleus, binds to interferon stimulated response elements (ISREs), and promotes transcription of interferon stimulated genes (ISGs); phosphorylation of STAT1 and STAT2 peak about 2 hours after treatment with a type I interferon. Long-term signaling is driven by unphosphorylated STAT1 and STAT2 complexed with IRF9, and peaks around 72 hours after treatment with type I interferons. Genes listed in order of decreasing magnitude of log fold-change.

A

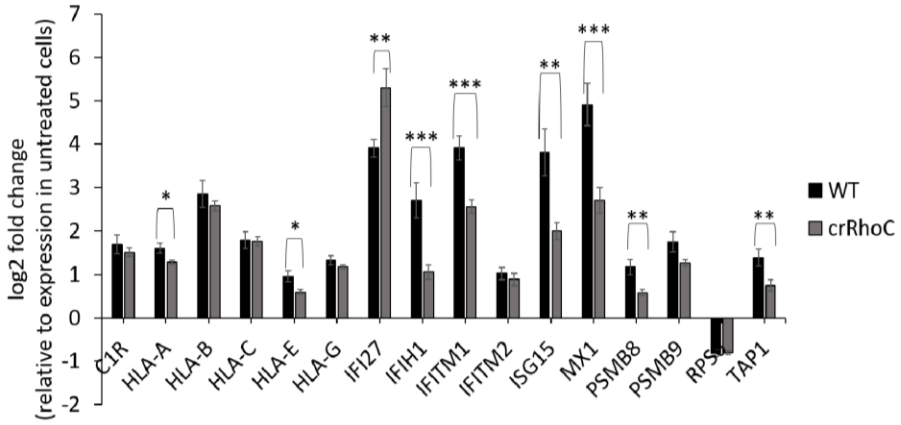
log2 fold change
(relative to expression in untreated cells)
WT
crRhoC
C1R
HLA-A
HLA-B
HLA-C
HLA-E
HLA-G
IFI27
IFIH1
IFITM1
IFITM2
ISG15
MX1
PSMB8
PSMB9
RPS9
TAP1

B

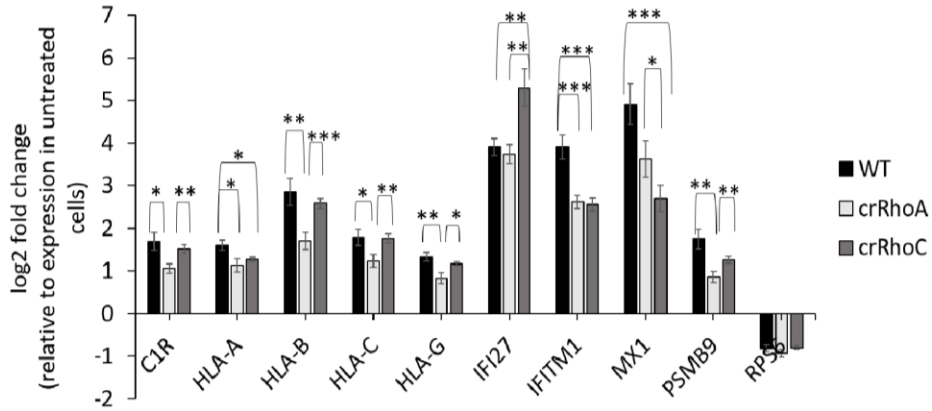
log2 fold change
(relative to expression in untreated cells)
WT
crRhoA
crRhoC
C1R
HLA-A
HLA-B
HLA-C
HLA-G
IFI27
IFITM1
MX1
PSMB9
RPS9

C

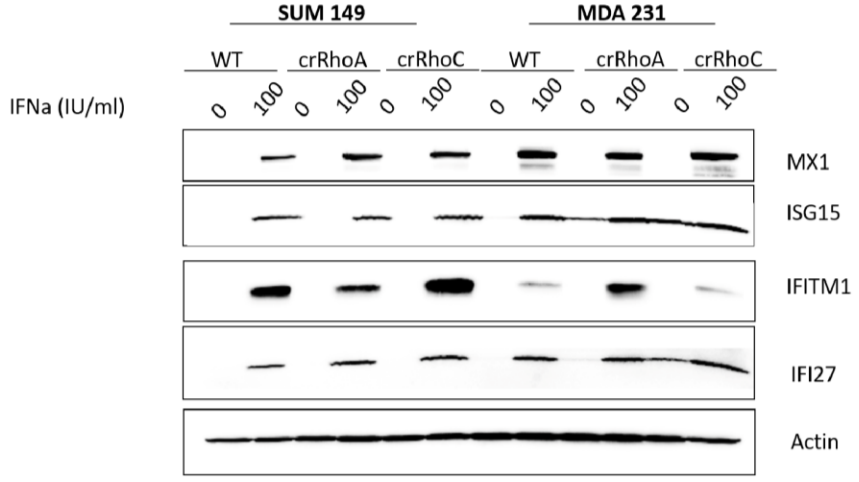
SUM 149
MDA 231
WT
crRhoA
crRhoC
IFNa (IU/ml)
0
100
MX1
ISG15
IFITM1
IFI27
Actin

Figure 3.8 Rho expression alters expression of interferon stimulated genes. (A) RNA expression of interferon stimulated genes in response to 72 hours of IFN-α treatment (100 IU/ml). Wild-type cells had larger increases in gene expression with IFN-α treatment compared to crRhoC cells. Black bars are expression in wild-type cells, dark grey bars are expression in crRhoC cells. **(B)** RNA expression of interferon stimulated genes in response to 72 hours of IFN-α treatment (100 IU/ml). Wild-type cells had larger increases in gene expression with IFN-α treatment compared to crRhoA and crRhoC cells. Black bars are expression in wild-type cells, light grey bars are expression in crRhoA cells, dark grey bars are expression in crRhoC cells. *: $p < 0.05$; **: $p < 0.01$; ***: $p < 0.001$. **(C)** Protein expression of interferon stimulated genes in response to 72 hours of IFN-α treatment (100 IU/ml).

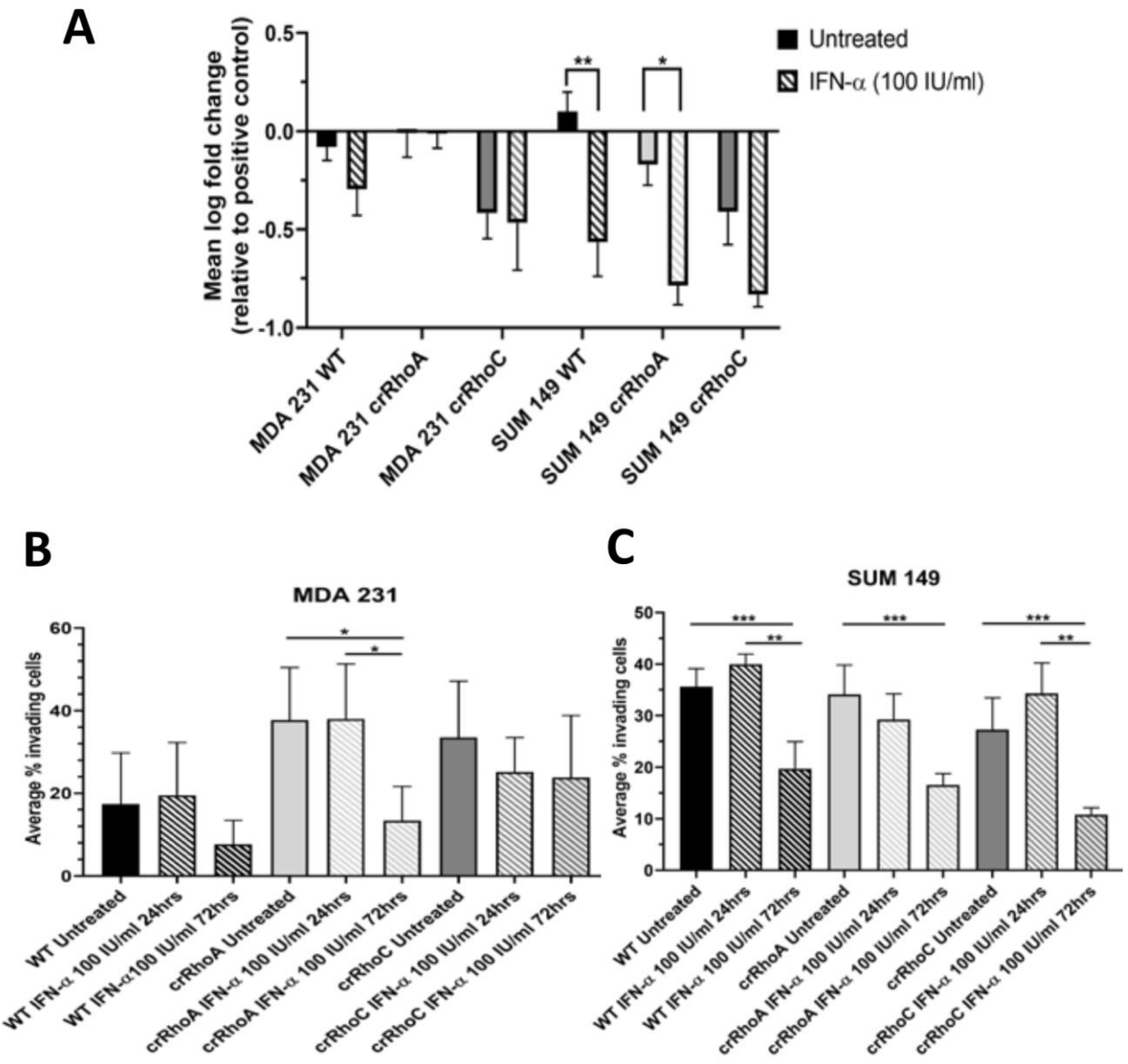

Figure 3.9 RhoC expression modulates cells' functional response to interferon. (A) Quantification of difference in fluorescent intensity with IFN-α treatment between positive control (non-adhering) and test wells in centrifugation adhesion assay (n = 3 biological replicates); decreases in fluorescent intensity correspond to increases in cell-cell adhesiveness. Treatment with IFN-α at 100 IU/ml for 72 hours led to increased adhesion for all cells, but the increases were larger and more significant in wild-type and crRhoA cells compared to crRhoC cells. **(B)** Quantification of transwell invasion with IFN-α treatment (n = 3 biological replicates) in MDA 231 and in **(C)** SUM 149. Treatment with IFN-α led to decreased invasion for all cells; in MDA 231 wild-type and crRhoA cells had larger and more significant decreases than in crRhoC cells, whereas in SUM 149 crRhoC cells had the largest relative decrease in invasion. Downward-slanting stripes represent IFN-α treatment; black bars are wild-type, light grey bars are crRhoA cells, and dark grey bars are crRhoC cells. *: $p < 0.05$; **: $p < 0.01$; ***: $p < 0.001$.

TABLES

Table 3.1 crRhoC cells have predicted inhibition of IRF9 and STAT2 signaling compared to wild-type cells. iPathwayGuide analysis of RNAseq data identified multiple genes downregulated in crRhoC compared to wild-type cells ("consistent (-)") that were also identified as downstream of IRF9 and STAT2 based on KEGG ("DE targets"). Significance determined by $p < 0.05$ and indicated by *.

	crRhoC vs WT									
	SUM 149		MDA 231		VARI 068		SUM 190		MCF7	
Gene	Consistent (-)/DE targets	FDR-adjusted p-value	Consistent (-)/DE targets	FDR-adjusted p-value	Consistent (-)/DE targets	FDR-adjusted p-value	Consistent (-)/DE targets	FDR-adjusted p-value	Consistent (-)/DE targets	FDR-adjusted p-value
IRF9	13/15	0.148	15/16*	0.003	23/23*	2.29e-14	0/1	1.00	5/5	0.736
STAT2	13/15	0.230	15/17*	0.018	24/24*	2.29e-14	0/1	1.00	5/5	0.736

Table 3.2 Genes downstream of Type I interferon signaling are downregulated in crRhoC cells compared to wild-type. Combining the RNAseq results of crRhoC vs WT in all cell lines assessed (SUM 149, MDA 231, VARI 068, SUM 190, and MCF7), 17 genes downstream of IRF9 and STAT2 were significantly downregulated in crRhoC cells compared to wild-type, with significance determined by $p < 0.05$.

Gene	LogFC	FDR-adjusted p-value
IFI27	-2.90	1.00e-6
BST2	-2.10	1.00e-6
RSAD2	-1.81	1.00e-6
IFI6	-1.31	1.00e-6
OAS2	-1.27	2.29e-4
XAF1	-1.20	1.00e-6
MX1	-1.07	1.00e-6
PSMB8	-1.00	1.00e-6
IFIT1	-0.886	3.59e-4
IFIT3	-0.783	3.133-4
IFI35	-0.758	1.00e-6
ISG20	-0.756	2.03e-4
IFITM3	-0.681	1.00e-6
OASL	-0.678	0.002
IFIT2	-0.673	0.004
OAS3	-0.667	3.01e-4
IRF5	-0.610	1.36e-5

Table 3.3 RhoC knockout dampens IFN-driven increase in cell-cell adhesion. Adhesion was measured using the fluorimetric centrifugation adhesion assay. Log fold change in fluorescence corresponds to change in adhesiveness. Significance determined by $p < 0.05$ and indicated by *.

Cell Line	|Log fold change| with IFN-α tx	p value with IFN-α tx
MDA 231 WT	3.63	0.250
MDA 231 crRhoA	1.30	0.982
MDA 231 crRhoC	1.12	0.864
SUM 149 WT	5.69*	0.037
SUM 149 crRhoA	4.59*	0.007
SUM 149 crRhoC	2.02	0.120

Table 3.4 RhoC knockout modulates IFN-driven inhibition of cell invasion. Cells were treated with IFN-α for 72 hours and transwell invasion assays were conducted. Fold change between the percent invading cells for untreated and treated cells was calculated. Significance determined by $p < 0.05$ and indicated by *.

Cell Line	Fold change with IFN-α tx 72 hr	p value with IFN-α tx 72 hr
MDA 231 WT	0.559	0.431
MDA 231 crRhoA	0.645*	0.012
MDA 231 crRhoC	0.289	0.809
SUM 149 WT	0.447*	2E-4
SUM 149 crRhoA	0.514*	1E-4
SUM 149 crRhoC	0.604*	9E-4

REFERENCES

1. Kondo T, Sentani K, Oue N, Yoshida K, Nakayama H, Yasui W. Expression of RhoC is associated with metastasis of gastric carcinomas. *Pathobiology*. 2004;71(1):19-25. doi:10.1159/000072958
2. Wang W, Yang LY, Yang ZL, Huang GW, Lu WQ. Expression and significance of RhoC gene in hepatocellular carcinoma. *World J Gastroenterol*. 2003;9(9):1950-1953.
3. Kamai T, Tsujii T, Arai K, et al. Significant association of Rho/ROCK pathway with invasion and metastasis of bladder cancer. *Clin Cancer Res*. 2003;9(7):2632-2641. doi:10.1126/science.279.5350.509
4. Suwa H, Ohshio G, Imamura T, et al. Overexpression of the rhoC gene correlates with progression of ductal adenocarcinoma of the pancreas. *Br J Cancer*. 1998;77(1):147-152. doi:10.1038/bjc.1998.23
5. Clark E a, Golub TR, Lander ES, Hynes RO. Genomic Analysis of metastasis reveals an essential role for RhoC. *Nature*. 2000;406(6793):532-535. doi:10.1038/35018520
6. Kleer CG, Griffith KA, Sabel MS, et al. RhoC-GTPase is a novel tissue biomarker associated with biologically aggressive carcinomas of the breast. *Breast Cancer Res Treat*. 2005;93(2):101-110. doi:10.1007/s10549-005-4170-6
7. van Golen KL, Wu ZF, Qiao XT, Bao L, Merajver SD. RhoC GTPase overexpression modulates induction of angiogenic factors in breast cells. *Neoplasia*. 2000;2(5):418-425. doi:http://dx.doi.org/10.1038/sj.neo.7900115
8. Hakem A, Sanchez-Sweatman O, You-Ten A, et al. RhoC is dispensable for embryogenesis and tumor initiation but essential for metastasis. *Genes Dev*. 2005;19(17):1974-1979. doi:10.1101/gad.1310805
9. Wu M, Wu ZF, Rosenthal DT, Rhee EM, Merajver SD. Characterization of the roles of RHOC and RHOA GTPases in invasion, motility, and matrix adhesion in inflammatory and aggressive breast cancers. In: *Cancer*. Vol 116. ; 2010:2768-2782. doi:10.1002/cncr.25181
10. Etienne-Manneville S, Hall A. Rho GTPases in cell biology. *Nature*. 2002;420(6916):629-635. doi:10.1038/nature01148
11. Hartsock A, Nelson WJ. Adherens and tight junctions: Structure, function and connections to the actin cytoskeleton. *Biochim Biophys Acta - Biomembr*. 2008;1778(3):660-669. doi:10.1016/j.bbamem.2007.07.012
12. Wheeler AP, Ridley AJ. Why three Rho proteins? RhoA, RhoB, RhoC, and cell motility. *Exp Cell Res*. 2004. doi:10.1016/j.yexcr.2004.08.012
13. Citi S, Guerrera D, Spadaro D, Shah J. Epithelial junctions and Rho family GTPases: The zonular signalosome. *Small GTPases*. 2014. doi:10.4161/21541248.2014.973760
14. Harris TJC, Tepass U. Adherens junctions: from molecules to morphogenesis. *Nat Rev Mol Cell Biol*. 2010;11(7):502-514. doi:10.1038/nrm2927
15. Martin TA, Watkins G, Mansel RE, Jiang WG. Loss of tight junction plaque molecules in breast cancer tissues is associated with a poor prognosis in patients with breast cancer. *Eur J Cancer*. 2004. doi:10.1016/j.ejca.2004.08.008
16. Hoover KB, Liao SY, Bryant PJ. Loss of the tight junction MAGUK ZO-1 in breast cancer: Relationship to glandular differentiation and loss of heterozygosity. *Am J Pathol*. 1998. doi:10.1016/S0002-9440(10)65691-X
17. Kaihara T, Kusaka T, Nishi M, et al. Dedifferentiation and decreased expression of

adhesion molecules, E-cadherin and ZO-1, in colorectal cancer are closely related to liver metastasis. *J Exp Clin Cancer Res*. 2003.
18. Rendón-Huerta EP, Torres-Martínez A, Charles-Niño C, et al. Pegylated interferon-α2b and ribavirin decrease claudin-1 and E-cadherin expression in HepG2 and Huh-7.5 cells. *Ann Hepatol*. 2013. doi:10.1016/s1665-2681(19)31346-8
19. Cao X, Sun L, Lechuga S, Naydenov NG, Feygin A, Ivanov AI. A Novel pharmacological approach to enhance the integrity and accelerate restitution of the intestinal epithelial barrier. *Inflamm Bowel Dis*. 2020. doi:10.1093/ibd/izaa063
20. Chaigne-Delalande B, Deuve L, Reuzeau E, et al. RhoGTPases and p53 are involved in the morphological appearance and interferon-α response of hairy cells. *Am J Pathol*. 2006. doi:10.2353/ajpath.2006.050345
21. Badr G, Saad H, Waly H, et al. Type I interferon (IFN-α/β) rescues B-lymphocytes from apoptosis via PI3Kδ/Akt, Rho-A, NFκB and Bcl-2/BclXL. *Cell Immunol*. 2010. doi:10.1016/j.cellimm.2010.02.012
22. Buess M, Nuyten DSA, Hastie T, Nielsen T, Pesich R, Brown PO. Characterization of heterotypic interaction effects in vitro to deconvolute global gene expression profiles in cancer. *Genome Biol*. 2007. doi:10.1186/gb-2007-8-9-r191
23. Aw Yong KM, Ulintz PJ, Caceres S, et al. Heterogeneity at the invasion front of triple negative breast cancer cells. *Sci Rep*. 2020;10(1). doi:10.1038/s41598-020-62516-8
24. Allen SG, Chen Y-C, Madden JM, et al. Macrophages Enhance Migration in Inflammatory Breast Cancer Cells via RhoC GTPase Signaling. *Sci Rep*. 2016;6(1):39190. doi:10.1038/srep39190
25. Weetall M, Hugo R, Friedman C, et al. A homogeneous fluorometric assay for measuring cell adhesion to immobilized ligand using V-well microtiter plates. *Anal Biochem*. 2001. doi:10.1006/abio.2001.5140
26. Draghici S, Khatri P, Tarca AL, et al. A systems biology approach for pathway level analysis. *Genome Res*. 2007;17(10). doi:10.1101/gr.6202607
27. Khatri P, Draghici S, Tarca AL, Hassan SS, Romero R. A system biology approach for the steady-state analysis of gene signaling networks. In: *Lecture Notes in Computer Science (Including Subseries Lecture Notes in Artificial Intelligence and Lecture Notes in Bioinformatics)*. Vol 4756 LNCS. ; 2007. doi:10.1007/978-3-540-76725-1_4
28. Tarca AL, Draghici S, Khatri P, et al. A novel signaling pathway impact analysis. *Bioinformatics*. 2009;25(1). doi:10.1093/bioinformatics/btn577
29. Kanehisa M, Goto S, Sato Y, Kawashima M, Furumichi M, Tanabe M. Data, information, knowledge and principle: Back to metabolism in KEGG. *Nucleic Acids Res*. 2014;42(D1). doi:10.1093/nar/gkt1076
30. Ashburner M, Lewis S, Subramaniam, Noble, Kanehisa. On ontologies for biologists: The gene ontology - Untangling the web. In: *Novartis Foundation Symposium*. Vol 247. ; 2002. doi:10.1002/0470857897.ch6
31. Harris MA, Clark J, Ireland A, et al. The Gene Oncology (GO) database and informatics resource. *Nucleic Acids Res*. 2004;32(DATABASE ISS.). doi:10.1093/nar/gkh036
32. Szklarczyk D, Gable AL, Lyon D, et al. STRING v11: Protein-protein association networks with increased coverage, supporting functional discovery in genome-wide experimental datasets. *Nucleic Acids Res*. 2019;47(D1). doi:10.1093/nar/gky1131
33. Oughtred R, Rust J, Chang C, et al. The BioGRID database: A comprehensive biomedical resource of curated protein, genetic, and chemical interactions. *Protein Sci*. 2021;30(1).

doi:10.1002/pro.3978
34. Draghici S. *Statistics and Data Analysis for Microarrays Using R and Bioconductor*. second. (Chapman, Hall, eds.). CRC; 2011.
35. Kaye DH, Freedman D a. Reference Guide on Statistics. *Ref Man Sci Evid*. 2011.
36. Lechner J, Krall M, Netzer A, Radmayr C, Ryan MP, Pfaller W. Effects of interferon α-2b on barrier function and junctional complexes of renal proximal tubular LLC-PK1 cells. *Kidney Int*. 1999. doi:10.1046/j.1523-1755.1999.00487.x
37. Cheon H, Holvey-Bates EG, Schoggins JW, et al. IFNβ-dependent increases in STAT1, STAT2, and IRF9 mediate resistance to viruses and DNA damage. *EMBO J*. 2013. doi:10.1038/emboj.2013.203
38. Wang W, Yin Y, Xu L, et al. Unphosphorylated ISGF3 drives constitutive expression of interferon-stimulated genes to protect against viral infections. *Sci Signal*. 2017;10(476). doi:10.1126/scisignal.aah4248
39. Provance OK, Lewis-Wambi J. Deciphering the role of interferon alpha signaling and microenvironment crosstalk in inflammatory breast cancer. *Breast Cancer Res*. 2019. doi:10.1186/s13058-019-1140-1
40. Cervantes-Badillo MG, Paredes-Villa A, Gómez-Romero V, et al. IFI27/ISG12 Downregulates Estrogen Receptor α Transactivation by Facilitating Its Interaction With CRM1/XPO1 in Breast Cancer Cells. *Front Endocrinol (Lausanne)*. 2020. doi:10.3389/fendo.2020.568375
41. Szekely B, Bossuyt V, Li X, et al. Immunological differences between primary and metastatic breast cancer. *Ann Oncol*. 2018. doi:10.1093/annonc/mdy399
42. Chiang KC, Huang ST, Wu RC, et al. Interferon α-inducible protein 27 is an oncogene and highly expressed in cholangiocarcinoma patients with poor survival. *Cancer Manag Res*. 2019. doi:10.2147/CMAR.S196485
43. Li S, Xie Y, Zhang W, et al. Interferon alpha-inducible protein 27 promotes epithelial-mesenchymal transition and induces ovarian tumorigenicity and stemness. *J Surg Res*. 2015. doi:10.1016/j.jss.2014.06.055
44. Wang H, Qiu X, Lin S, Chen X, Wang T, Liao T. Knockdown of IFI27 inhibits cell proliferation and invasion in oral squamous cell carcinoma. *World J Surg Oncol*. 2018. doi:10.1186/s12957-018-1371-0
45. Chen R-H, Xiao Z-W, Yan X-Q, et al. Tumor Cell-Secreted ISG15 Promotes Tumor Cell Migration and Immune Suppression by Inducing the Macrophage M2-Like Phenotype. *Front Immunol*. 2020. doi:10.3389/fimmu.2020.594775
46. Kariri Y, Alsaleem M, Joseph C, et al. The prognostic significance of interferon-stimulated gene 15 (ISG15) in invasive breast cancer. *Breast Cancer Res Treat*. 2021;185(2):293-305. https://pubmed.ncbi.nlm.nih.gov/33073304/.
47. Liang R, Li X, Zhu X. Deciphering the Roles of IFITM1 in Tumors. *Mol Diagnosis Ther*. 2020. doi:10.1007/s40291-020-00469-4
48. Little AC, Pathanjeli P, Wu Z, et al. IL-4/IL-13 stimulated macrophages enhance breast cancer invasion via rho-GTPase regulation of synergistic VEGF/CCL-18 signaling. *Front Oncol*. 2019. doi:10.3389/fonc.2019.00456
49. Zhuang PY, Shen J, Zhu XD, et al. Direct Transformation of Lung Microenvironment by Interferon-α Treatment Counteracts Growth of Lung Metastasis of Hepatocellular Carcinoma. *PLoS One*. 2013. doi:10.1371/journal.pone.0058913
50. Zhang Z, Zhu Y, Xu D, et al. IFN-α facilitates the effect of sorafenib via shifting the M2-

like polarization of TAM in hepatocellular carcinoma. *Am J Transl Res*. 2021. https://www.ncbi.nlm.nih.gov/pmc/articles/PMC7847501/.
51. Gresser I, Brouty-Boyé D, Thomas MT, Macieira-Coelho A. Interferon and cell division. Ii. influence of various experimental conditions on the inhibition of l1zl0 cell multiplication in vitro by interferon preparations12. *J Natl Cancer Inst*. 1970. doi:10.1093/jnci/45.6.1145
52. Berraondo P, Sanmamed MF, Ochoa MC, et al. Cytokines in clinical cancer immunotherapy. *Br J Cancer*. 2019. doi:10.1038/s41416-018-0328-y
53. Caraglia M, Dicitore A, Marra M, et al. Type I Interferons: Ancient Peptides with Still Under-Discovered Anti-Cancer Properties. *Protein Pept Lett*. 2013. doi:10.2174/092986613805290372
54. Medrano RFV, Hunger A, Mendonça SA, Barbuto JAM, Strauss BE. Immunomodulatory and antitumor effects of type I interferons and their application in cancer therapy. *Oncotarget*. 2017. doi:10.18632/oncotarget.19531
55. Doherty MR, Cheon HJ, Junk DJ, et al. Interferon-beta represses cancer stem cell properties in triple-negative breast cancer. *Proc Natl Acad Sci U S A*. 2017. doi:10.1073/pnas.1713728114
56. Rosenthal DT, Zhang J, Bao L, et al. RhoC impacts the metastatic potential and abundance of breast cancer stem cells. *PLoS One*. 2012;7(7). doi:10.1371/journal.pone.0040979

Chapter 4 : Conclusions and Future Directions

IBC is the most aggressive form of breast cancer, and is highly heterogeneous[1]. The adoption of trimodality therapy (neoadjuvant chemotherapy, mastectomy, and radiation) and the advent of targeted therapies for HER2+ cancers has improved IBC survival significantly[2], however the increase in survival has plateaued at about 40% 5-year survival[3]. Thus, there is still significant room for improvement in IBC survival, and the identification of IBC-specific targeted therapies would further that goal. As no IBC-specific targeted therapies have yet been adopted for clinical use, molecular drivers of IBC need to be further investigated.

This thesis work finds that although IBC survival has improved over the past four decades, racial disparities in survival persist. This work further explores the contribution of RhoC to the aggressive behavior of IBC and other breast cancers, and finds that RhoC modulates cell adhesion, cell invasion, and cellular response to interferon signaling in an interconnected manner relevant to the development of therapeutic strategies targeting aggressive breast cancers like IBC.

In order to accurately analyze the epidemiology of IBC, a standard definition of IBC in the SEER database is needed. We hypothesized that expanding the currently recommended coding for IBC (ICD-O-3 “8530” and AJCC 6th Edition T “T4d”) to include codes that reflect the clinical signs of IBC (EoD-CS-Ext codes 510 – 750) would best capture authentic IBC cases in the SEER database, and indeed we found that using a combination of all of these codes results in a larger number of cases with similar survival statistics. This implies that many genuine cases of

IBC are being overlooked and that adoption of these clinically-relevant codes as a new coding standard would be beneficial for future IBC studies. We further find that there are marked racial disparities in the epidemiology of IBC: in comparison with white patients, black patients have significantly higher incidence of IBC, younger age at diagnosis, and worse survival outcomes. The increased incidence and decreased survival of black patients with IBC compared to white patients have been persistent trends over several decades—indeed, although overall IBC survival has significantly improved for all races, for several decades the gap between the survival of white and black patients has not narrowed. The persistance of this disparity in survival is an important finding that prompts investigation into why measures that have improved overall IBC survival have not also led to equal survival outcomes between races.

In future research, we will validate our proposed clinically-informed IBC coding standard in a prospective cohort of patients presenting at the cancer centers in our region, to assess whether female breast cancer patients assigned as ICD-O-3 “8530”, AJCC “T4d”, or EoD-CS-Ext codes 510-750 and having the same metastatic status (with or without metastases at diagnosis) would be considered by physicians to need similar treatment and whether they would have similar survival outcomes. Additionally, our study would have been strengthened by the inclusion of more patients identifying as Asian/Pacific Islander or as American Indian/Alaska Native, so in composing a prospective patient cohort we would work with physicians in cancer centers in our region to encourage recruitment of IBC patients from these ethnic backgrounds.

In investigating molecular drivers of IBC and other aggressive breast cancers, we found that RhoC affects cell junction protein expression, junction functionality, and cellular response to interferon treatment. In both the triple-negative breast cancer (TNBC) cell lines we studied, one IBC and one non-IBC, loss of RhoC expression led to a trend towards increased protein

expression of cell junction markers and increased colocalization of these markers at points of cell-cell contact instead of diffusely spread through the cytoplasm. Interestingly, loss of RhoC did not lead to significant differences in the RNA expression of these same junction genes, suggesting that RhoC influences post-translational modifications in junction signaling, or potentially trafficking of transmembrane junction proteins in a manner that affects the accumulation or degradation of junction proteins. Nevertheless, the observed changes in protein expression correlated with significant increases in cell-cell adhesion and decreases in cell invasion in crRhoC cells. Seeking to assess whether RhoC's effect on cell invasion was due to RhoC's effect on junction function, we performed transient knockdown of the tight junction protein ZO-1, whose expression was most significantly affected by RhoC expression, and found that it did not significantly change the invasiveness of wild type or crRhoC cells. It is possible that one reason that ZO-1 knockdown alone did not significantly change invasion was that other junction proteins compensated functionally in the absence of ZO-1; future studies investigating inducible knockdown of multiple junction proteins in conjunction could further assess the contribution of cell junctions to RhoC's ability to promote cancer invasion.

We found also that crRhoC cells had significantly decreased expression of interferon stimulated genes compared to wild type cells at baseline, without IFN-α treatement; when treated with low-dose IFN-α for 72 hours, crRhoC cells had smaller increases both in RNA and protein expression of interferon stimulated genes compared to wild type cells. Functionally, crRhoC cells also had a blunted response to IFN-α treatment, having smaller increases in adhesion and decreases in invasiveness than wild type cells. The finding that RhoC contributes to interferon signaling is a novel contribution to the fields of both Rho GTPase study and Type I interferon study. In the context of IBC and potential interactions with immune cells in the tumor

microenvironment, the link between RhoC and interferon signaling would be particularly interesting to further investigate. Moreover, the finding that RhoC expression modulates cell adhesion in response to interferon suggests that RhoC's regulation of junction expression and interferon response may be interconnected.

We will further our studies on this topic by a combination of *in vitro* and *in vivo* work. We will measure the expression of junction proteins in wild type and crRhoC cells treated with IFN-α, and if IFN-α leads to increases in junction protein expression, we will study whether transient knockdown of junction proteins would inhibit interferon-driven decreases in cell invasion. To investigate the mechanism by which RhoC affects interferon signaling, we would start by assessing NF-κB signaling in these cell lines. RhoA is known to contribute to NF-κB signaling by activating Rho-associated protein kinase (ROCK), which in turn phosphorylates I-kappa B kinase alpha (IκBα), leading IκBα to dissociate from the NF-κB complex and thus allowing the NF-κB complex to translocate into the nucleus and activate gene transcription[4,5]. Previous work from our lab found that pomegranate fruit extract inhibited NF-κB signaling in MDA 231 and SUM 149 while also decreasing the expression of RhoA and RhoC[6]. NF-κB signaling is also known to be activated by Type I interferons, via STAT3, Akt, and PI3K[7]. The convergence of Rho signaling and interferon signaling on the NF-κB pathway (**Figure 4.1**) would therefore be our first avenue of exploration, starting with assessing whether NF-κB is activated by low-dose IFN-α treatment and whether the level of NF-κB activation is different in wild-type cells compared to crRhoC cells. Interestingly, the RhoGAP DLC1, which localizes with junction proteins α-catenin and E-cadherin, has been shown to inhibit NF-κB signaling in prostate cancer cells, although this inhibition is dependent on stable cell-cell junctions and is lost when junctions are disrupted by removal of Ca^{2+} from the media[8]. This study highlights the

contributions of RhoGAPs and RhoGEFs to RhoC signaling, and also points to a potential mechanism linking RhoC, junction function, and interferon signaling through NF-κB. We would therefore also want to study whether expression of RhoGAPs like DLC1 are affected by low-dose IFN-α treatment and by RhoC expression in our breast cancer cell lines.

To assess the impact of RhoC expression on interferon response in cancer cells in the presence of a subset of immune cells, we will grow cells in a co-culture system, with wild-type and crRhoC cancer cells seeded into the top chamber of transwells while human-derived M1 or M2 macrophages are seeded into the bottom chamber, based on our lab's previous work studying aggressive breast cancers and their interaction with macrophages[9,10]. Cells would be treated with IFN-α and the impact on cancer cells' viability, adhesion and invasion would be measured and compared to cancer cells treated with IFN-α and not co-cultured with macrophages. We hypothesize that co-culture with macrophages would enhance the effects of IFN-α treatment we observed in the work described above, namely increased cell adhesion and decreased invasion, and that in crRhoC cells these effects would remain blunted even in the presence of M2 macrophages.

If we do observe increased anti-cancer impact in experiments in the co-culture system compared to cell culture without macrophages, we would expand the work to *in vivo* studies in NOD SCID gamma (NSG) mice seeded with human hematopoietic stem cells and allowed to develop a "humanized" immune cell milieu. We would orthotopically transplant RhoC-high wild-type or crRhoC human breast cancer cells into the mammary fat pads of these mice, and after engraftment of the tumors would begin treatment with IFN-α. We would then assess whether long term low-dose IFN-α treatment impacts metastatic progression or survival in these mice, hypothesizing that metastases would be reduced and survival increased in all treated mice,

but more significantly in the mice with wild-type breast cancer compared to crRhoC cells. We would also assess the toxicity of long term low-dose IFN-α treatment.

The above-mentioned studies would utilize breast cancer cells that are RhoC-high (in wild-type) and are also TNBCs, as in our work described above we identified RhoC expression modulating interferon response more significantly in TNBC compared to non-TNBC based on our RNAseq data. However, we could also perform functional studies with non-TNBC cancer cells that are RhoC-high (for instance, the IBC cell lines SUM 190, which is ER-/PR-/HER2+, or MDA IBC 1, which is ER+/PR-/HER2-) to assess whether RhoC expression contributes to interferon response in these cell lines. If we do not see significant differences between wild-type and crRhoC cells' response to IFN-α in these cell lines, that would suggest an important mechanistic link between hormone receptor or EGFR expression, RhoC, and interferon which could be further explored. Additionally, it would point to IFN-α as a potential targeted therapy for TNBC, which is sorely needed in clinical practice.

While studying the epidemiology of IBC and the contribution of RhoC to junction function and interferon response appear to be very different projects, studying them in conjunction could fill an important gap in the field of breast cancer—namely, the reasons for racial disparity in IBC survival. Future studies could use IBC tumor microarrays to assess whether differences in RhoC expression, junction expression, or interferon response in IBC patients of different races could impact survival. To our knowledge, no studies have yet assessed whether RhoC expression in aggressive cancers varies by patients' race/ethnicity. Work from our lab studying IBC in North Africa did identify high RhoC expression[11], which appeared higher than typically seen in IBC patients in Michigan, so it seems possible that RhoC expression may differ by race and thereby impact patient survival. Very few studies examine differences in cell

junction expression in cancer patients of different races—Tan et al. find that the adhesion-related protein ALCAM is decreased in the primary tumors of African American breast cancer patients compared to Caucasian breast cancer patients[12]. On the other hand, multiple studies do show differences in immune response between patients of different races. For hepatitis C patients treated with interferon, African American patients tend to have decreased sustained virologic response (SVR) compared to Hispanic and Caucasian patients, and patients from Asia tend to have increased SVR compared to patients from Western countries[13,14]; certain polymorphisms in the IL28B gene correlate with SVR and the distribution of these polymorphisms among patients of different races also correlates with the differences in SVR between races[15]. In the context of breast cancer, African American TNBC patients have higher expression of immune checkpoint inhibitors than Caucasian patients, while Caucasian patients have larger areas of tumor-infiltrating lymphocytes than African American patients[16]. On the other hand, African American breast cancer patients also had increased Tregs, increased tumor-associated macrophages, increased M2 macrophages, and increased expression of interferon stimulated genes compared to white patients[17]. So far these are observational studies and are not directly correlated with survival; future work could address black patients' increased tumor-promoting immune expression by clinical trials of neoadjuvant treatment with IFN-α in addition to normal trimodality therapy, to assess whether IFN-α would be an efficacious intervention to improve survival for black patients with TN-IBC to be at least equal to the survival of white patients.

Overall, the field of IBC has progressed significantly over the past several decades to provide improved survival outcomes for patients in a disease that is nevertheless still extremely aggressive. Especially as improvements in survival have plateaued since the early 2000's and the introduction of trastuzumab, there is a significant need to better understand the molecular

mechanisms that drive IBC and identify targeted therapies to further improve IBC survival. We hope that the contributions of this thesis work will continue to progress the field of IBC by identifying a link between RhoC expression, cell junction function, and interferon response, and thereby laying the groundwork for studies examining types of immunotherapy that could be effective against IBC as well as studies that will ultimately close the survival gap between IBC patients of different races, so that someday any patient presenting with IBC will have an equal chance to survive and thrive cancer-free.

FIGURES

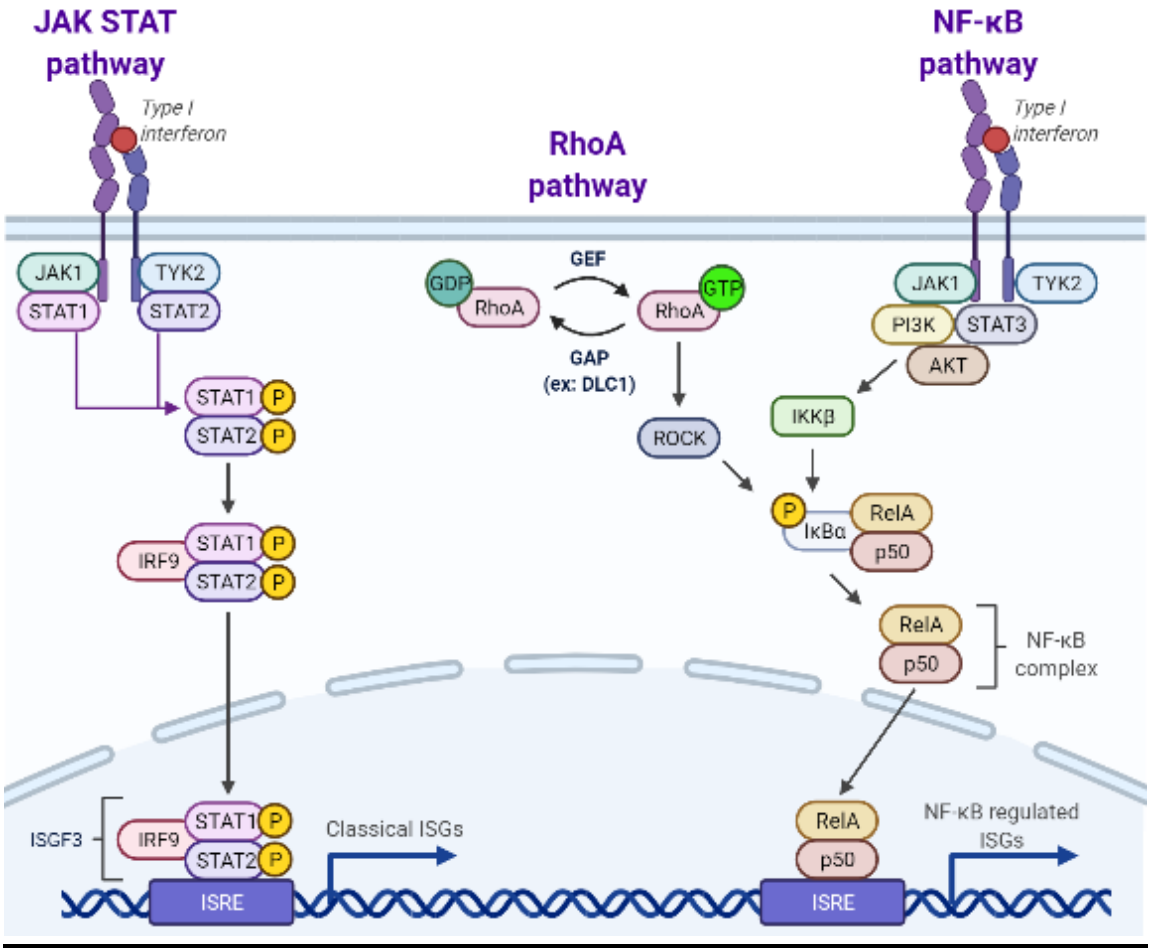

Figure 4.1 Rho, interferon, and NF-κB signaling pathways. Current understanding of the intersection between Rho GTPase signaling and Type I interferon signaling, which both converge on the NF-κB signaling pathway. IκBα phosphorylation leads to degradation of IκBα and release of the NF-κB complex, which translocates to the nucleus and regulates transcription. Both Rho kinase (ROCK) and interferon-stimulated signaling through STAT3-PI3K-Akt can lead to phosphorylation of IκBα and thus activated NF-κB signaling. Diagram created using Biorender.

REFERENCES

1. Van Laere SJ, Ueno NT, Finetti P, et al. Uncovering the molecular secrets of inflammatory breast cancer biology: An integrated analysis of three distinct affymetrix gene expression datasets. *Clin Cancer Res*. 2013. doi:10.1158/1078-0432.CCR-12-2549
2. van Uden DJP, van Laarhoven HWM, Westenberg AH, de Wilt JHW, Blanken-Peeters CFJM. Inflammatory breast cancer: An overview. *Crit Rev Oncol Hematol*. 2015. doi:10.1016/j.critrevonc.2014.09.003
3. van Uden DJP, Bretveld R, Siesling S, de Wilt JHW, Blanken-Peeters CFJM. Inflammatory breast cancer in the Netherlands; improved survival over the last decades. *Breast Cancer Res Treat*. 2017;162(2):365-374. doi:10.1007/s10549-017-4119-6
4. Park SY, Lee SW, Lee WS, et al. RhoA/ROCK-dependent pathway is required for TLR2-mediated IL-23 production in human synovial macrophages: Suppression by cilostazol. *Biochem Pharmacol*. 2013;86(9):1320-1327. doi:10.1016/j.bcp.2013.08.017
5. Segain JP, De la Blétière DR, Sauzeau V, et al. Rho kinase blockade prevents inflammation via nuclear factor κB inhibition: Evidence in Crohn's disease and experimental colitis. *Gastroenterology*. 2003;124(5):1180-1187. doi:10.1016/S0016-5085(03)00283-X
6. Khan GN, Gorin MA, Rosenthal D, et al. Pomegranate Fruit Extract Impairs Invasion and Motility in Human Breast Cancer. *Integr Cancer Ther*. 2009;8(3):242-253. doi:10.1177/1534735409341405
7. Pfeffer LM. The role of nuclear factor κb in the interferon response. *J Interf Cytokine Res*. 2011;31(7):553-559. doi:10.1089/jir.2011.0028
8. Tripathi V, Popescu NC, Zimonjic DB. DLC1 suppresses NF-κB activity in prostate cancer cells due to its stabilizing effect on adherens junctions. *Springerplus*. 2014;3(1):1-12. doi:10.1186/2193-1801-3-27
9. Allen SG, Chen Y-C, Madden JM, et al. Macrophages Enhance Migration in Inflammatory Breast Cancer Cells via RhoC GTPase Signaling. *Sci Rep*. 2016;6(1):39190. doi:10.1038/srep39190
10. Little AC, Pathanjeli P, Wu Z, et al. IL-4/IL-13 stimulated macrophages enhance breast cancer invasion via rho-GTPase regulation of synergistic VEGF/CCL-18 signaling. *Front Oncol*. 2019. doi:10.3389/fonc.2019.00456
11. Schairer C, Hablas A, Eldein IABS, et al. Clinico-pathologic and mammographic characteristics of inflammatory and non-inflammatory breast cancer at six centers in North Africa. *Breast Cancer Res Treat*. 2019;176(2):407-417. doi:10.1007/s10549-019-05237-5
12. Tan F, Mosunjac M, Adams AL, et al. Enhanced down-regulation of ALCAM/CD166 in African-American Breast Cancer - PubMed. *BMC Cancer*. 2014;14(715). doi:10.1186/1471-2407-14-715
13. Park C, Jiang S, Lawson KA. Efficacy and safety of telaprevir and boceprevir in patients with hepatitis C genotype 1: A meta-analysis. *J Clin Pharm Ther*. 2014;39(1):14-24. doi:10.1111/jcpt.12106
14. Chuang WL, Yu ML. Host factors determining the efficacy of hepatitis C treatment. *J Gastroenterol*. 2013;48(1):22-30. doi:10.1007/s00535-012-0669-x
15. Lisker-Melman M, Walewski JL. The impact of ethnicity on hepatitis C virus treatment decisions and outcomes. *Dig Dis Sci*. 2013;58(3):621-629. doi:10.1007/s10620-012-2392-0

16. Ogony JW, Radisky DC, Ruddy KJ, et al. Immune responses and risk of triple-negative breast cancer: Implications for higher rates among African American women. *Cancer Prev Res*. 2020;13(11):901-910. doi:10.1158/1940-6207.CAPR-19-0562
17. Kim G, Pastoriza JM, Condeelis JS, et al. The Contribution of Race to Breast Tumor Microenvironment Composition and Disease Progression. *Front Oncol*. 2020;10. doi:10.3389/fonc.2020.01022